METHODOLOGIES FOR THE OPTIMIZATION OF FIBRE-REINFORCED COMPOSITE STRUCTURES WITH MANUFACTURING UNCERTAINTIES

RYAN JASON HAMILTON

A THESIS SUBMITTED IN COMPLIANCE WITH THE
REQUIREMENTS FOR THE MASTERS DEGREE IN TECHNOLOGY
TO THE DEPARTMENT OF MECHANICAL ENGINEERING AT
THE DURBAN UNIVERSITY OF TECHNOLOGY

APPROVED FOR FINAL SUBMISSION

PROFESSOR MARK WALKER
DATE
SUPERVISOR

DURBAN, SOUTH AFRICA
MAY 2006

Declaration

I declare that this thesis is my own unaided work except where due acknowledgment is made to others. This thesis is being submitted for the Masters Degree in Technology to the Department of Mechanical Engineering at the Durban University of Technology, and has not been submitted previously for any other degree or examination.

Ryan Jason Hamilton Date

Acknowledgement

I would like to thank Professor Mark Walker for giving me the opportunity to study towards my masters of technology degree. I would also like to thank my parents for their support throughout all of my studies and to Bianca Carroll for her assistance with the imaging and typing.

Contents

List of Figures

List of Tables

Abstract

Fibre Reinforced Plastics (FRPs) have been used in many practical structural applications due to their excellent strength and weight characteristics as well as the ability for their properties to be tailored to the requirements of a given application. Thus, designing with FRPs can be extremely challenging, particularly when the number of design variables contained in the design space is large. For example, to determine the ply orientations and the material properties optimally is typically difficult without a considered approach. Optimization of composite structures with respect to the ply angles is necessary to realize the full potential of fibre-reinforced materials. Evaluating the fitness of each candidate in the design space, and selecting the most efficient can be very time consuming and costly. Structures composed of composite materials often contain components which may be modelled as rectangular plates or cylindrical shells, for example. Modelling of components such as plates can be useful as it is a means of simplifying elements of structures, and this can save time and thus cost.

Variations in manufacturing processes and user environment may affect the quality and performance of a product. It is usually beneficial to account for such variances or tolerances in the design process, and in fact, sometimes it may be crucial, particularly when the effect is of consequence. The work conducted within this project focused on methodologies for optimally designing fibre-reinforced laminated composite structures with the effects of manufacturing tolerances included. For this study it is assumed that the probability of any tolerance value occurring within the tolerance band, compared with any other, is equal, and thus the techniques are aimed at designing for the worst-case scenario.

This thesis thus discusses four new procedures for the optimization of composite structures with the effects of manufacturing uncertainties included. Five design problems are investigated, and the first methodology is used to solve problems 1 and 2. The remaining problems are solved with the remaining methodologies. In all cases, the methodologies are flexible enough to allow any appropriate design fitness formulation and search algorithm (and, where necessary, failure criterion) to be used.

The problems are:

Problem 1 - A technique for optimally designing fibre-reinforced plates with manufacturing uncertainties for maximum buckling strength. Here, a procedure to design symmetrically lami-

nated plates for maximum buckling load with manufacturing uncertainty in the ply angle, which is the design variable, is described. Classical Lamination Theory is implemented, three different tolerance scenarios are used for the purposes of illustrating the methodology, and plates with varying aspect ratios and loading ratios are optimally designed and compared.

Problem 2 - A methodology for the optimally designing fibre-reinforced laminated structures with design variable tolerances for maximum buckling strength. In this problem, which is similar to the first, the finite element method is implemented and used to determine the fitness of each design candidate, and so the effects of bending-twisting coupling are accounted for. As before, three different tolerance scenarios are used for the purposes of illustrating the methodology, and, by way of example, plates with varying aspect and loading ratios, as well as differing boundary conditions, are chosen to demonstrate the technique, and optimally designed and compared.

Problem 3 - A technique for optimally designing fibre-reinforced laminated plates under in-plane loads for minimum weight with manufacturing uncertainties accounted for. Here, a procedure to design symmetrically laminated plates under buckling loads for minimum weight with manufacturing uncertainty in the ply angle, which is the design variable, is described. A minimum buckling load capacity is the design constraint implemented and the effects of bending-twisting coupling are neglected in implementing the procedure. As before, three different tolerance scenarios are used for the purposes of illustrating the methodology, and plates with varying aspect ratios and loading ratios are optimally designed and compared.

Problem 4 - A methodology for optimally designing fibre-reinforced laminated plates under in-plane loads for minimum weight with manufacturing uncertainty accounted for. Here, a procedure to design symmetrically laminated plates under buckling loads for minimum weight with manufacturing uncertainty in the ply angle and plate thickness, which are the design variables, is described. A minimum buckling load capacity is the design constraint implemented. The effects of bending-twisting coupling are neglected in implementing the procedure, and the Downhill Simplex method is used as the search technique. Two different tolerance scenarios are used for the purposes of illustrating the methodology, and plates with varying aspect ratios and loading ratios are optimally designed and compared.

Problem 5 - A technique for optimally designing fibre-reinforced laminated structures for minimum weight with manufacturing uncertainties accounted for. Here, a methodology to

design symmetrically laminated structures under transverse loads for minimum weight with manufacturing uncertainty in the ply angle, is described. The ply angle and the ply thickness are the design variables, and the Tsai-Wu failure criteria is the design constraint used. The finite element method is implemented, and thus effects like bending-twisting coupling are accounted for. In order to demonstrate the procedure, laminated plates with varying aspect ratios and boundary conditions are optimally designed and compared.

Chapter 1

Literature Review

1.1 The Finite Element Method

1.1.1 Introduction

The most distinctive feature of the finite element method that separates it from others is the division of a given domain into a set of simple subdomains, called finite elements [1]. Any geometric shape that allows computation of the solution or its approximation, or provides necessary relations among the values of the solution at selected points, called nodes, of the subdomain, qualifies as a finite element. The number of elements is determined by two factors: The capabilities of the processor being used, and the desired accuracy of the results [2].

The elements that compose the object are of finite size and hence the name of the method (FEM). The smaller the size, the smaller the errors, and as a result, the solution obtained approaches the true solution. In essence, the finite element method translates a complex design problem into a system of linear algebraic equations.

Today, the finite element method is indispensable in aircraft, automotive, and other industries.

Compatibility

Although the basic approach of separating a body into finite elements has been explained, the continuity of the body's response must not be forgotten. To prove continuity, a body, being

seen as an assembly of separate elements, contains an assumed existence of forces acting on the elements through interconnecting joints. To obtain a workable solution, the following two requirements must be fulfilled:

(a) Elements joined by a particular node must have the same displacement at that node.

(b) The interface between two elements is subject to displacements that are functions of the nodes on the interface, and those nodes only.

These two requirements are called the *compatibility conditions* of the finite element model and provide the mathematical justification of the polynomial relationship, called the *shape function* [2].

1.1.2 Convergence requirements

As the finite element method is a numerical technique, a sequence of approximate solutions is obtained as the element size is successively reduced [3]. This sequence will converge to the exact solution if the interpolation polynomial satisfies the following convergence requirements:

(1) The field variable must be continuous within the elements. This requirement is easily satisfied if continuous functions are chosen as interpolation models. Since polynomials are inherently continuous, they easily satisfy this requirement.

(2) All uniform states of the field variable ϕ and its partial derivatives up to the highest order appearing in the functional $I(\phi)$ should have representation in $\phi^{(e)}$ when, in the limit, the element size reduces to zero.

(3) At element interfaces (boundaries) the field variable ϕ and any of its partial derivatives up to one order less than the highest order derivative appearing in $I(\phi)$ must be continuous.

The elements whose interpolation polynomials satisfy the requirements (1) and (3) are called *compatible* or *conforming* elements and those satisfying condition (2) are called *complete* elements. If the r^{th} derivative of the field variable ϕ is continuous, then ϕ is said to have C^r continuity. In terms of this notation, the completeness requirement implies that ϕ must have C^r continuity within an element, while the compatibility requirement implies that ϕ must have C^{r-1} continuity at element interfaces.

In the case of general solid and structural mechanics problems, this requirement implies that the element must deform without causing openings, overlaps or discontinuities between

adjacent elements. In the case of beam, plate and shell elements, the first derivatives of the displacement across inter-element boundaries must also be continuous.

If the interpolation polynomial satisfies all three requirements, the approximate solution converges to the correct solution when the mesh is refined and an increasing number of smaller elements are used. In order to prove the convergence mathematically, the mesh refinement has to be made in a regular fashion so as to satisfy the following conditions [4]:

(1) The elements must be made smaller in such a way that every point of the solution region can always be within an element;

(2) All previous (coarse) meshes must be contained in the refined meshes and

(3) The form of the interpolation polynomial must remain unchanged during the process of mesh refinement.

These three conditions are illustrated in Figure 1-1, where a simple two dimensional solution domain in the form of an equilateral triangle is discretized with an increasing number of three node elements.

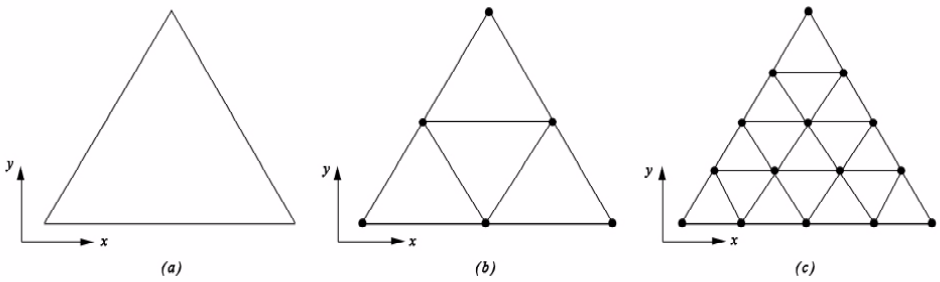

Figure 1-1: Example of successive mesh refinements: (a) Original soluton domain; (b) Discretization with 4 triangular elements; (c) Discretization with 16 triangular elements

Conditions (1) and (2) are illustrated in Figure 1-1, where a two-dimensional region is discretised with increasing number of triangular elements. From Figure 1-2, where the solution region is assumed to have a curved boundary, it can be seen that conditions (1) and (2) are not satisfied if elements with straight boundaries are used. In structural problems, interpolation polynomials satisfying all the convergence requirements always lead to the convergence of the displacement solution from below, while nonconforming elements may converge either from below or from above.

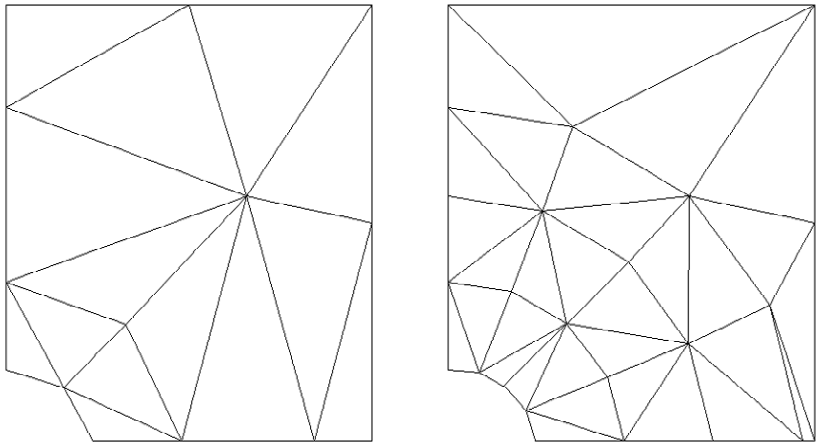

(a) Idealization I (N = 2) (b) Idealization II (N = 4)

Figure 1-2: Finite element idealization of a quarter plate with a circular hole where N is the number of subdivisions of a quarter hole.

1.1.3 Two-dimensional (quadrilateral) element

The displacement at any point within element e is a function of its location which can be seen in Figure 1-3. It can be expressed in the vector form [2]:

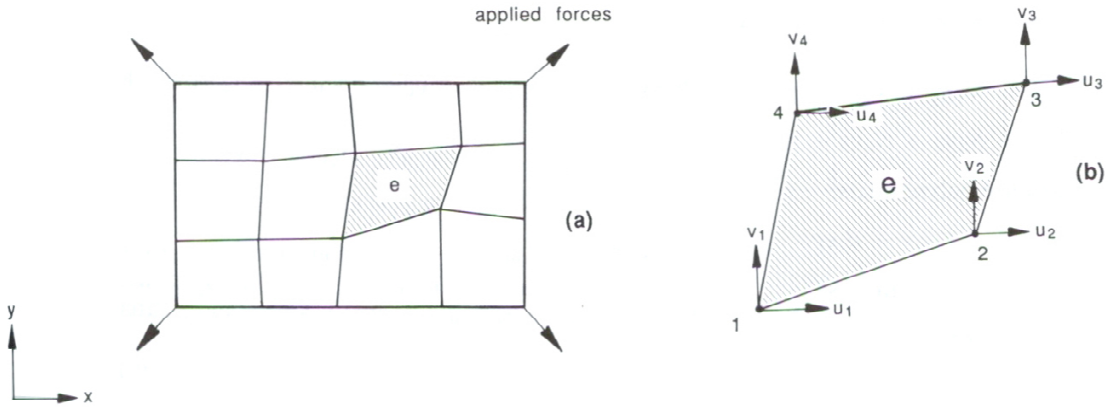

Figure 1-3: A finite element model - (a) assembly of elements (b) an enlarged element

$$\{\mathbf{a}\,(x,y)\} = \begin{Bmatrix} u(x,y) \\ v(x,y) \end{Bmatrix} \tag{1.1}$$

At the corner nodes, the displacement becomes

$$\{\mathbf{a}_i\} = \begin{Bmatrix} u_i \\ v_i \end{Bmatrix} \tag{1.2}$$

where i = 1,2,3 and 4. All four node displacements can be grouped together under one vector:

$$\{\mathbf{a}\}^e = \begin{Bmatrix} u_1 \\ v_1 \\ u_2 \\ v_2 \\ u_3 \\ v_3 \\ u_4 \\ v_4 \end{Bmatrix} \tag{1.3}$$

The components of the displacement vector, Equation 1.1, can be expressed by the polynomials

$$u(x, y) = A_u + B_u x + C_u y + D_u xy \tag{1.4}$$

$$v(x, y) = A_v + B_v x + C_v y + D_v xy \tag{1.5}$$

Equations 1.4 and 1.5, when expressed in terms of corner displacements, become

$$u(x, y) = N_1 u_1 + N_2 u_2 + N_3 u_3 + N_4 u_4 \tag{1.6}$$

$$v(x, y) = N_1 v_1 + N_2 v_2 + N_3 v_3 + N_4 v_4 \tag{1.7}$$

$N_1$to $N_4$are second-degree four-term polynomials:

$$N_i = a_i + b_i x + c_i y + d_i xy \tag{1.8}$$

Polynomial $N_1$is chosen so as to fit the conditions:

$$\begin{aligned} N_1 &= 1 \text{ at node 1,} \\ N_1 &= 0 \text{ at nodes 2, 3 and 4} \end{aligned} \tag{1.9}$$

with similar conditions for N_2 to N_4. Equations 1.6 and 1.7 can be written in vector form:

$$\begin{Bmatrix} u(x,y) \\ v(x,y) \end{Bmatrix} = \begin{bmatrix} N_1 & 0 & N_2 & 0 & N_3 & 0 & N_4 & 0 \\ 0 & N_1 & 0 & N_2 & 0 & N_3 & 0 & N_4 \end{bmatrix} \begin{Bmatrix} u_1 \\ v_1 \\ u_2 \\ v_2 \\ u_3 \\ v_3 \\ u_4 \\ v_4 \end{Bmatrix} \tag{1.10}$$

or abbreviated:

$$\{\mathbf{a}(x,y)\} = [N]\{\mathbf{a}\}^e \tag{1.11}$$

where $[N]$ is called the shape function.

To determine $[N]$, first consider a rectangular element, as shown in Figure 1-4. The coordinates of its four corner nodes are $(-b,-a),(b,-a),(b,a)$ and $(-b,a)$. Thus the shape function components are

$$\begin{aligned} N_1 &= \tfrac{1}{4ab}(b-x)(a-y) \quad N_2 = \tfrac{1}{4ab}(b+x)(a-y) \\ N_3 &= \tfrac{1}{4ab}(b+x)(a+y) \quad N_4 = \tfrac{1}{4ab}(b-x)(a+y) \end{aligned} \tag{1.12}$$

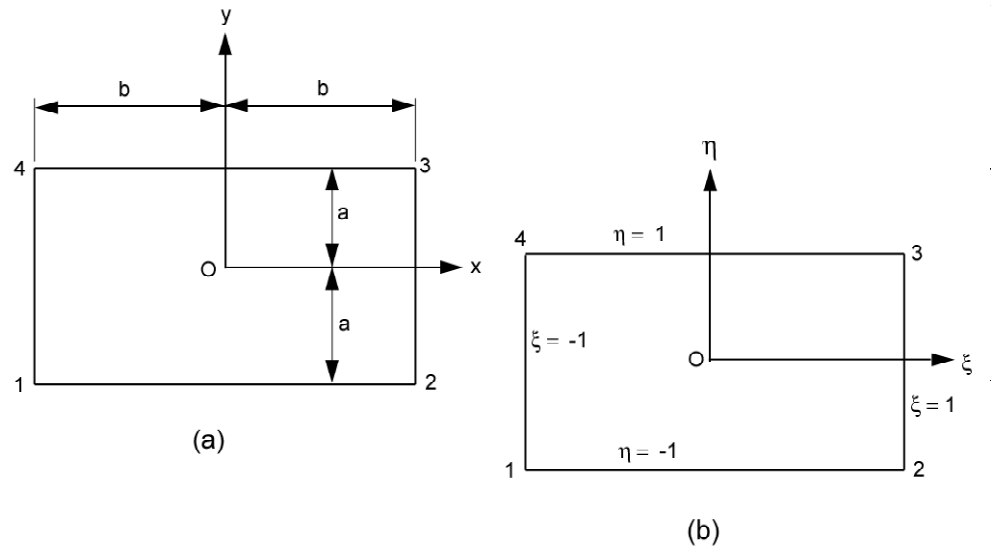

Figure 1-4: A rectangular element - (a) element in a local Cartesian coordinate system (b) element in a local natural coordinate system

The shape-function components can be expressed in a nondimensional form by introducing new coordinates:

$$\xi = \frac{x}{b} \quad \eta = \frac{y}{a} \tag{1.13}$$

Then Equation 1.12 becomes

$$\begin{aligned} N_1 &= \tfrac{1}{4}(1-\xi)(1-\eta) \quad N_2 = \tfrac{1}{4}(1+\xi)(1-\eta) \\ N_3 &= \tfrac{1}{4}(1+\xi)(1+\eta) \quad N_4 = \tfrac{1}{4}(1-\xi)(1+\eta) \end{aligned} \tag{1.14}$$

The $\xi\eta$ coordinates form a natural local coordinate system as shown in Figure 1-5.

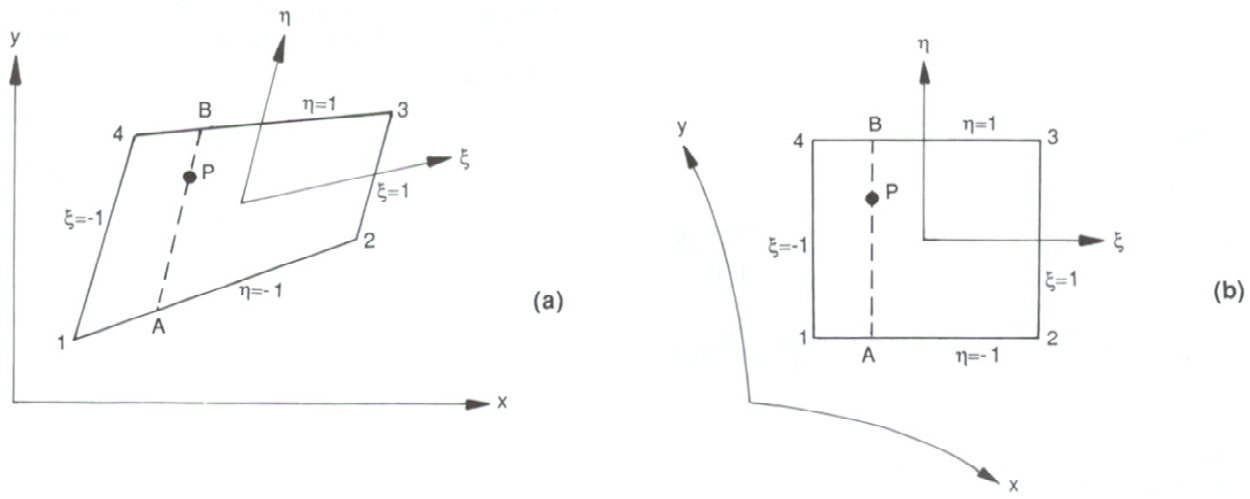

Figure 1-5: A general quadrilateral element - (a) element in a global Cartesian coordinate system (b) element in a local natural coordinate system

The natural coordinate system can be applied as well to general quadrilaterals, with the shape-function expressions remaining the same. Consider the general quadrilateral shown in Figure 1-5(a). It is located in a global xy coordinate system. A natural $\xi\eta$ coordinate system is introduced by assuming the following relations along the quadrilateral sides

$\eta = -1$ along side 12

$\xi = +1$ along side 23

$\eta = +1$ along side 34

$\xi = -1$ along side 41

The origin of the $\xi\eta$ system lies in the middle of the element. The two coordinates are directed toward the middle of the right side and the upper side, respectively, as shown in Figure 1-5(a). Consider point $P(\xi, \eta)$; $A(\xi, -1)$and $B(\xi, +1)$ are its projections on sides 12 and 34, respectively. Concerning coordinate x_p, the following geometrical relation applies:

$$\frac{x_P - x_A}{x_B - x_A} = \frac{1+\eta}{2} \tag{1.15}$$

From this relation, we obtain

$$\begin{aligned} x_P &= N_1 x_1 + N_2 x_2 + N_3 x_3 + N_4 x_4 \\ y_P &= N_1 y_1 + N_2 y_2 + N_3 y_3 + N_4 y_4 \end{aligned} \tag{1.16}$$

This leads to the expression for the transformation from the $\xi\eta$ to the xy coordinate system:

$$\left\{ \begin{array}{c} x \\ y \end{array} \right\} = \left[\begin{array}{cccccccc} N_1 & 0 & N_2 & 0 & N_3 & 0 & N_4 & 0 \\ 0 & N_1 & 0 & N_2 & 0 & N_3 & 0 & N_4 \end{array} \right] \left\{ \begin{array}{c} x_1 \\ y_1 \\ x_2 \\ y_2 \\ x_3 \\ y_3 \\ x_4 \\ y_4 \end{array} \right\} \tag{1.17}$$

The relation between N_i derivatives in the two systems is expressed by

$$\left\{ \begin{array}{c} \frac{\partial N_i}{\partial \xi} \\ \frac{\partial N_i}{\partial \eta} \end{array} \right\} = \left[\begin{array}{cc} \partial x/\partial \xi & \partial y/\partial \xi \\ \partial x/\partial \eta & \partial y/\partial \eta \end{array} \right] \left\{ \begin{array}{c} \partial N_i/\partial x \\ \partial N_i/\partial y \end{array} \right\} \tag{1.18}$$

The first right-hand matrix is the Jacobian:

$$[\jmath] = \left[\begin{array}{cc} \partial x/\partial \xi & \partial y/\partial \xi \\ \partial x/\partial \eta & \partial y/\partial \eta \end{array} \right] = \left\{ \begin{array}{c} \partial/\partial \xi \\ \partial/\partial \eta \end{array} \right\} \left[\begin{array}{cc} x & y \end{array} \right] \tag{1.19}$$

$$= \frac{1}{4} \left[\begin{array}{cccc} -(1-\eta) & (1-\eta) & (1+\eta) & -(1+\eta) \\ -(1-\xi) & (1-\xi) & (1+\xi) & -(1+\xi) \end{array} \right]$$

1.1.4 Finite elements for plates

A plate is a thin solid that may be modelled using 3D elements as shown in Figure 1-6(a) [5]. But a solid element has unnecessary degrees of freedom, as it computes transverse normal

stress and transverse shear stresses, all of which are considered negligible in a thin plate. Also, thin 3D elements create problems produced by ill-conditioning because stiffness associated with thickness-direction ε_z is very much larger than other stiffnesses. The plate element shown in Figure 1-6(b) has half as many degrees of freedom as the comparable solid element and omits ε_z from its formulation. In Figure 1-6(b), the thickness t may appear to be zero, but the physically correct value is used in formulating element stiffness matrices.

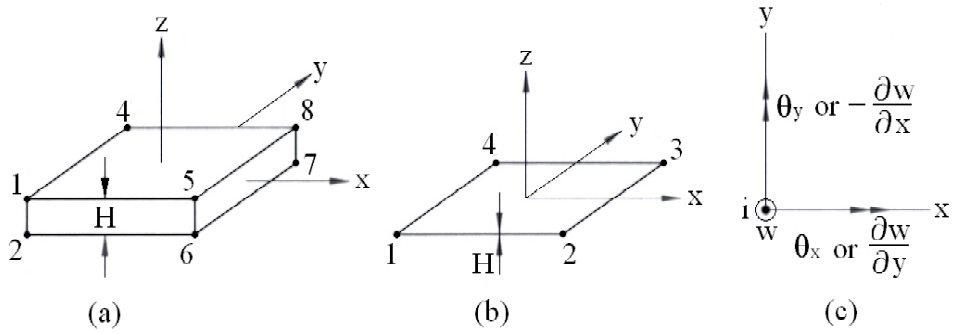

Figure 1-6: (a) A 3D solid element. (b) The comparble plate element. (c) Plate d.o.f. at a typical node i, viewed normal to the xy plane

A *plane* element must be able to display states of constant σ_x, σ_y and τ_{xy} if it is to pass patch tests. A plate element must be able to display these states in each $z = constant$ layer, which means that a valid plate element must pass patch tests for states of constant M_x, M_y, and M_{xy}. Figure 1-7 depicts a patch test for constant M_x, which requires constant $\partial\theta_y/\partial x$ in Mindlin theory (see below) if the test is to be passed. If $v \neq 0$, rotations about the x axis must be prevented at nodes 1, 3, 4, 6, and 7 as shown in Figure 1-7.

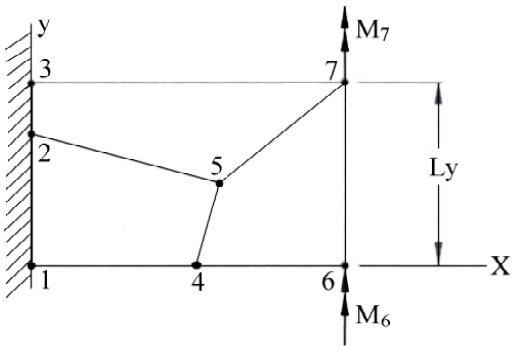

Figure 1-7: A patch test for constant curvature (or for constant M_x). Nodal moment loads are $M_6 = M_7 = M_x L_y/2$.

Mindlin plate theory To account for transverse shear deformation, the assumption that right angles in a cross-section are preserved must be abandoned [6]. This means that planes initially normal to the mid-surface may experience rotations different from rotations of the mid-surface itself. Thus the differential element in Figure 1-8 has the deformations depicted in Figure 1-9, where θ_x and θ_y are rotation components of a line initially normal to the mid-surface.

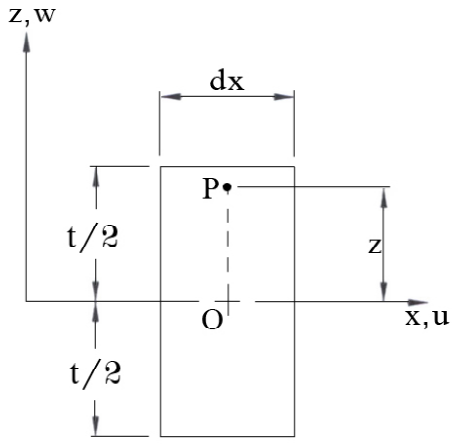

Figure 1-8: Differential slice of a plate of thickness t before loading

Combining these displacements with Equations 1.20

$$\varepsilon_x = \frac{\partial u}{\partial x} \qquad \varepsilon_y = \frac{\partial v}{\partial y} \qquad \gamma_{xy} = \frac{\partial u}{\partial y} + \frac{\partial v}{\partial x} \tag{1.20}$$

Equations 1.21 are obtained

$$\begin{array}{llll} u = z\theta_y & \varepsilon_x = z\frac{\partial \theta_y}{\partial x} & \gamma_{xy} = z\left(\frac{\partial \theta_y}{\partial y} - \frac{\partial \theta_x}{\partial x}\right) \\ v = -z\theta_x & \varepsilon_y = -z\frac{\partial \theta_x}{\partial y} & \gamma_{yz} = \frac{\partial w}{\partial y} - \theta_x \\ & & \gamma_{zx} = \frac{\partial w}{\partial x} + \theta_y \end{array} \tag{1.21}$$

instead of Equations 1.22.

$$\varepsilon_x = -z\frac{\partial^2 w}{\partial x^2} \qquad \varepsilon_y = -z\frac{\partial^2 w}{\partial y^2} \qquad \gamma_{xy} = -2z\frac{\partial^2 w}{\partial x \partial y} \tag{1.22}$$

Equations 1.21 are the main equations of Mindlin Plate Theory. If $\theta_x = \partial w/\partial y$ and $\theta_y = -\partial w/\partial x$, transverse shear deformation vanishes and Equations 1.21 reduce to Equations 1.22.

Loads and supports Loads in the z-direction, either distributed or concentrated, may be applied to lateral surfaces $z = \pm t/2$ or to edges of a plate. Such loads are called *lateral* loads.

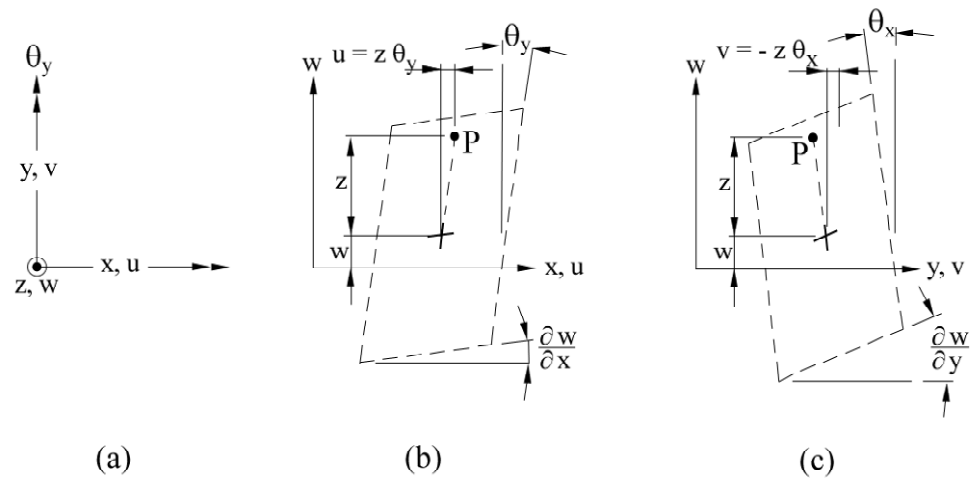

Figure 1-9: (a) Displacements and positive directions for rotations θ_x and θ_y viewed normal to the xy plane. (b)Mindlin theory displacements in an xz-parallel cross-section. (c) Mindlin theory displacemment in a yz-parallel cross-section.

Distributed load has dimensions [force/length^2] on a lateral surface or [force/length] on an edge. A plate edge may also be loaded by a bending moment whose vector is tangent to the edge. The same kinds of edge loads may be applied to the plate by supports.

At the point where a concentrated lateral (z-direction) force is applied, Mindlin theory predicts infinite bending moments and infinite displacement. In reality no force can be truly concentrated, and in plate theory the infinities disappear if the *concentrated* load is applied over a small area instead [6].

Mindlin plate elements A Mindlin element is based on three fields [5]: $w = w(x, y)$, $\theta_x = \theta_x(x, y)$, and $\theta_y = \theta_y(x, y)$. Each is interpolated from nodal values. If all interpolations use the same polynomial, then for an element of n nodes,

$$\left\{ \begin{array}{c} w \\ \theta_x \\ \theta_y \end{array} \right\} = \sum_{i=1}^{n} \left[\begin{array}{ccc} N_i & 0 & 0 \\ 0 & N_i & 0 \\ 0 & 0 & N_i \end{array} \right] \left\{ \begin{array}{c} w_i \\ \theta_{xi} \\ \theta_{yi} \end{array} \right\} = \mathbf{Nd} \tag{1.23}$$

From Equations 1.21 and 1.23 a strain-displacement matrix $\boldsymbol{\beta}$ can be formed. In the stiffness matrix formula,

$$k = \int \boldsymbol{\beta}^T \mathbf{E} \boldsymbol{\beta} dv \tag{1.24}$$

where $\mathbf{E}$ is a 5 by 5 matrix that includes the 3 by 3 $\mathbf{E}$ of plane stress and also shear moduli associated with the two transverse shear strains. Integration of $\boldsymbol{\beta}^T \mathbf{E} \boldsymbol{\beta}$ with respect to z is done explicitly. Integration in the plane of the element is done numerically if the element is isoparametric.

The N_i are given by Equation 1.14 for a four-node quadrilateral element. In any $z =$ constant layer, strains vary in the same way as in the corresponding plane element provided that all terms of the integrand are integrated by the same quadratic rule. This is not usually done, for reasons discussed below.

Consider the bending mode shown in Figure 1-10. Element strains ε_x are independent of x, therefore, any order of quadrature will report the same strain energy for pure bending. However, this element displays spurious shear strain. If a/t is large, transverse shear strain γ_{zx} becomes large and the element is too stiff in bending, unless γ_{zx} is evaluated at $x = 0$, where γ_{zx} vanishes. But one-point quadrature for all strains would introduce four instability modes. This observation suggests "selective" integration, in which one-point quadrature is applied to bending terms. Then two instability modes remain. They may be controlled by "stabilization" matrices. Calculated stresses are usually most accurate at Gauss points.

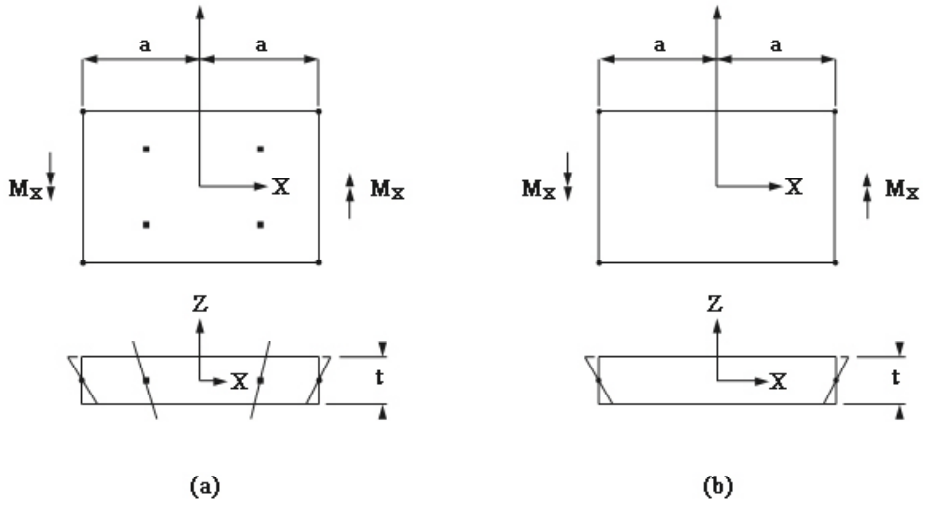

Figure 1-10: A bending deformation in a four-node Mindlin plate element. (a) Four-point intergration rule. (b) One-point intergration rule.

1.2 Composite materials

Composites are produced when two or more materials are joined to give a combination of properties that cannot be attained in the original materials. Composite materials may be selected to give unusual combinations of stiffness, strength, weight, high-temperature performance, corrosion resistance, hardness, or conductivity.

Composites can be placed into three categories based on their shapes of the materials; particulate, fibre, and laminar. Concrete, a mixture of cement and gravel, is a particulate composite; fibreglass, containing glass fibres embedded in a polymer, is a fibre-reinforced composite; and plywood, having alternate layers of wood veneer, is a laminar composite. If the reinforcing particles are uniformly distributed, particulate composites have isotropic properties; fibre composites may be either isotropic or anisotropic; laminar composites always display anisotropic behavior.

1.2.1 Fibre reinforced composites (FRCs)

A fibre reinforced composite is a material which is reinforced with high-strength synthetic fibrous material such as ceramic, metal, or polymeric material in a softer, more ductile matrix [7]. The matrix material transmits the force to the fibres, which carry most of the applied force.

Many types of reinforcing materials are employed. Straw has been used to strengthen mud bricks for centuries. Steel reinforcing bars are introduced into concrete structures. Glass fibres in a polymer matrix produce fibreglass for transportation and aerospace applications. Fibres made of boron, carbon, polymers, and ceramics provide exceptional reinforcement in advanced composites based on matrices of polymers, metals, ceramics, and even intermetallic compounds.

The rule of mixtures for fibre-reinforced composites

As for particulate composites, the rule of mixtures always predicts the density of fibre-reinforced composites [7]:

$$\rho_c = f_m \rho_m + f_f \rho_f \tag{1.25}$$

where $f_m = 1 - f_f$ and m and f refer to the matrix and fibre.

In addition, the rule of mixtures accurately predicts the electrical and thermal conductivity of fibre-reinforced composites along the fibre direction if the fibres are continuous and unidirectional:

$$K_c = f_m K_m + f_f K_f \tag{1.26}$$

$$\sigma_c = f_m \sigma_m + f_f \sigma_f \tag{1.27}$$

where K is the thermal conductivity and σ is the electrical conductivity..

In a composite with a metal matrix and ceramic fibres, the bulk of the energy would be transmitted through the fibres. When the fibres are not continuous or unidirectional, the simple rule of mixtures may not apply. For example, in a metal fibre-polymer matrix composite, electrical conductivity would be low and would depend on the length of the fibres, and how often the fibres touch each other.

Modulus of Elasticity

The rule of mixtures is used is used to predict the modulus of elasticity when the fibres are continuous and unidirectional. Parallel to the fibres, the modulus of elasticity may be as high as:

$$E_c = f_m E_m + f_f E_f \tag{1.28}$$

However, when the applied stress is very large, the matrix begins to deform and the stress strain curve is no longer linear. Since the matrix now contributes little to the stiffness of the composite, the modulus can be approximated by:

$$E_c = f_f E_f \tag{1.29}$$

When the load is applied perpendicular to the fibres, each component of the composite acts independently of each other. The modulus of the composite is now:

$$\frac{1}{E} = \frac{f_m}{E_m} + \frac{f_f}{E_f} \tag{1.30}$$

Again, if the fibres are not continuous and unidirectional, the rule of mixtures does not apply.

1.2.2 Fibre-reinforced plastic composite materials (FRPs)

A fibre reinforced plastic is a polymer matrix composite composed primarily of plastic and in which fibrous (graphite, glass, aramid) reinforcements are imbedded with strength properties superior to those of the base resin. Two of the most important matrix plastic resins for fibre-reinforced plastics are unsaturated polyester and epoxy resins. The polyester resins are lower in costs but are usually not as strong as the epoxy resins. Unsaturated polyesters are widely used for matrices of fibre-reinforced plastics. Applications for these materials include boat hulls, building panels, and structural panels for automobiles, aircraft, and appliances. Epoxy resins cost more but have special advantages such as good strength properties and lower shrinkage after curing than polyester resins. Epoxy resins are commonly used as matrix materials for carbon and aramid-fibre composites.

Glass fibres for reinforced plastics

Glass fibres are used to reinforce plastic matrices to form structural composites and moulding compounds. Glass-fibre plastic composite materials have the following favourable characteristics: high strength-to-weight ratio; good dimensional stability; good resistance to heat, cold, moisture, and corrosion; good electrical insulation properties; ease of fabrication; and relatively low cost.

The two most important types of glass used to produce glass fibres for composites are E (electrical) and S (high strength) glasses.

E glass is the most commonly used glass for continuous fibres while S glass has a higher strength to weight ratio and is more expensive than E glass and is used primarily for military and aerospace applications.

Glass fibres are produced by drawing monofilaments of glass from a furnace containing

molten glass and gathering a large number of these filaments to form a strand of glass fibres. The strands are then used to make glass fibre rovings that consist of a collection of bundles of continuous filaments. The rovings may be in continuous strands or woven to make woven roving. Glass fibre reinforced mats are made of continuous strands or chopped strands. The strands are usually held together with a resinous binder.

Carbon fibres for reinforced plastics

Composite materials made by using carbon fibres for reinforcing plastic resin matrices such as epoxy are characterized by having a combination of light weight, very high strength and high stiffness [8]. These properties make the use of carbon fibre plastic composite materials useful for aerospace applications. In general, carbon fibres are produced from polyacrylonitrile (PAN) precursor fibres by three processing stages: (1) stabilization, (2) carbonization and (3) graphitization.

Stabilization, the PAN fibres are first stretched to align each fibre parallel to the fibre axis and then they are oxidized in air at about 200 to 220^oC while held in tension.

Carbonization, the stabilized PAN-based fibres are heated until they become transformed into carbon fibres by the elimination of O, H and N from the precursor fibre. During the carbonization process, ribbons are formed within each fibre that greatly increase the tensile strength of the material.

Graphitization is used if an increase in the modulus of elasticity is desired at the expense of high tensile strength. During graphitization the preferred orientation of the crystallites within each fibre is increased.

Aramid fibres for reinforced plastics

Aramid fibre is the generic name for aromatic fibres. Aramid fibres were introduced under the trade name of Kevlar and at present there are two commercial types. Kevlar 29 and 49. Kevlar 29 is a low density, high strength aramid fibre designed for applications such as bullet proof vests, ropes and cables. Kevlar 49 is a low density and high strength and modulus used as reinforcements in composites for aerospace, marine and automotive applications.

Kevlar aramid is used for high-performance composite applications where light weight, high

strength and stiffness, damage resistance to fatigue and stress rupture are important.

The tensile properties and density of E-glass, carbon and aramid fibres are compared in Table 1.1. It is noted that glass fibres have a lower tensile strength and modulus than carbon and aramid fibres but higher elongation. The density of glass fibres is also higher than carbon and aramid fibres. However, because of their low cost and versatility, glass fibres are by far the most commonly used reinforcing fibres for plastics.

Property	Glass (E)	Carbon (HT)	Aramid (Kevlar 49)
Tensile strength (MPa)	3100	3450	3600
Tensile modulus (GPa)	76	228	131
Elongation at break (%)	4.5	1.6	2.8
Density (g/cm^3)	2.54	1.8	1.44

Table 1.1: Comparative properties of fibre reinforcements for plastics

1.2.3 Laminated fibre reinforced plastics and their properties

Material orthotropy Laminate properties (i.e. strength, stiffness, thermal, etc.) depend on the form of the reinforcement. The directional nature of the fibres introduce directional dependence to most of the properties. Materials whose properties are independent of direction are called *isotropic* materials. Conversely, those materials with different properties in different directions are called *anisotropic*. A special case of anisotropy is the existence of two mutually perpendicular planes of symmetry in the material properties. Such materials are referred to as *orthotropic*. Continuous fibre composites are orthotropic in nature and their properties are defined in the plane of the layer in two directions; the direction along the fibres and the direction perpendicular to the fibre orientation.

Stiffness is an example of an orthotropic material property of unidirectional fibre-reinforced laminates. Both the matrix and fibres are generally isotropic. However, when combined, the properties become anisotropic. Consider a fibre-reinforced material shown in Figure 1-11, loaded along either the fibre direction, x_1, or transverse to the fibre direction, x_2.

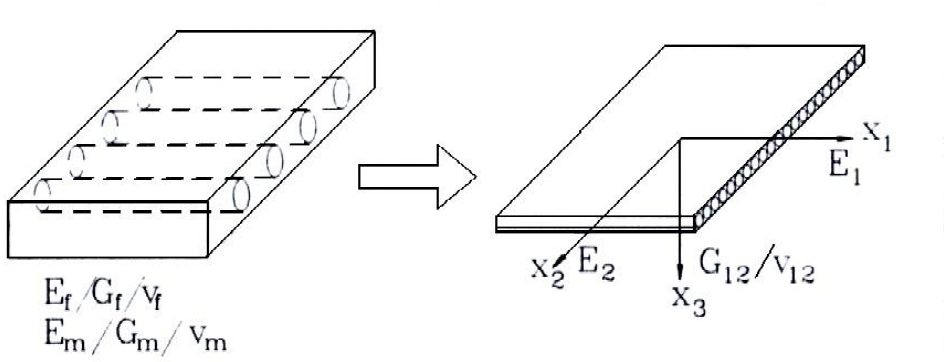

Figure 1-11: Elastic properties of a unidirectional fibre-reinforced composite layer

When the material is loaded along the fibre direction, the deformation is small and the tensile strength is high as shown in Figure 1-12. This figure shows that as the fibre orientation varies from 0^o to 90^o, the maximum tensile strength of the material decreases. Since the amount of deformation under a specified load reflects the stiffness of a material, the unidirectional composite has different stiffness properties along these two mutually perpendicular directions. The stiffness of the laminate in the fibre direction is much closer to that of the fibre stiffness, E_f, and the stiffness perpendicular to the fibre direction is governed mostly by the properties of the matrix, E_m, G_m, and ν_m. Directions that are along the fibre and perpendicular to the fibre directions are commonly referred to as the principal material directions or principal axes of the material.

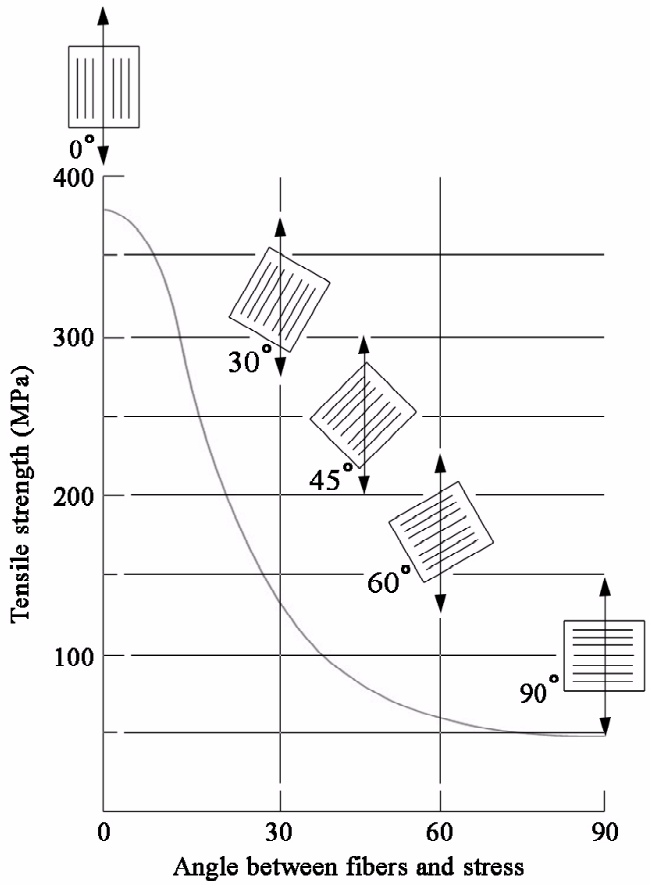

Figure 1-12: Effect of fibre orientation on the tensile strength of E-glass fibre reinforced epoxy composites

Four elastic stiffness properties, commonly referred to as the engineering constants, describe the mechanical properties of an orthotropic layer in its plane. These are two Young's moduli, E_1 and E_2, along the fibre and transverse to the fibre directions, respectively, and the shear modulus G_{12} and Poisson's ratio ν_{12} in the plane of the layer. These properties are related to the amount of fibre present in the composite layer. A quantity, V_f, referred to as the *fibre volume fraction*, is commonly used to measure the amount of fibre in a composite material. Typical stiffness properties of various unidirectional composite materials are given in Table 1.2, along with the fibre volume fraction. The properties are for cured laminates made up of T300/5208 Graphite/Epoxy.

Material	P_i	ρ (kg/m^3)	E_1 (GPa)	E_2 (GPa)	G_{12} (GPa)	ν	V_f
T300/5208	5	1600	181	10.34	7.17	0.28	0.70

Table 1.2: Properties of T300/520

Laminate definition

The laminae discussed thus far are described according to a standard notation called the *stacking sequence* [9], which lists fibre orientations as being measured from the laminate reference axis. If the orientation is counterclockwise from the reference direction, it is considered positive. The standard stacking sequence lists orientations of the different layers, starting from the top of the laminate to the bottom. A laminate with N layers is represented as $[\theta_1/\theta_2/.../\theta_N]$ and is *symmetric* when the fibre orientations of the bottom half of the laminate are mirror images of the fibre orientations above the midplane of the laminate; for example, $[-45/30/0/45/45/0/30/-45]$. Symmetric laminates with an even number of layers are represented by the portion of the stacking sequence above the laminate midplane followed by the subscript 's' after the closing bracket, $[-45/30/0/45]_s$. If the layers within the brackets are repeated, the number of repetitions can also be placed after the bracket before the subscript 's'. That is the laminate $[45/0/45/0/0/45/0/45]$ can be represented as $[45/0]_{2s}$. A laminate is said to be *anti-symmetric* if the magnitude of the ply orientation angle below the laminate midplane is a mirror image of the ply orientations above the midplane with the signs reversed. For example, $[45/-45/45/-45]$ is an anti-symmetric laminate. It can be desirable to place a negative θ orientation for every positive θ orientation. These laminates are called *balanced laminates*. Pairs of positive and negative orientations do not have to be placed adjacent to one another.

Several unique cases of laminate stacking sequence definitions can also be used. Laminates that have alternating orientations of 0^o and 90^o plies are known as *cross-ply laminates*. Examples of cross-ply laminates include $[0/90]$, $[0/90]_s$, and $[0_3/90]_s$. Laminates consisting of an equal number of equal-thickness layers at $+\theta$ and $-\theta$ fibre orientations are known as *angle-ply laminates*. For example, a 30^o symmetric angle-ply laminate could be $[30/-30/30/-30]_s$. All the layers of an angle-ply laminate have the same fibre orientation angle, say $\theta = \alpha$, with

an alternating sign. A very important and common class of laminates is called *quasi-isotropic* because the in-plane effective elastic response of this class of laminates is isotropic. All symmetric laminates with $2N$ equal-thickness layers ($N \geq 3$) and N equal angles between fibre orientations shown in Figure 1-13, are quasi-isotropic. For N equal angles of $\Delta\theta$ between fibre orientations:

$$\Delta\theta = \frac{\pi}{N} \tag{1.31}$$

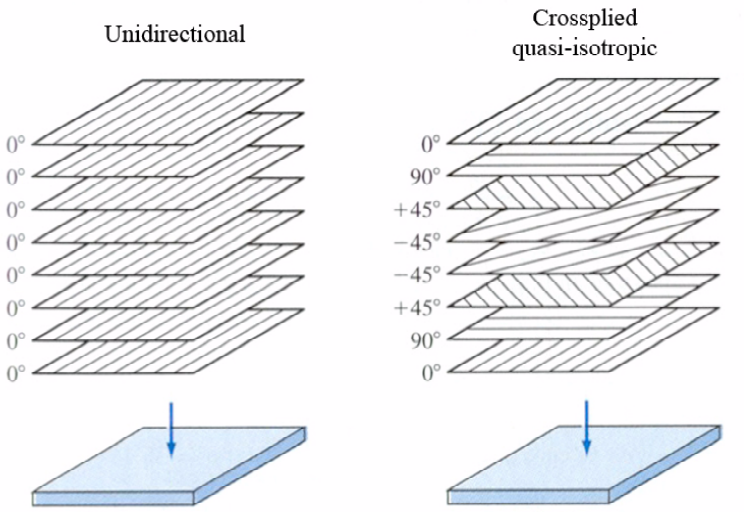

Figure 1-13: An example of a quasi-isotropic laminate with angles $\Delta\theta$ fibres of 0^o, 45^o ($\pi/4$), 90^o ($\pi/2$), etc.

Mechanics of FRP laminates

To design a structure that will meet the requirements of certain response quantities such as displacements, stresses or buckling loads, the response for a specific loading must be determined. Elastic properties form the relation between stresses and strains and are the fundamental quantities that govern the material response. Quantities such as deformations, stresses and buckling loads depend on elastic properties such as the elastic modulus, shear modulus and Poisson's ratio. In designing structures made up of monolithic materials these properties are normally given and are not included among the set of parameters that the designer varies in order to improve the performance of the structure. For composite materials, part of the effort is to

design the elastic properties of the laminate.

Thin structures made from thin layers of material can carry loads through two different types of mechanisms. The first involves stretching or compressing the layers in their own plane and is referred to as *membrane action*. The second mechanism involves bending of the layers.

Orthotropic layers

The effective properties of a unidirectional fibrous composite with the fibres orientated off-axis can be modeled as a homogeneous anisotropic material [10]. As indicated in Figure 1-14, two Cartesian coordinate systems are identified: the $x_1 - x_2 - x_3$ system and the $x - y - z$ system. The x_1 direction is the fibre direction, with x_2 and x_3 directions perpendicular to the fibre direction. The $x - y - z$ coordinates are obtained by a rotation about the x_3 axis. The material exhibits symmetry with respect to the $x - y$ or $y - z$ plane. Such layers are referred to as orthotropic and the $x_1$and x_2 axes are the principle axes of orthotropy. When the principal axes of orthotropy are oriented at an angle, θ, with respect to the axes of the laminate (an off-axis layer), the laminar behavior will appear to have the characteristics of an anisotropic material.

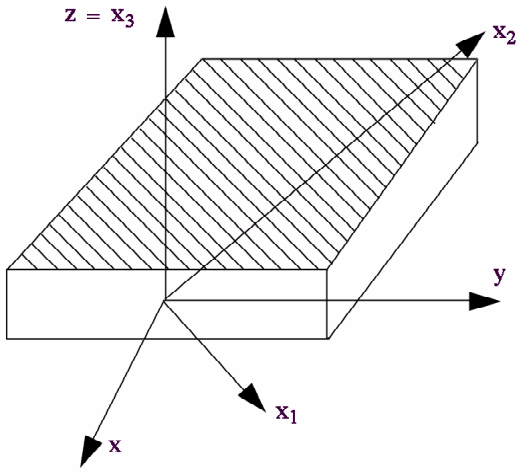

Figure 1-14: Plains of material symmetry for an orthotropic layer

For a material such as a unidirectional laminate the conditions of transverse anisotropy apply. The stress/ strain relationship can be written as:

$$\varepsilon_i = S_{ij}\sigma_j \tag{1.32}$$

where ε_i and σ_j are components of stress and strain and the stiffness matrix S_{ij} is given by:

$$S_{ij} = \begin{bmatrix} 1/E_1 & -\nu_{12}/E_1 & 0 \\ -\nu_{12}/E_1 & 1/E_2 & 0 \\ 0 & 0 & 1/G_{12} \end{bmatrix} \tag{1.33}$$

Equation 1.32 shows the constitutive relationship for a unidirectional laminate in plane stress and indicates how the terms in the compliance matrix can be related to engineering constants. This equation can be inverted to obtain the stress/strain relationships:

$$\begin{Bmatrix} \sigma_1 \\ \sigma_2 \\ \tau_{12} \end{Bmatrix} = \begin{bmatrix} Q_{11} & Q_{12} & 0 \\ Q_{21} & Q_{22} & 0 \\ 0 & 0 & Q_{66} \end{bmatrix} \begin{Bmatrix} \varepsilon_1 \\ \varepsilon_2 \\ \gamma_{12} \end{Bmatrix} \tag{1.34}$$

where the terms of Q_{ij} are:

$$\begin{aligned} Q_{11} &= \frac{E_1}{1-\nu_{12}\nu_{21}}, \quad Q_{22} = \frac{E_2}{1-\nu_{12}\nu_{21}} \\ Q_{12} &= \frac{\nu_{12}E_2}{1-\nu_{12}\nu_{21}} = \frac{\nu_{21}E_1}{1-\nu_{12}\nu_{21}} \\ Q_{66} &= G_{12} \end{aligned} \tag{1.35}$$

and the Poisson's ratios are:

$$\frac{\nu_{21}}{E_2} = \frac{\nu_{12}}{E_1} \tag{1.36}$$

To determine lamina properties with respect to other coordinate axes, the stiffness matrix must be transformed. For rotation by angle θ to axes x, y, it can be shown that

$$\begin{bmatrix} \sigma_x \\ \sigma_y \\ \tau_{xy} \end{bmatrix} = \left[\overline{Q}\right] \begin{bmatrix} \varepsilon_x \\ \varepsilon_y \\ \gamma_{xy} \end{bmatrix} \tag{1.37}$$

The transformed stiffnesses matrix is $\overline{Q}$, the elements of which are

$$\begin{aligned}
\overline{Q}_{11} &= Q_{11}m^4 + 2(Q_{12} + 2Q_{66})n^2m^2 + Q_{22}n^4 \\
\overline{Q}_{12} &= (Q_{11} + Q_{22} - 4Q_{66})m^2n^2 + Q_{12}(n^4 + m^4) \\
\overline{Q}_{22} &= Q_{11}n^4 + 2(Q_{12} + 2Q_{66})n^2m^2 + Q_{22}m^4 \\
\overline{Q}_{16} &= (Q_{11} - Q_{12} - 2Q_{66})nm^3 + (Q_{12} - Q_{22} + 2Q_{66})n^3m \\
\overline{Q}_{26} &= (Q_{11} - Q_{12} - 2Q_{66})n^3m + (Q_{12} - Q_{22} + 2Q_{66})nm^3 \\
\overline{Q}_{66} &= (Q_{11} + Q_{22} - 2Q_{12} - 2Q_{66})n^2m^2 + Q_{66}(n^4 + m^4)
\end{aligned} \tag{1.38}$$

where $m = \cos\theta$ and $n = \sin\theta$

These equations can be put into a simpler form by using trigonometric identities to replace the terms with powers of sines and cosines of the fibre orientation angle θ with the sine and cosine of multiple angles 2θ and 4θ. Tsai and Pagano [11] defined the following material properties:

$$\begin{aligned}
U_1 &= \frac{1}{8}(3Q_{11} + 3Q_{22} + 2Q_{12} + 4Q_{66}) \\
U_2 &= \frac{1}{2}(Q_{11} - Q_{22}) \\
U_3 &= \frac{1}{8}(Q_{11} + Q_{22} - 2Q_{12} - 4Q_{66}) \\
U_4 &= \frac{1}{8}(Q_{11} + Q_{22} + 6Q_{12} - 4Q_{66}) \\
U_5 &= \frac{1}{8}(Q_{11} + Q_{22} - 2Q_{12} + 4Q_{66})
\end{aligned} \tag{1.39}$$

which yield a simpler form of the transformed reduced material stiffness matrix as

$$
\begin{aligned}
\overline{Q}_{11} &= U_1 + U_2 \cos 2\theta + U_3 \cos 4\theta \\
\overline{Q}_{12} &= U_4 - U_3 \cos 4\theta \\
\overline{Q}_{22} &= U_1 - U_2 \cos 2\theta + U_3 \cos 4\theta \\
\overline{Q}_{16} &= \frac{1}{2} U_2 \sin 2\theta + U_3 \sin 4\theta \\
\overline{Q}_{26} &= \frac{1}{2} U_2 \sin 2\theta - U_3 \sin 4\theta \\
\overline{Q}_{66} &= U_5 - U_3 \cos 4\theta
\end{aligned}
\tag{1.40}
$$

Both the U's and the Q's are independent of the ply orientation, but the $\overline{Q}$'s are dependent on ply orientation for orthotropic materials. An advantage of the form of the reduced stiffnesses in Equation 1.40 is the constant parts of $\overline{Q}_{11}$, $\overline{Q}_{12}$, $\overline{Q}_{22}$, and $\overline{Q}_{66}$ given in terms of the U_1, U_4, and U_5 which do not depend on the ply orientation. Based on this feature, the U's are sometimes called the *material invariants*.

Elastic properties of FRP laminates The in-plane, bending and coupling stiffness matrices are sufficient to describe the elastic response characteristics of a laminate under combined in-plane and bending loads [9]. Due to the complex couplings that exist between the different deformation modes for laminates, it is not possible to associate the stiffness properties of a laminate with quantities that are similar to the classical elastic material properties.

Unless the lamination sequence is symmetric with respect to the laminate midplane, there exists a coupling ($B \neq 0$) between in-plane and bending deformations. A more intricate coupling is due to the B_{16} and B_{26} terms. These terms may induce twisting deformations in laminates even if there is no applied twisting action. Laminates loaded by in-plane loads inducing uniform in-plane stress states will experience twisting curvatures. The B_{16} and B_{26} terms are often referred to as the *extension-twisting coupling* terms and are caused by the existence of off-axis layers that are not symmetric with respect to the laminate midplane.

When restricted to symmetric stacking sequences, vanishing of the **B** matrix eliminates coupling between the in-plane and out-of-plane responses of a laminate. In this case, the midplane strains are only related to the in-plane stress resultants and the curvatures to the

moment resultants.

For the bending stiffness matrix, the stiffness terms D_{16} and D_{26} couple the moment resultants M_x and M_y with the twisting curvature. The resulting effect is the tendency of the laminate to curl under applied uniform bending moments. Thus, the D_{16} and D_{26} terms are referred to as the *bending-twisting coupling* terms. These terms exist for all laminates that have layers with off-axis orientations. Their relative magnitude compared to the other bending stiffness terms may be made small by manipulating the stacking sequence, but unless the off-axis layers are removed from the laminate they will have a finite value.

Similarly, the existence of the A_{16} and A_{26} terms in the in-plane stiffness matrix yields a coupling behavior termed *shear-extension coupling*. The net effect of these terms on the laminate response is the induction of shearing deformation under in-plane normal stress resultants N_x and N_y. Although the primary reason for the existence of these terms is the presence of layers with off-axis fibre orientations, unlike the bending-twisting terms, these terms may be eliminated quite easily by enforcing a balanced condition of the off-axis layers. Balanced laminates have to be placed adjacent to each other, but can be at separate through-thickness locations. However, the distance between them has a direct influence on the D_{16} and D_{26} terms. Balanced laminates with adjacent layers of plus and minus θ orientations will have smaller bending-twisting terms compared to ones that have layers with the same orientations grouped together and separated from the layers with negative angles.

In cross-ply laminates the D_{16} and D_{26} terms are zero since the $\overline{Q}_{16}$ and $\overline{Q}_{26}$ terms are zero**.** The A_{16} and A_{26} terms are zero for angle ply laminates.

Laminate theories

Classical Laminate Theory Classical Laminate Theory (CLT) applies to plates that are infinitely long and wide. In other words it ignores edges. In many real situations laminates will have edges, for example a plate containing a hole or a plate of finite width [12]. At such edges the assumptions of CLT break down and the in-plane stresses (σ_x,σ_y,σ_{xy}) alone are found not to satisfy local equilibrium on the stress-free boundaries. The through thickness direct (σ_z) and shear (τ) stresses shown in Figure 1-15, can be calculated from advanced applied mechanics theories or from finite element analysis. It is found that within one plate thickness from the edge

these stresses can be sufficiently high to exceed the (low) through-thickness strengths. Both their magnitude and sense (tension or compression) are determined by the laminates sequence. Hence it is possible to minimize their effect and reduce the chance of failure, by interlaminar shear or tension, initiating at an edge.

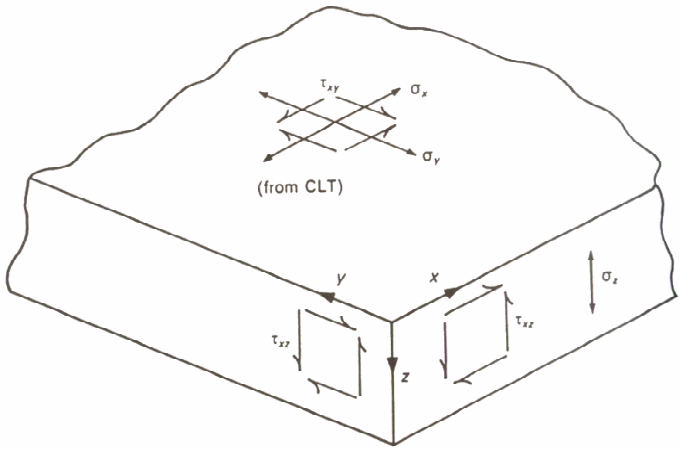

Figure 1-15: Stresses at laminate edge in the thickness (z) direction

A simple illustration of this situation is given by a cross-ply laminate when loaded in tension parallel to the 0^o plies. With a $(0/90^o)_s$ stacking sequence the through-thickness direct stress on the edges parallel to the load is tensile, whilst for a $(90/0^o)_s$ stacking sequence the stress is compressive. Clearly the former stacking sequence is preferred.

Assumptions of CLT The following assumptions are fundamental to laminate theory [10]:

1. The laminae are perfectly bonded.

2. Each layer is a homogenous material with known effective properties.

3. Individual layer properties can be isotropic, orthotropic or transversely isotropic.

4. Each layer is in a state of plane stress.

5. The laminate deforms according to the following Kirchhoff assumptions for bending and stretching of thin plates:

5a. Normals to the midplane remain straight and normal to the deformed midplane after deformation.

5b. Normals to the midplane do not change length.

Laminates of orthotropic plies CLT assumes that N orthotropic layers are perfectly bonded together with an infinitely thin bond-line and the in-plane deformations across the bond-line are continuous [9]. The mechanical behavior of laminated plates is characterized by the following relationship:

$$N^T = A\varepsilon^o + BK \tag{1.41}$$

$$M^T = B\varepsilon^o + DK \tag{1.42}$$

where $N^T = (N_x, N_y, N_{xy})$ is the vector of in-plane force resultants; $M^T = (M_x, M_y, M_{xy})$ is the vector of moment resultants; $\varepsilon^o = \left(\varepsilon^o_x, \varepsilon^o_y, \varepsilon^o_{xy}\right)$ and $K = (K_x, K_y, K_{xy})$ are the midplane strains and plate curvatures, respectively. Using CLT u, v and w being the midplane displacements in the x, y and z directions:

$$\begin{aligned} \varepsilon^o_x &= u_{,x} & K &= -w_{,xx} \\ \varepsilon^o_y &= v_{,y} & K_y &= -w_{,yy} \\ \varepsilon^o_{xy} &= u_{,y} + v_{,x} & K_{xy} &= -2w_{,xy} \end{aligned} \tag{1.43}$$

Equations 1.41 and 1.42 collectively are known as the 'plate constitutive equations', and the associated analysis as 'Classical Laminate Theory'.

The elements of the A, B and D matrices are

$$A_{ij} = \sum_{k=1}^{N} \left(\overline{Q}_{ij}\right)_{(k)} (z_k - z_{k-1}) \tag{1.44}$$

$$B_{ij} = \frac{1}{2} \sum_{k=1}^{N} \left(\overline{Q}_{ij}\right)_{(k)} \left(z_k^2 - z_{k-1}^2\right) \tag{1.45}$$

$$D_{ij} = \frac{1}{3} \sum_{k=1}^{N} \left(\overline{Q}_{ij}\right)_{(k)} \left(z_k^3 - z_{k-1}^3\right) \tag{1.46}$$

with $i = 1, 2, 6$ and $j = 1, 2, 6$ and where the $\overline{Q}^{ij}|_k$ are the elements of the reduced stiffness matrix of layer k and z_k the coordinates of the interface between ply k and ply $k+1$.

Equation 1.44 represents the *in-plane stiffness matrix*, Equation 1.45 represents the *cou-*

pling or *bending-extension stiffness matrix*, and Equation 1.46 represents the *material flexural stiffness matrix*.

Examination of the plate constitutive Equations 1.41 and 1.42 allows us to identify similar couplings for laminates, the appended for thus becomes

$$\begin{bmatrix} N_x \\ N_y \\ N_{xy} \end{bmatrix} = \begin{bmatrix} A_{11} & A_{12} & A_{13} \\ A_{21} & A_{22} & A_{23} \\ A_{31} & A_{32} & A_{33} \end{bmatrix} \begin{bmatrix} \varepsilon_x^o \\ \varepsilon_y^o \\ \varepsilon_{xy}^o \end{bmatrix} + \begin{bmatrix} B_{11} & B_{12} & B_{13} \\ B_{21} & B_{22} & B_{23} \\ B_{31} & B_{32} & B_{33} \end{bmatrix} \begin{bmatrix} K_x \\ K_y \\ K_{xy} \end{bmatrix} \tag{1.47}$$

$$\begin{bmatrix} M_x \\ M_y \\ M_{xy} \end{bmatrix} = \begin{bmatrix} B_{11} & B_{12} & B_{13} \\ B_{21} & B_{22} & B_{23} \\ B_{31} & B_{32} & B_{33} \end{bmatrix} \begin{bmatrix} \varepsilon_x^o \\ \varepsilon_y^o \\ \varepsilon_{xy}^o \end{bmatrix} + \begin{bmatrix} D_{11} & D_{12} & D_{13} \\ D_{21} & D_{22} & D_{23} \\ D_{31} & D_{32} & D_{33} \end{bmatrix} \begin{bmatrix} K_x \\ K_y \\ K_{xy} \end{bmatrix}$$

noting that $A_{12} = A_{21}$ etc.

We can make the following associations:

- A_{13} and A_{23} relate in-plane direct forces to in-plane shear strain, or in-plane shear force to in-plane direct strains.
- B_{11}, B_{12} and B_{22} relate in-plane direct forces to plane curvatures, or bending moments to in-plane direct strains.
- B_{13} and B_{23} relate in-plane direct forces to plate twisting, or torque to in-plane direct strains.
- B_{33} relates in-plane shear force to plate twisting, or torque to in-plane shear strain.
- D_{13} and D_{23} relate bending moments to plate twisting, or torque to plate curvatures.

In applications where symmetric laminates are used, the B matrix representing the bending-extension coupling vanishes and:

$$\{N\} = [A]\{\varepsilon^o\} \tag{1.48}$$

$$\{M\} = [D]\{K\} \tag{1.49}$$

The FEM and the analysis of laminated plates The layered nature of laminates means that only certain types of elements can be used efficiently within the FEM. It would, in theory, be possible to stack three-dimensional solid elements with one layer of solids representing a laminate ply. This is impractical for two reasons. It would be expensive to run such a model if the lay-up had more than a few plies and a real structure was being represented. In addition, layering solid elements through the thickness of relatively thin plates leads to ill-conditioned sets of equations. For these reasons solids tend to be used either where the lay-up is very thick or the geometry is more solid than plate-like, or where there is a three-dimensional field in the material, as can occur at the free edges of plates. In the latter case the 3D nature of the stress field is only significant over a short length, typically 3-5 thicknesses, and a small 3D sub-model of the region can be used [5].

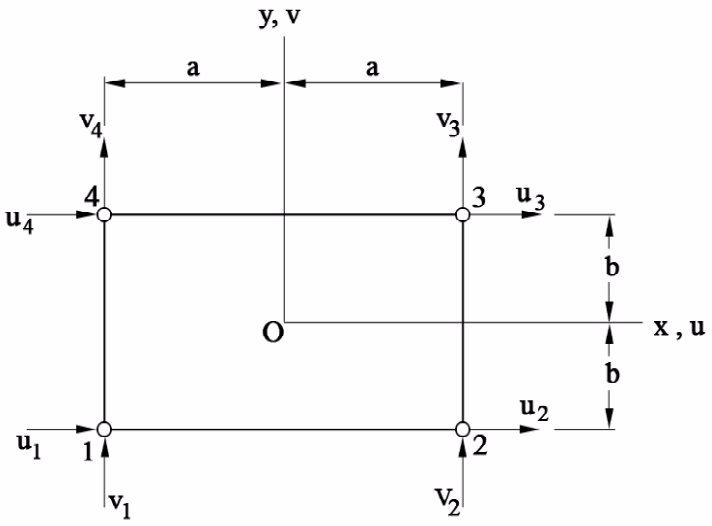

Figure 1-16: A bilinear quadrilateral and its eight nodal degrees of freedom

Figure 1-16 shows a typical four node quadrilateral flat plate element with only in-plane displacements. Such elements are widely used in composite analysis for modelling the in-plane behavior of flat plates. However, care must be taken to ensure that both the stresses and the displacements are zero out of the element's plane, otherwise the model is not valid. With

layered composites this depends upon the orientation of the plies. If the lay-up is not balanced then this 2D element cannot be used.

In practice it is more usual to employ a plate or shell element. The shell is modelled in terms of its mid-surface plane rather than the complete volume. The standard bending theory assumption that the strains only have a combination of constant and linear variation through the thickness of the shell is then used. This means that the deformation of the shell can then be defined by stretching (for the constant strain components) and rotation (for the linear strain components) of the shell's mid-thickness surface.

Both the two-dimensional solid and the general plate element can occur as quadrilaterals or triangles. They all have nodes at the corners of the element.

Provided that the shell is thin, then shell theory gives a good description of its behavior. It is assumed that there is no stress or strain in the direction normal to the plane of the mid-surface. With this idealized behavior it is only necessary to define displacements and rotations as the degrees of freedom on the element mid-surface plane. However, if Kirchhoff thin shell theory is used it is found to be very difficult to derive finite elements for other than very simple (rectangular) geometries. This arises from the need to differentiate the transverse displacements twice to derive the bending strains. Definition of the shape functions and determination of the Jacobian matrix for arbitrary shaped elements has not proven to be simple in such cases. Instead, other shell theories have been used, typically the Mindlin theory [5]. These allow for transverse shear strains to occur so that the bending strains take the form:

$$\varepsilon_{x'x'} = \frac{\partial u'}{\partial x'} + z' \frac{\partial \theta_{y'}}{\partial x'} \tag{1.50}$$

where the "prime" denotes that these are coordinates and displacements in local coordinates in the plane and normal to the mid-thickness surface. There are other similar terms for the other bending strains. This definition of strain only requires first derivatives to be found, which greatly simplifies the determination of the Jacobian matrix. In addition, the formulation allows for the transverse displacements w' and the rotations $\theta_{x'}$ and $\theta_{y'}$ to be interpolated independently of each other. It is this which greatly simplifies the definition of the shape functions. Standard shape functions of the form:

$$w' = [N_1 N_2 N_3 ... N_m] \begin{bmatrix} w_1 \\ w_2 \\ . \\ w_m \end{bmatrix} \tag{1.51}$$

and

$$\theta_{x'} = [N_1 N_2 N_3 ... N_m] \begin{bmatrix} \theta_{x1} \\ \theta_{x2} \\ . \\ \theta_{xm} \end{bmatrix} \tag{1.52}$$

can be used, where the shape function for the ith node, N_i, is the standard simple form used for many 2D membrane plate and solid elements.

The Mindlin theory allows shear strains to occur and so these must also be included in the element behavior and take the typical form (constant through the thickness):

$$\varepsilon_{x'} = \frac{\partial w'}{\partial x'} + \theta_{y'} \tag{1.53}$$

In reality the transverse strains cannot be constant through the thickness since they must be zero on the top and bottom faces of the plate, and they will generally vary in some parabolic form through the thickness. The transverse shears in the Mindlin theory therefore represent average through-thickness values. For thin plates the consequence of the variation through the thickness is second order and this average value is quite sufficient for good accuracy.

1.2.4 Buckling of fibre-reinforced flat plates

Fibre-reinforced laminates can fail by a phenomenon known as buckling when subjected to compressive or shear loads [13]. This is especially true if the laminates are thin. The characteristic of buckling is that the panel retains its original configuration until the initial buckling load is reached, at which point large out-of-plane displacements occur. The magnitude of the load is determined by the stiffness of the laminate, together with the geometry and edge supports.

Most structures can continue to sustain load over and above the initial buckling strength. Final failure will be determined by the strength of the laminate and it is usual for the design load to be equal to, or less than the initial buckling load.

Classical Laminate Theory

Consider a symmetrically laminated rectangular plate of length a, width b and thickness H which consists of n orthotropic layers with fibre angles $\theta_k, k = 1, 2, ..., K$, as shown in Figure 1-17.

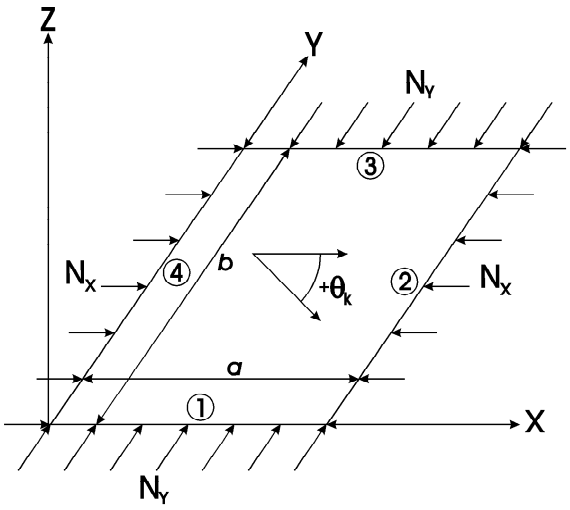

Figure 1-17: Geometry and loading of plate

The plate is defined in the Cartesian coordinates x, y and z with axes x and y lying on the middle surface of the plate, and is subjected to biaxial compressive forces N_x and N_y in the x and y directions, respectively, with the load ratio defined as $\lambda = N_y/N_x$ (where $0 \leq \lambda \leq 1$ is the proportionality constant) as shown in Figure 1-17.

If the effects of transverse shear deformation are neglected, then it may be shown that the buckling load is given by

$$N(m,n) = \frac{n^2\pi^2}{b^2(1+\lambda\alpha_{mn}^2)} \left[\begin{array}{c} D_{11}\alpha_{mn}^{-2} + 2(D_{12}+ \\ + 2D_{66}) + D_{22}\alpha_{mn}^2 \end{array} \right] \tag{1.54}$$

where m and n represent the half wave numbers, $\alpha_{mn} = na/mb$ and D_{ij} are the bending stiffnesses.

The critical load is obtained by minimising $N(m,n)$ over the integer parameters m and n. Thus the *critical* buckling load is given by

$$N_{mn} = \min_{m,n} N(m,n) \tag{1.55}$$

In Equation 1.54, the terms involving bending/twisting coupling stiffnesses D_{16} and D_{26} have been omitted. Their effect on the buckling load becomes negligible provided the following conditions are satisfied

$$D_{16}/(D_{11}D_{12}^3)^{1/4} \leq 0.2, \;\; D_{26}/(D_{22}D_{12}^3)^{1/4} \leq 0.2 \tag{1.56}$$

First-order shear deformable theory

If the effects of transverse shear deformation are to be included, a first-order shear deformable theory can be employed to analyse the problem. For example, assume the following displacement field:

$$\begin{aligned} u &= u_0(x,y) + z\psi_x(x,y) \\ v &= v_0(x,y) + z\psi_y(x,y) \\ w &= w(x,y) \end{aligned} \tag{1.57}$$

where u_o, v_o and w_o are the displacements of the reference surface in the x, y and z direction, respectively, and ψ_x, ψ_y are the rotations of the transverse normal about the x and y axes.

The in-plane strain components can be written as a sum of the extensional and flexural parts and they are given as

$$\{\epsilon\} = \{\epsilon_p\} + z\{\epsilon_f\} \tag{1.58}$$

where

$$\{\epsilon\}^T = (\epsilon_x, \epsilon_y, \epsilon_{xy})$$

and

$$\{\epsilon_p\} = \begin{pmatrix} u_{o,x} \\ v_{o,y} \\ u_{o,y} + v_{o,x} \end{pmatrix}, \ \{\epsilon_f\} = \begin{pmatrix} \psi_x \\ \psi_y \\ \psi_x + \psi_y \end{pmatrix} \tag{1.59}$$

Here, a subscript after the comma denotes differentiation with respect to the variable following the comma.

The transverse shear strains are obtained from

$$\{\gamma\} = \begin{pmatrix} \gamma_{xz} \\ \gamma_{yz} \end{pmatrix} = \begin{pmatrix} w_{o,x} + \psi_x \\ w_{o,y} + \psi_y \end{pmatrix} \tag{1.60}$$

The equations for in-plane stresses of the k-th layer under a plane stress state may be written as

$$\begin{pmatrix} \sigma_x \\ \sigma_y \\ \sigma_{xy} \end{pmatrix}_{(k)} = \begin{pmatrix} \bar{Q}_{11} & \bar{Q}_{12} & \bar{Q}_{16} \\ \bar{Q}_{12} & \bar{Q}_{22} & \bar{Q}_{26} \\ \bar{Q}_{16} & \bar{Q}_{26} & \bar{Q}_{66} \end{pmatrix}_{(k)} \begin{pmatrix} \epsilon_x \\ \epsilon_y \\ \epsilon_{xy} \end{pmatrix} = [\bar{Q}]_{(k)}\{\epsilon\} \tag{1.61}$$

and similarly for the transverse shear stresses as

$$\begin{pmatrix} \tau_{yz} \\ \tau_{xz} \end{pmatrix}_{(k)} = \alpha \begin{pmatrix} \bar{Q}_{44} & \bar{Q}_{45} \\ \bar{Q}_{45} & \bar{Q}_{55} \end{pmatrix}_{(k)} \begin{pmatrix} \gamma_{yz} \\ \gamma_{xz} \end{pmatrix} = \alpha[C]_{(k)}\{\gamma\} \tag{1.62}$$

where α is a shear correction factor [14], and $\bar{Q}_{ij}$ are the transformed stiffnesses. Equations 1.61 and 1.62 may be written in compact form as

$$\boldsymbol{\sigma}_k = \bar{Q}_k \boldsymbol{\epsilon} \tag{1.63}$$

where $\bar{Q}_k$ refers to the full matrix with elements $(\bar{Q}_{ij})_{k,}$, and $\boldsymbol{\sigma}_k$ and $\boldsymbol{\epsilon}$ represent in-plane and transverse stresses and strains, respectively. The resulting shear forces and moments acting on the plate are obtained by integrating the stresses through the laminate thickness, viz.

$$\{V\}^T = (V_x, V_y) = \int_{-h/2}^{h/2} (\tau_{xz}, \tau_{yz}) dz$$

$$\{M\}^T = (M_x, M_y, M_{xy}) = \int_{-h/2}^{h/2} (\sigma_x, \sigma_y, \sigma_{xy}) z dz \tag{1.64}$$

The relations between V and M, and the strains are given by

$$\{V\} = [S]\{\gamma\},\ \{M\} = [D]\{\epsilon_f\} \tag{1.65}$$

where the stiffness matrices $[S]$ and $[D]$ are computed from

$$[S] = \alpha \sum_{k=1}^{K} \int_{h_{k-1}}^{h_k} [C]_{(k)} dz$$

$$[D] = \sum_{k=1}^{K} \int_{h_{k-1}}^{h_k} [\bar{Q}]_{(k)} z^2 dz \tag{1.66}$$

From the condition that the potential energy of the plate is stationary at equilibrium, and neglecting the pre-buckling effects, the equations governing the biaxial buckling of the shear deformable laminate are obtained as

$$M_{x,xx} + 2M_{xy,xy} + M_{y,yy} + N_x w_{,xx} + N_y w_{,yy} = 0$$

$$M_{x,x} + M_{xy,y} - V_x = 0 \tag{1.67}$$

$$M_{y,y} + M_{xy,x} - V_y = 0$$

where N_x and N_y are the pre-buckling stress components which are shown in Figure 1-17. As no simplifications are assumed on the elements of the $[D]$ matrix, Equations 1.67 include the bending-twisting coupling as exhibited by virtue of $D_{16} \neq 0$, $D_{26} \neq 0$.

Finite Element Method The shear deformable model can be easily solved using the finite element method. Consider the finite element formulation of the problem based on Mindlin type theory. Let the region S of the plate be divided into n sub-regions S_r ($S_r \in S; r = 1, 2, ..., n$) such that

$$\Pi(u) = \sum_{r=1}^{n} \Pi^{Sr}(u) \tag{1.68}$$

where Π and Π^{Sr} are potential energies of the plate and the element, respectively, and u is the displacement vector. Using the same shape functions associated with node i ($i = 1, 2, ..., n$), $S_i(x, y)$, for interpolating the variables in each element, we can write

$$u = \sum_{i=1}^{n} S_i(x, y) u_i \tag{1.69}$$

where u_i is the value of the displacement vector corresponding to node i, and is given by

$$u = \{u_o^{(i)}, v_o^{(i)}, w_o^{(i)}, \psi_x^{(i)}, \psi_y^{(i)}\}^T \tag{1.70}$$

The static buckling problem reduces to a generalized eigenvalue problem of the conventional form, viz.

$$([K] + \lambda[K_G])\{u\} = 0 \tag{1.71}$$

where $[K]$ is the stiffness matrix and $[K_G]$ is the initial stress matrix. The lowest eigenvalue of the homogeneous system seen in Equation 1.71 yields the buckling load. Note that here λ denotes the eigenvalue, and should not be confused with the proportionality constant: $\lambda = N_y/N_x$.

1.2.5 Flexural response of fibre reinforced flat plates

The major difference between designing for in-plane response and flexural response is in the importance of the stacking sequence. For in-plane response, only the total thickness of the layers of a given orientation matters, whereas for flexural response, the order of the layers with different orientations is as important as their total thickness. Layers that are located on the outside of the laminate contribute much more to the overall flexural stiffness than identical layers that are located near the midplane. Unlike in-plane response, flexural stiffness response often depends not only on the thickness of the laminate but also on its other dimensions.

Consider a symmetrically laminated rectangular plate of length a, width b and thickness

H under a transverse bending load $q(x, y)$, as shown in Figure 1-18. The plate is located in the x, y, z plane and constructed of an arbitrary number K of orthotropic layers of thickness t_k and fibre orientation θ_k where $k = 1, 2, ..., K$. The displacement of a point (x^0, y^0, z^0) on the reference surface is denoted by (u^0, v^0, w^0).

The governing equation for the deflection w in the z direction under a transverse load q is given by [15]:

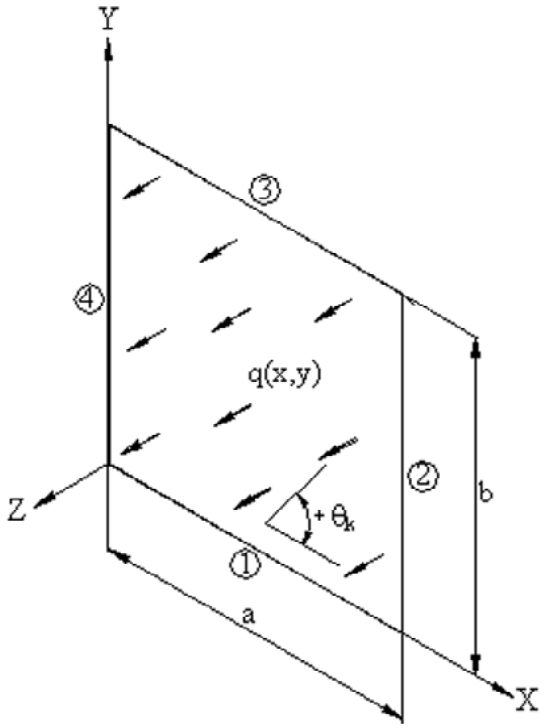

Figure 1-18: Geometry and loading of plate

$$D_{11}w_{,xxxx} + 4D_{16}w_{,xxxy} + 2(D_{12} + 2D_{66})w_{,xxyy} + 4D_{26}w_{,xyyy} + D_{22}w_{,yyyy} = q \qquad (1.72)$$

where variables after the comma denote differentiation with respect to that variable.

As no simplifications are assumed on the elements of the $[D]$ matrix, Equation 1.72 includes bending-twisting coupling as exhibited by virtue of $D_{16} \neq 0, D_{26} \neq 0$.

Finite Element Method This model can be solved using the finite element method. Consider a finite element formulation of the problem based on Mindlin type theory. Let the region S of the plate be divided into n sub-regions S_r ($S_r \in S; r = 1, 2, ..., n$) such that

$$\Pi(u) = \sum_{r=1}^{n} \Pi^{Sr}(u) \tag{1.73}$$

where Π and Π^{Sr} are potential energies of the plate and the element, respectively, and u is the displacement vector. Using the same shape functions associated with node j ($j = 1, 2, ..., n$), $S_j(x, y)$, for interpolating the variables in each element, we can write

$$u = \sum_{j=1}^{n} S_j(x, y) u_j \tag{1.74}$$

where u_j is the value of the displacement vector corresponding to node j, and is given by

$$u = \{u^{(j)}, v^{(j)}, w^{(j)}, \phi_1^{(j)}, \phi_2^{(j)}\}^T \tag{1.75}$$

The displacements $\{u, v, w, \phi_1, \phi_2\}$ are approximated as

$$u = \sum_{j=1}^{n} u_j \psi_j(x, y), \; v = \sum_{j=1}^{n} v_j \psi_j(x, y), \; w = \sum_{j=1}^{n} w_j \psi_j(x, y) \tag{1.76}$$

$$\phi_1 = \sum_{j=1}^{n} S_j^1 \psi_j(x, y), \; \phi_2 = \sum_{j=1}^{n} S_j^2 \psi_j(x, y) \tag{1.77}$$

where ψ_j are Lagrange family of interpolation functions. From the equilibrium equations of the first order theory, and Equation 1.76, we obtain the finite element model of the first-order theory,

$$\sum_{\beta=1}^{5} \sum_{j=1}^{n} K_{ij}^{\alpha\beta} \Delta_j^{\beta} - F_i^{\alpha} = 0, \; (\alpha = 1, 2, ..., 5) \tag{1.78}$$

or

$$[K]\{\Delta\} - \{F\} = \{0\} \tag{1.79}$$

where K and F are the stiffness and force coefficients respectively, and the variable Δ denotes the nodal values of w and its derivatives.

1.2.6 Failure criteria

For the determination of strength of any material it is the usual practice to estimate the stress at the time and location when failure occurs. In the case of conventional materials we need only to determine the maximum tensile, compressive, or shear stress and can then make some observation about the failure and the failure mechanism. This process is relatively straightforward because isotropic materials have no preferential orientation and usually one strength constant will suffice. The isotropic material is essentially a one-dimensional or one-constant material. The Young's modulus for stiffness will suffice because Poisson's ratio is taken to be about 0.3, and the uniaxial tensile strength will also suffice because the shear strength is taken to be about 50 to 60 percent of the tensile.

For composite materials, however, the one-constant approach for stiffness or for strength is no longer adequate. Six constants for the strength of unidirectional composites are needed. The number of constants however do not introduce conceptual difficulty. We know that unidirectional composites have highly directionally dependent strength. The longitudinal strength can be twenty times that of the transverse and shear strength. So for any state of applied stress, all three stress components must be examined before a judgment on the cause of failure can be made. We cannot say quickly the specific stress component that is responsible for the failure. Probably all three components are responsible. The effect of combined stresses must be systematically determined and can be regarded as a way of life for composites.

The determination of strength using failure criteria is based on the assumption that the material is homogeneous (properties do not vary from point to point) and its strength can be experimentally measured with simple tests. Failure criteria provide the analytic relation for the strength under combined stresses. There is another approach of strength using fracture mechanics. A material is assumed to contain flaws. The dominant flaw based on its size, shape and location determines the strength when its growth cannot be stopped.

For composite materials, we need a failure criterion for the unidirectional plies. The strength of a laminated composite will be based on the strength of the individual plies within a laminate.

We would expect successive ply failure as the applied load to a laminate increases. We will have the first ply failure (FPF) to be followed by other ply failures until the last ply failure which would be the ultimate failure of the laminate. The ply stress and ply strain calculations for symmetric and general laminates are intended for strength determination.

Tsai-Wu failure criterion

A general form of the failure criterion for orthotropic materials under plane stress assumption is known as the *Tsai-Wu failure criterion* [16],[17], which stipulates that the condition for non-failure for any particular ply is:

$$F(\theta) = F_{11}\sigma_1^{(k)}\sigma_1^{(k)} + F_{22}\sigma_2^{(k)}\sigma_2^{(k)} + F_{66}\tau_{12}^{(k)}\tau_{12}^{(k)} + 2F_{12}\sigma_1^{(k)}\sigma_2^{(k)} + F_1\sigma_1^{(k)} + F_2\sigma_2^{(k)} \leq 1 \quad (1.80)$$

where the strength parameters $F_{11}, F_{22}, F_{66}, F_1, F_2$ and F_{12} are given by

$$\begin{array}{lll} F_{11} = 1/(X_t X_c) & F_{22} = 1/(Y_t Y_c) & F_{66} = 1/G^2 \\ F_1 = 1/X_t - 1/X_c & F_2 = 1/Y_t - 1/Y_c & F_{12} = -\frac{1}{2}\sqrt{F_{11}F_{22}} \end{array} \quad (1.81)$$

and X_t, X_c, Y_t, Y_c are the tensile and compressive strengths of the composite material in the fibre and transverse directions, and G is the in-plane shear strength.

Typical strength properties for T300/5208 unidirectional laminae are given in Table 1.3

Material	Longitudinal tensile X	Longitudinal compression X'	Transverse tensile Y	Transverse compression Y'	Shear
T300/5208	1500 MPa	1500 MPa	40 MPa	246 MPa	68 MPa

Table 1.3: Strength properties of T300/5208

1.3 Robust design

Tolerances of design variables due to variations in manufacturing processes and user environment may affect the quality and performance of a product [18]. It is usually beneficial to account for such variances in the design process, and in fact, sometimes it may be crucial, particularly when the effect is of consequence. Robust Design Optimization (RDO) is intended to yield a system that performs with minimal variability in the face of input variations or uncertainties. RDO methods generally seek to minimize the variation of an Aggregate Objective Function (AOF) and to maintain design feasibility under input variations. The optimization outcome depends on (i) the acceptable level of variations in performance, and (ii) the level of input variations [19]. Robust design, then, is an approach that explicitly recognizes the effects of these variations and seeks to minimize their consequences - without eliminating their sources.

Various researchers have used robust optimization techniques in the design optimization of structures. For example, Sandgren & Cameron [20] studied the robust design optimization of structures under the presence of variation in loading, geometry and material properties. They used a Monte Carlo simulation embedded into a genetic algorithm, together with a hybrid genetic/non-linear algorithm and a multi-objective formulation to determine a design solution that is optimal under the primary design criteria, but insensitive to variation. Liou & Jang [21] describe a procedure for considering stress distributions in forged products and use the finite element method together with a robust design approach. In order to extend the operating life of products and satisfy the quality of operation during the customer usage, it is necessary to monitor residual stresses during the forging operations. The finite element method and robust design methodology were utilized to identify the controlling process parameters which can monitor the residual stresses in forged products. Lee & Park [22] describe a robust optimization strategy for dealing with discrete constrained design problems. A relatively simple method is proposed to select discrete and robust optimum. At first, the discrete design is achieved as the postprocess of conventional optimization. An orthogonal array is established around a conventional optimum, and the characteristic functions are evaluated. The characteristic function is defined by considering the robustness of the objective and constraints. The parameter design of the Taguchi method is introduced to obtain the robust solution in discrete space. The method is insensitive to variations of the design variables within the selected discrete values enhancing the

feasibility of constraints. Several structural problems are solved to demonstrate the technique. In another paper, Lee & Park [23] propose a robust optimization technique which accounts for tolerances of design variables. The approach suggested in the paper was developed to obtain an optimum value insensitive to variations on design variables within a feasible region, and is performed by using a mathematical programming algorithm. A multiobjective function is defined to have the mean and the standard deviation of the original objective function, while the constraints are supplemented by adding a penalty term to the original constraints. This method has an advantage in that the second derivatives of the constraints are not required. Several standard problems for structural optimization are solved to check the usefulness of the suggested method.

1.4 Design optimization procedures

Researchers and designers use various design optimization techniques to optimize the design of structures and make them more efficient. With the advent of fibre-reinforced laminated composites, these optimization techniques have helped engineers minimize the calculation time and simplify complexity to produce optimal structures.

1.4.1 Minimization or maximization of functions

Consider a function f that depends on one or more independent variables [24]. The value of those variables where f takes on a maximum or a minimum value must then be found. The value of f that achieves the maximum or minimum can then be calculated. The computational requirements are to perform the computation quickly and economically and to use as little memory as possible. Often the computational effort is dominated by the cost of evaluating f. In such cases it is necessary to evaluate f as few times as possible.

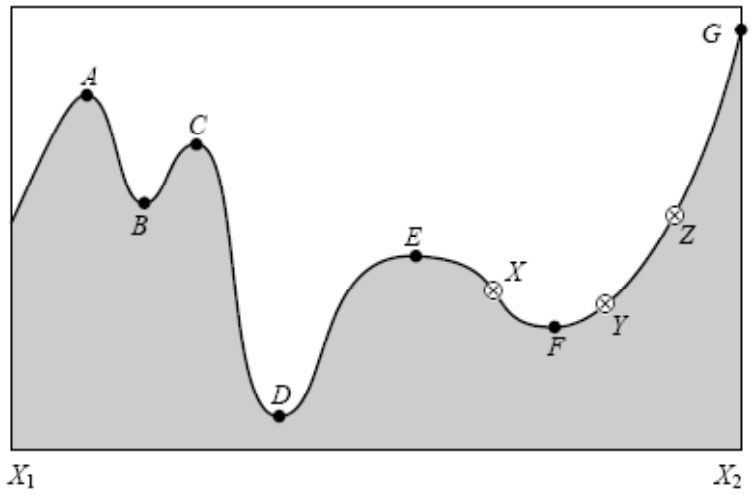

Figure 1-19: Extrema of a function in an interval. Points A, C, and E are local maxima. Points B and F are local minima. The global maximum occurs at G, while the global minimum is at D. The points X, Y , and Z are said to bracket the minimum F, since Y is less than both X and Z.

An extremum can be either global or local as shown in Figure 1-19. Finding a global extremum is often very difficult and two standard heuristics are often used. The first is to find

the local extrema by starting from widely varying values of the independent variables (perhaps chosen quasi-randomly), and then pick the most extreme of these. The second is to perturb a local extremum by taking a finite amplitude step away from it, and see if the routine returns to a better point, or returns to the original point.

1.4.2 Examples of search routines

There are various techniques for finding maxima or minima, including *Simulated Annealing*, *Linear Programming*, *Monte Carlo* and the *Golden Section* method. Simulated Annealing is a relatively new optimization routine and has solved problems previously thought to be unsolvable. This routine directly addresses the problem of finding global extrema in the presence of large numbers of undesired local extrema. Linear Programming is a well developed area of *Constrained Optimization* where both the function to be optimized and the constraints happen to be linear functions of the independent variables.

The Golden Section method

The Golden Section method is a simple one-dimensional search routine that works as follows [24]: The root is bracketed in an interval (a_p, b_p). The function is then evaluated at an intermediate point x_p and a new, smaller bracketing interval, either (a_p, x_p) or (x_p, b_p) is obtained. This process continues until the bracketing interval is acceptably small. It is optimal to choose x_p to be the midpoint of (a_p, b_p) so that the decrease in the interval length is maximised when the function is as uncooperative as it can be. The position of x_p is found by manipulation and the end result is:

$$w = \frac{3 - \sqrt{5}}{2} = 0.38197 \tag{1.82}$$

There is a precise translation of these considerations to the minimization problem. To bracket a minimum involves bracketing a pair of points, a_p and b_p, when the function has opposite sign at these two points, which gives the root of a function. A minimum, by contrast, is known to be bracketed only when there is a *triplet* of points, $a_p < b_p < c_p$ (or $c_p < b_p < a_p$), such that $f(b_p)$ is less than both $f(a_p)$ and $f(c_p)$. In this case it is known that the function (if it is nonsingular) has a minimum in the interval (a_p, c_p).

The analog of bisection is to choose a new point x_p, either between a_p and b_p or between b_p and c_p. If the latter choice is made, then $f(x_p)$ is evaluated. If $f(b_p) < f(x_p)$, then the new bracketing triplet of points is (a_p, b_p, x_p); if $f(b_p) > f(x_p)$, then the new bracketing triplet is (b_p, x_p, c_p). In all cases the middle point of the new triplet is the abscissa whose ordinate is the best minimum achieved thus far. The process is continued until the distance between the two outer points of the triplet is tolerably small.

The Downhill Simplex method

The Downhill Simplex algorithm gives a robust method that does not rely on derivatives to provide function minimization for any order dimensional space, but at the expense of convergence speed due to the increased number of function calls in comparison to other optimization algorithms.

In a sense the simplex rolls downhill due to computation of the function values at the vertices of the simplex, replacing vertices (except the low value) within each iteration of the algorithm.

The simplex method in N dimensions uses $N+1$ points within the merit space to define the simplex. Selection of these points can be prescribed, but random selection allows the potential to fully investigate the merit space. The function values are found at each of these points. The points with the low (P_L), high (P_1), and second high (P_2) function values are determined. Next, the centroid of the points except P_1, $\overline{P}$, is determined. The simplex method essentially has four steps possible during each iteration: reflection, contraction in one dimension, contraction around the low vertex, and expansion. The basis for each step is provided here:

(1) Reflection: A reflected point, P_R, is found by reflecting P_1 through $\overline{P}$ with the equation:

$$P_R = (1+\alpha)\,\overline{P} - \alpha P_1 \tag{1.83}$$

where α is the reflection factor (Nelder and Mead [25]: $\alpha = 1$). P_R replaces P_1 if $f(P_L) < f(P_R) < f(P_1)$.

(2) Expansion: if $f(P_R) < f(P_L)$ then the simplex grows along the centroid direction with the hope that the expansion point, P_E, is better than P_L. The expansion is determined with the equation:

$$P_E = (1-\gamma)\overline{P} + \gamma P_R \tag{1.84}$$

where γ is the expansion factor (Nelder and Mead [25]: $\gamma = 2$). P_E replaces P_1 if $f(P_E) < f(P_L)$

(3) 1D Contraction: if $f(P_R) > f(P_2)$ then the simplex contracts along the centroid direction with the hope that the contracted point, P_C, is better than P_2. The 1D contraction is determined with the equation:

$$P_C = (1-\beta_1)\overline{P} + \beta_1 P_0 \tag{1.85}$$

where β_1 is the 1D contraction factor (Nelder and Mead [25]: $\beta_1 = 0.5$) and P_0 is the selection of P_1 or P_R which has the lowest function value. P_C replaces P_1 if $f(P_C) < f(P_0)$

(4) Full contraction: if $f(P_C) > f(P_0)$ then 1D contraction does not suffice, and the whole simplex is contracted around P_L. The full contraction is determined with the equation:

$$P_i = (1-\beta_2)P_L + \beta_2 P_i \tag{1.86}$$

where β_2 is the full contraction factor (Nelder and Mead [25]: $\beta_2 = 0.5$) and P_i represents all the points except P_L.

Typically, when a point replaces P_1 the current iteration is completed. Next the termination condition is checked. If the tolerance is not met then the next iteration is started. If the tolerance is met, then the optimization is complete.

1.5 Design optimization of laminated composites

The use of laminated composite materials as structural components is becoming widespread in several branches of engineering. An advantage of FRC materials over conventional ones is the possibility of tailoring their properties to the specific requirements of a given application. The tailoring is mostly achieved by maximizing the mechanical properties as a result of selecting the layer fibre angles optimally.

1.5.1 Design optimization with buckling loads

An important failure mode for FRC structures is buckling under in-plane loading. The in-plane load carrying capacity of these structures can be maximized by using the ply angle as a design variable and determining the optimal angles. Optimization of composite structures with respect to ply angles to maximize the critical buckling load is necessary to realise the full potential of fibre-reinforced materials. Numerous researchers have demonstrated the benefits of design optimization and some examples that account for in-plane loading are Refs [26]-[33]. The effects of boundary conditions and of bending twisting coupling on the buckling load of symmetric angle ply laminates have been investigated in Refs [34],[35]-[37]. In Ref [38] the fibre orientations, laminae thicknesses and material combinations are used as design variables, and the technique proposed is used to select the best combination for minimum cost for plates subject to compressive loads. In Ref [39] a method of feasible ply directions is used to determine optimal thickness distributions over the plate that yield maximum uniaxial and biaxial buckling loads.

1.5.2 Design optimization for minimum weight

A number of studies concerning the minimum weight design of composite structures appear in the literature. Angle-ply laminates subjected to uncertain loads were considered by Adali *et al.* [40] who used a convex modelling approach in their analysis. The optimal design of symmetrically laminated plates under transverse loads was given by Tauchert and Adibhatla [41] using the minimum strain energy criterion, by Quian *et al.* [42] and by Kengtung [43] using the minimum structural compliance criterion. A maximum stiffness design for both symmetric

and antisymmetric laminates was considered by Kam and Chang [44]. Adali *et al.* [45] investigated the minimum weight and deflection design of thick sandwich laminates via symbolic computation. Phillips and Gürdal [46] and Triantafillou *et al* [47] detailed the optimal design of composite panels and hybrid box beams, respectively. The former used analysis routines in conjunction with an optimization package to provide design schemes for geodesically stiffened minimum weight aircraft wing rib panels. Optimal weight design of shells was considered by Min and Charanteney [48], who investigated sandwich cylinders under combined loadings. A study by Ostwald [49] considered the combined loading cases of external pressure and axial compression in the optimization of thin walled shells. The Bubnov-Galerkin method was used to solve the stability problem. A paper by Walker *et al.* [33] focuses on the minimum deflection and weight designs of laminated composite plates. The finite element method using Mindlin plate theory was used in conjunction with optimization routines in order to obtain the optimal designs. Comparative results are presented for minimum weight priority design as an alternative to minimum deflection/minimum weight priority design to investigate the effect of priority on the deflection and weight.

Various researchers have investigated the design of composite structures under in-plane loads for minimum weight. For instance, Lucoshevichyus [50] and Shin *et al* [51] investigated the design optimization of plates, while Walker *et al* [52] dealt with laminated cylinders.

1.5.3 Robust design for laminated structures

Very few researchers have dealt with the robust design of composite structures. Chiang [53] used a robust design approach to improve the accuracy of the Iosipescu shear test specimen. The statistical design of experiments based on the finite element method was employed, and was able to identify the influential design variables. Refs [54],[55] describe a methodology which uses a random global search algorithm to explore near optimal designs for different tolerances.

1.5.4 Design methodologies for the design of laminated structures

Various researchers have proposed design methodologies or techniques for the optimization of composite structures, and some consist of two or more stages. For example, Walker *et al* [56] describes a describes a methodology that can be used to select the best material combinations

and optimize the design of hybrid composite plates subject to minimum weight and cost.

In the Refs [38]-[61], Walker and Smith describe several different techniques for the design optimization of composite structures. In the first, the fibre orientations, laminae thicknesses and material combinations are used as design variables, and the technique is used to select the best combination for minimum cost for plates subject to compressive loads. This is a refinement of the technique detailed in [56]. The second details a similar procedure for minimizing the weight of sandwich cylindrical shells and particularly tubes. Ref [58] presents a procedure to design composite structures for a maximum combination of torque and in-plane loads, and is tailored for tubes, which are used as examples to illustrate the technique. Ref [59] describes a simple-self design methodology that can be used to minimize the weight of composite structures. The procedure is based on the finite element method, and suitable elements are removed without affecting the overall structural integrity. Here, a failure criterion is implemented. Refs [60] and [61] describe techniques for using genetic algorithms and finite element analysis to optimize the design of laminated structures. In both cases, the implementation of the GA is unique, and convergence is rapid. In the first paper, the aim is to minimize the weight, whilst in the second, a multiobjective approach is used to minimize the weight and deflection.

Chapter 2

Optimization of laminated structures with manufacturing uncertainties accounted for - design problems and solution procedures

2.1 Introduction

When composite laminates are manufactured, the desired fibre orientation in different plies may deviate from their intended design values by a few degrees. These deviations are referred to as manufacturing uncertainties. For example, assume that the interval $0^o \leq \theta \leq 90^o$ is divided into i sub-intervals $[0^o \leq \theta \leq M^o]_1$, $[M^o \leq \theta \leq N^o]_2$, $[N^o \leq \theta \leq O^o]_3$... $[Y^o \leq \theta \leq Z^o]_i$, and that for each, a manufacturing uncertainty in the lay-up angle θ is incurred, and must be accounted for during the design stage, if optimal performance is required. Furthermore, assume that the probability of any tolerance value occurring within the tolerance band, compared with any other, is equal. Extensive research has been performed in the field of manufacturing tolerances but not incorporating it as part of the design optimization process. For example, for the interval $[0^o \leq \theta \leq M^o]_1$ there may be a maximum variation band of $+g$ or $-h$, with $0^o \leq g, h \leq 90^o$. In addition, when accounted for, it is assumed that $\theta + g \leq 90^o$ and $0^o \leq \theta + h$.

2.2 Problem 1: A technique for optimally designing fibre-reinforced laminated plates with manufacturing uncertainties for maximum buckling strength

Here, a procedure to design simply supported symmetrically laminated plates for maximum buckling load with manufacturing uncertainty in the ply angle, which is the design variable [62], is described. This procedure is implemented neglecting the effects of bending-twisting and the Golden Section method is used as the search technique, but the methodology is flexible enough to allow any appropriate problem formulation and search algorithm to be substituted. Three different tolerance scenarios are used for the purpose of illustrating the methodology, and plates with varying aspect ratios and loading ratios are optimally designed.

2.2.1 Optimal design problem formulation

The objective of the design problem is to maximize the buckling loads N_x and N_y, shown in Figure 1-17, for a given plate thickness H by optimally determining the fibre orientations given by $\theta_k = (-1)^{k+1}\theta$ for k $\leq K/2$ and θ_k = (-1)$^k\theta$ for k $\geq K/2+1$ (where k is the layer - or ply - number), with the manufacturing tolerances accounted for. The nominal buckling load is given by Equation 1.55.

If there were no manufacturing tolerances to consider, the design objective would be to maximize $N(\theta)$ with respect to θ,viz.

$$N_{\max} \stackrel{\triangle}{\equiv} \max_{\theta}[N(\theta)],\ 0^o \leq \theta \leq 90^o \tag{2.1}$$

where $N(\theta)$ is determined using Equation 1.55.

2.2.2 Solution procedure

In order to illustrate the problem, consider the following scenario. Assume that on the interval $[0^o \leq \theta \leq 22^o]_1$ a manufacturer incurs the following maximum tolerances: $\theta+13^o$ and $\theta-7^o$; viz. when trying to achieve the value θ, the actual value that results is $\theta - 7^o \leq \theta \leq \theta + 13^o$. On the interval $[22^o \leq \theta \leq 35^o]_2$, the tolerance is $\theta - 12^o \leq \theta \leq \theta + 6^o$, on the interval $[35^o \leq \theta \leq 70^o]_3$

the tolerance is $\theta - 17^o \leq \theta \leq \theta + 17^o$ and finally, for the interval $[70^o \leq \theta \leq 90^o]_4$, the tolerance is $\theta - 15^o \leq \theta \leq \theta + 5^o$. Figure 2-1 shows the effect of the tolerance in each of the four intervals on the buckling load for a laminated plate with eight symmetrically laminated layers of equal thickness (t) and with $\theta_1 = -\theta_2 = \theta_3 = -\theta_4 = -\theta_5 = \theta_6 = -\theta_7 = \theta_8 = \theta$. The plate has dimensions $a = 1.5m$, $b = 1m$ and the thickness ratio is specified as $H/b = 0.01$. Also, $\lambda = 1$. The material properties are those for a typical T300/5208 graphite/epoxy material as shown in Table 1.2. There are three trendlines given, and these represent the nominal buckling load (viz. the value of the buckling load at θ), along with the upper and lower bounds (viz. the buckling load at the values $\theta + g$ and $\theta + h$). Three discontinuities are easily identified, and these distinguish the four intervals described above. It is evident that the effect of the upper and lower tolerances is to shift the nominal trends right and left.

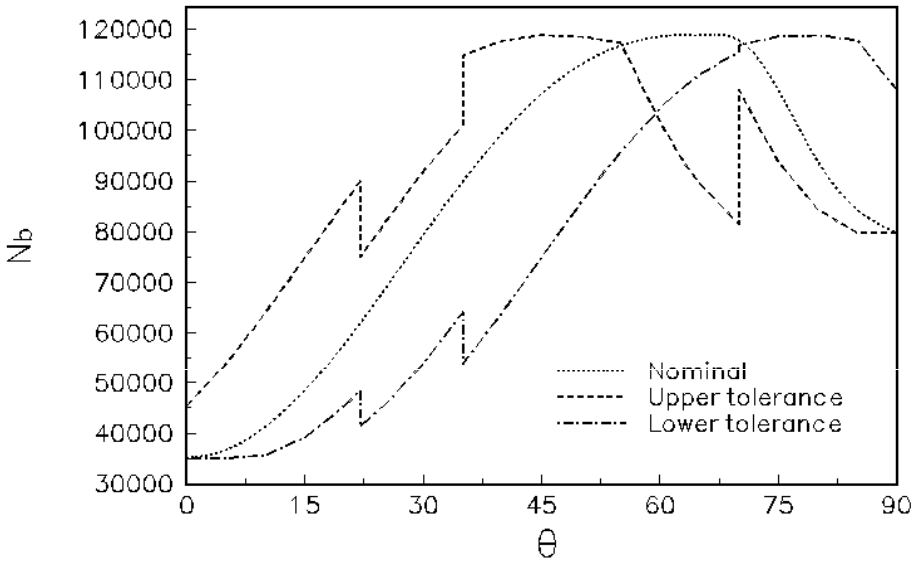

Figure 2-1: Effect of manufacturing tolerances on the buckling load of a plate with a/b = 1.5 and $\lambda = 1$

The design problem becomes one of determining the value of θ at which the buckling load is maximised, with the tolerances accounted for, which effectively becomes one of determining the value of θ for which the trend described by the lower solid line in Figure 2-2 (which needs no explanation) is maximum (viz. designing for the worst case scenario). In addition, the discontinuity points are ignored (for obvious reasons), and in the event that two or more values

of θ correspond to equal maximum buckling load values, the one that gives the best value contained within the upper solid line should logically be selected. In this case, the optimal value is 71^o (at 70^o a discontinuity exists and thus the optimal value must be 1^o to the right - here the required accuracy was to within 1^o) which corresponds to a buckling load of 104817 N. The optimal values for the nominal case are 63^o and 118847 N. It is apparent from this example that the values of the actual optimal results are quite different from those of the nominal, and that if we were to ignore the manufacturing tolerances and choose 63^o as the optimal fibre orientation, the corresponding buckling load could be as low as 93851 N, which is 10.5% less than the actual. This fact emphasizes the importance of carrying out optimization in design work with the effects of manufacturing tolerances included. Finally, it should be emphasized that by designing for the worst case scenario, the resulting outcome could be better.

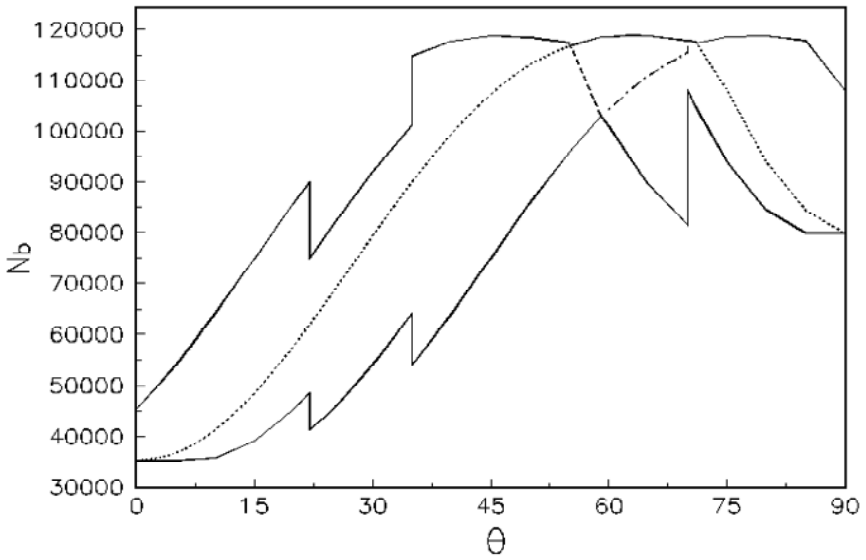

Figure 2-2

The optimization procedure thus involves the stages of evaluating the buckling load $N(\theta)$ for a given θ and $\theta + g$ and $\theta + h$, selecting the lowest of the three values, and improving the fibre orientation to maximize the least of the three. Thus, the computational solution consists of successive stages of analysis and optimization until a convergence is obtained and the optimal

angle θ_{opt} is determined within specified accuracy. In the optimization stage here, the Golden Section method is employed, and θ_{opt} is determined to within 1^o.

2.3 Problem 2: A methodology for the optimally designing fibre-reinforced laminated structures with design variable tolerances for maximum buckling strength.

Here, a procedure to design symmetrically laminated structures for maximum buckling load with manufacturing uncertainty in the ply angle - which is the design variable [63], is described. The finite element method, based on Mindlin plate and shell theory, is implemented and used to determine the fitness of each candidate, and so the effects of bending-twisting coupling are accounted for. The methodology is flexible enough to allow any appropriate finite element formulation and search algorithm to be substituted. Three different tolerance scenarios are used for the purpose of illustrating the methodology, and plates with varying aspect and loading ratios, as well as different boundary conditions, are chosen to demonstrate the technique, and optimally designed and compared.

2.3.1 Optimal design problem formulation

The objective of the design problem is the same as described in Section 2.1.1 which is to maximize $N(\theta)$ with respect to θ, using Equation 2.1, where $N(\theta)$ is determined from the finite element solution of the eigenvalue problem given by Equation 1.71.

2.3.2 Solution procedure

In order to illustrate the problem, consider the following scenario. Assume that on the interval $[0^o \leq \theta \leq 22^o]_1$ a manufacturer incurs the following maximum tolerances: $\theta+13^o$ and $\theta-7^o$; viz. when trying to achieve the value θ, the actual value that results is $\theta-7^o \leq \theta \leq \theta+13^o$. On the interval $[22^o \leq \theta \leq 35^o]_2$, the tolerance is $\theta-12^o \leq \theta \leq \theta+6^o$, on the interval $[35^o \leq \theta \leq 70^o]_3$ the tolerance is $\theta-17^o \leq \theta \leq \theta+17^o$ and finally, for the interval $[70^o \leq \theta \leq 90^o]_4$, the tolerance is $\theta-15^o \leq \theta \leq \theta+5^o$. Figure 2-3 shows the effect of the tolerance in each of the four intervals on the buckling load for a laminated CCCC (viz. clamped along each edge) plate with eight symmetrically laminated layers of equal thickness and with $\theta_1 = -\theta_2 = \theta_3 = -\theta_4 = -\theta_5 = \theta_6 = -\theta_7 = -\theta_8 = \theta$. The plate is square and the thickness ratio is specified as $H/b = 0.01$.

Also, $\lambda = 1$, and the buckling loads have all been non-dimensionalized by using the following:

$$N_b = \frac{N(\theta)b^2}{H^3 E_o} \tag{2.2}$$

where N is the critical buckling load and E_o is a reference value having the dimension of Young's modulus and is taken as $E_o = 1GPa$.

There are three trendlines given, and these represent the nominal buckling load (viz. the value of the buckling load at θ), along with the upper and lower bounds (viz. the buckling load at the values $\theta + g$ and $\theta + h$). Three discontinuities are easily identified, and these distinguish the four intervals described above. It is evident that the effect of the upper and lower tolerances is to shift the nominal trends right and left.

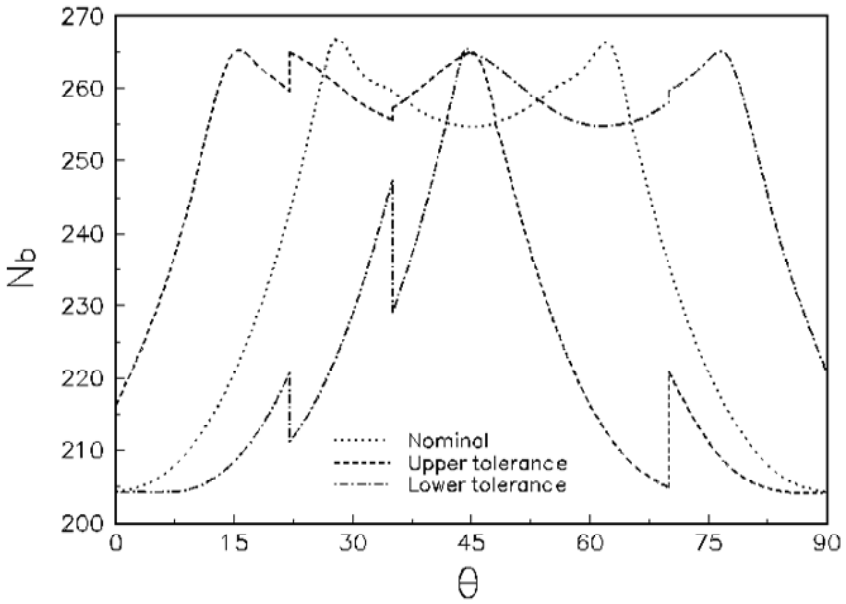

Figure 2-3: Effect of manufacturing tolerances on the buckling load of a plate with a/b = 1 and $\lambda = 1$

The design problem becomes one of determining the value of θ at which the buckling load is maximised, with the tolerances accounted for, which effectively becomes one of determining the value of θ for which the trend described by the lower solid line in Figure 2-4 (which needs

no explanation) is maximum (viz. designing for the worst case scenario). In addition, the discontinuity points are ignored (for obvious reasons), and in the event that two or more values of θ correspond to equal maximum buckling load values, the one that gives the best value contained within the upper solid line should logically be selected.

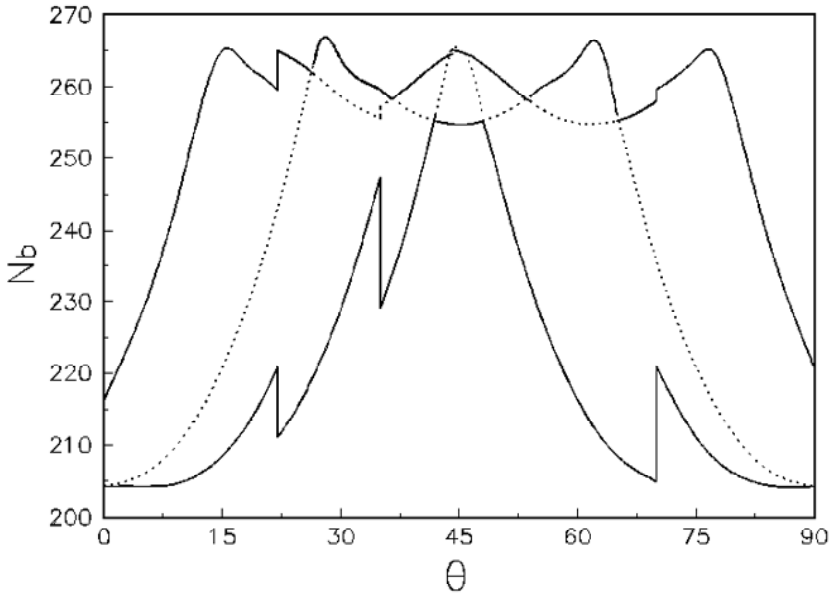

Figure 2-4

In this case, the optimal value is 42^o (or 48^o) - here the accuracy was to within 1^o- which corresponds to a buckling load of 255.2. The optimal values for the nominal case are 27^o or 63^o and 265.2. It is apparent from this example that the values of the actual optimal results are quite different from those of the nominal, and that if we were to ignore the manufacturing tolerances and choose 27^oor 63^o as the optimal fibre orientation, the corresponding buckling load could be as low as 211.1 (at 63^o) or 220.8 (at 27^o), which is 17.3% (or 13.5%) less than the actual. This fact emphasizes the importance of carrying out optimization in design work with the effects of manufacturing tolerances included. Finally, it should be emphasized that by designing for the worst case scenario, the resulting outcome could be better.

The optimization procedure thus involves the stages of evaluating the buckling load $N(\theta)$ for a given θ and $\theta + g$ and $\theta + h$, selecting the lowest of the three values, and improving the

fibre orientation to maximize the least of the three. Thus, the computational solution consists of successive stages of analysis and optimization until a convergence is obtained and the optimal angle θ_{opt} is determined within specified accuracy. In the optimization stage here, the Golden Section method is employed, and θ_{opt} is determined to within 1^o.

2.4 Problem 3: A technique for optimally designing fibre-reinforced laminated plates under in-plane loads for minimum weight with manufacturing uncertainties accounted for

Here, a procedure to design simply supported symmetrically laminated plates subject to a minimum buckling load capacity requirement for minimum weight with manufacturing uncertainty in the ply angle, which is the design variable [64], is described. The effects of bending-twisting coupling are neglected and the Golden Section method is used as the search technique, but the methodology is flexible enough to allow any appropriate problem formulation and search algorithm to be substituted. Three different tolerance scenarios are used to illustrate the methodology, and plates with varying aspect ratios and loading ratios are optimally designed.

2.4.1 Optimal design problem formulation

The objective of the design problem is to minimize the weight of the plate, subject to a minimum buckling load capacity constraint, shown in Figure 1-18, with manufacturing uncertainty in the layup angle and thickness accounted for. The problem can thus be stated as

$$W_{\min} \stackrel{\Delta}{\equiv} \min_{\theta,H} \left[W(\theta, H) \right], \qquad 0^o \leq \theta \leq 90^o \tag{2.3}$$

where the weight of a plate is given by

$$W = Hab\rho \tag{2.4}$$

and where H is the total thickness of the plate and ρ the density,

subject to

$$N \geq N_{\min} \tag{2.5}$$

where N is given by Equation 1.55.

2.4.2 Solution procedure

In order to illustrate the problem, consider the following scenario. Assume that on the interval $[0^o \leq \theta \leq 22^o]_1$ a manufacturer incurs the following maximum tolerances: $\theta+13^o$ and $\theta-7^o$; viz. when trying to achieve the value θ, the actual value that results is $\theta-7^o \leq \theta \leq \theta+13^o$. On the interval $[22^o \leq \theta \leq 35^o]_2$, the tolerance is $\theta-12^o \leq \theta \leq \theta+6^o$, on the interval $[35^o \leq \theta \leq 70^o]_3$ the tolerance is $\theta - 17^o \leq \theta \leq \theta + 17^o$ and finally, for the interval $[70^o \leq \theta \leq 90^o]_4$, the tolerance is $\theta-15^o \leq \theta \leq \theta+5^o$. Figure 2-5 shows the effect of the tolerance in each of the four intervals on the minimum required layer thicknesses for a laminated plate with eight symmetric layers of equal thickness and with $\theta_1 = -\theta_2 = -\theta_3 = \theta_4 = \theta$, The plate has dimensions $a = 1.5m$, $b = 1m$, with $\lambda = 1$ and the buckling load requirement here is 90 000N. There are three trendlines given, and these represent the nominal layer thickness (viz. the value at θ), along with the upper and lower bounds (viz. the values at $\theta+g$ and $\theta+h$). Three discontinuities are easily identified, and these distinguish the four intervals described above. It is evident that the effect of the upper and lower tolerances is to shift the nominal trends right and left.

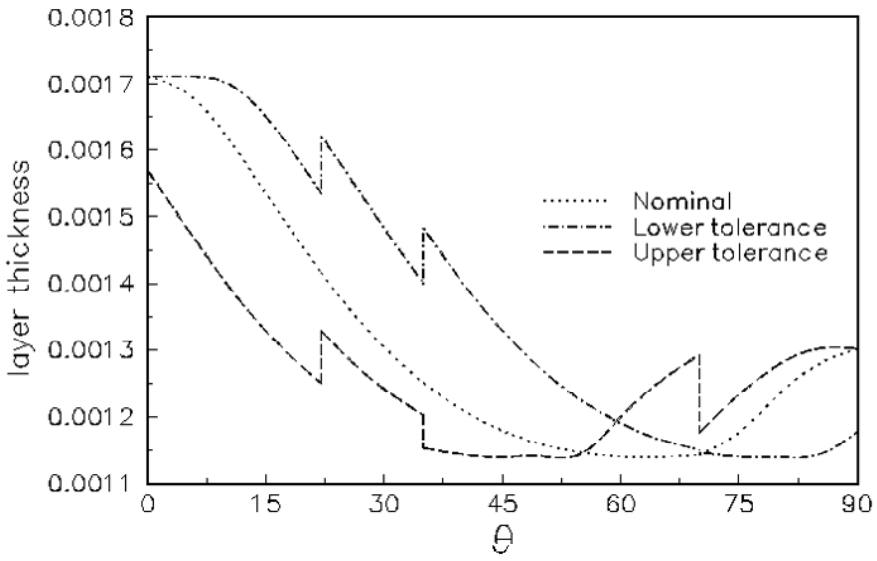

Figure 2-5: Effect of manufacturing tolerances on the layer thickness with a/b = 1.5 and λ =1

The design problem becomes one of determining the value of θ at which the layer thickness is minimized thus reducing the weight of the laminate, with the tolerances accounted for, which

effectively becomes one of determining the value of θ for which the trend described by the upper solid line in Figure 2-6 (which needs no explanation) is maximum (viz. designing for the worst case scenario). In addition, the discontinuity points are ignored (for obvious reasons), and in the event that two or more values of θ correspond to equal minimum thickness values, the one that gives the best value contained within the lower solid line should logically be selected. In this case, the optimal value is 71^o (at 70^o a discontinuity exists and thus the optimal value must be 1^o to the right - here the required accuracy was to within 1^o) which corresponds to a layer thickness of 0.00119m. The optimal values for the nominal case are 63^o and 0.00114m. It is apparent from this example that the values of the actual optimal results are quite different from those of the nominal, and that if we were to ignore the manufacturing tolerances and choose 63^o as the optimal fibre orientation, the corresponding buckling load could be as low as 71191N (at $63^o + 17^o$), which is 21% less than that required. This fact emphasizes the importance of carrying out optimization in design work with the effects of manufacturing tolerances included. Finally, it should be emphasized that by designing for the worst case scenario, the resulting buckling load will always be at least equal to that required.

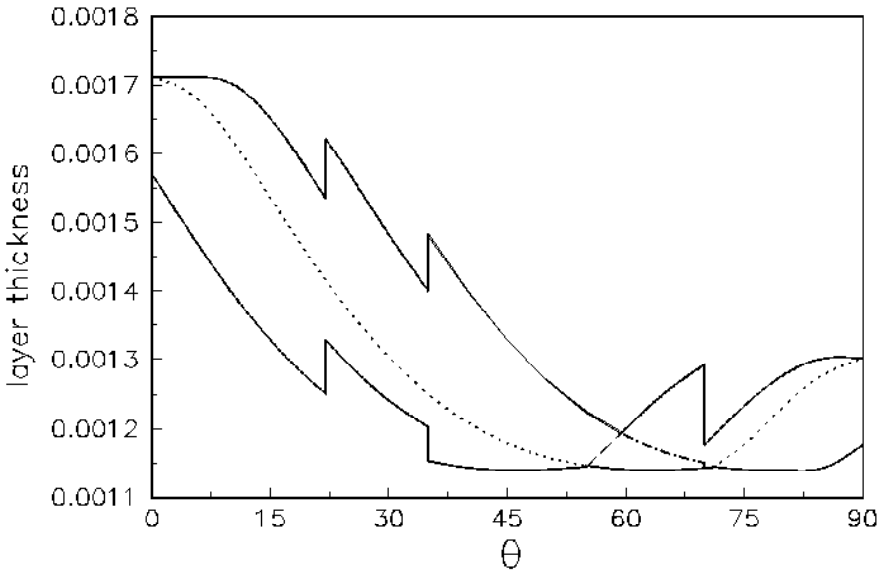

Figure 2-6

The optimization procedure thus involves the stages of determining the layer thickness

required for a given θ and $\theta+g$ and $\theta+h$, selecting the greatest of the three values, and improving the fibre orientation to minimize the greatest value. Thus, the computational solution consists of successive stages of analysis and optimization until convergence is obtained and the optimal angle θ_{opt} is determined within specified accuracy. In the optimization stage here, the Golden Section method is employed, and θ_{opt} is determined to within 1^o.

2.5 Problem 4: A methodology for optimally designing fibre-reinforced laminated plates under in-plane loads for minimum weight with manufacturing uncertainty accounted for

Here, a procedure to design simply supported symmetrically laminated plates subject to a minimum buckling load capacity requirement for minimum weight with manufacturing uncertainty in the ply angle *and the laminate thickness*, which are the design variables [65], is described. Like the previous problem, the effects of bending-twisting coupling are neglected. The Downhill Simplex method is used as the search technique, but the methodology is flexible enough to allow any appropriate problem formulation and search algorithm to be substituted. Three different tolerance scenarios are used to illustrate the methodology, and plates with varying aspect ratios and loading ratios are optimally designed.

2.5.1 Optimal design problem formulation

The objective of the design problem is to minimize the weight of the symmetrically laminated plate, subject to a minimum buckling load capacity constraint, shown in Figure 1-18, with manufacturing uncertainty in the lay-up angle and thickness accounted for. The problem can thus be stated as

$$W_{\min} \stackrel{\Delta}{\equiv} \min_{\theta,H} \left[W(\theta, H)\right], \qquad 0^o \leq \theta \leq 90^o, \ H_{\min} \leq H \leq H_{\max} \tag{2.6}$$

where the weight of a plate is given by

$$W = Hab\rho \tag{2.7}$$

where H is the total thickness of the plate and ρ the density.

The constraint may be stated as

$$N \geq N_{\min} \tag{2.8}$$

where N is given by Equation 1.55.

2.5.2 Solution procedure

Assume that for the interval $0^o \leq \theta \leq 90^o$ a manufacturing tolerance in the lay-up angle θ *and* thickness t is incurred, and must be accounted for during the design stage, if optimal performance is required. Furthermore, assume that the probability of any tolerance value occurring within the tolerance band, compared with any other, is equal. Extensive research has been performed in the field of manufacturing tolerances but not incorporating it as part of the design optimization process. For example, for θ there may be a maximum variation band of $+f$ or $-g$, with $0^o \leq f, g \leq 90^o$. In addition, when accounted for, it is assumed that $\theta + f \leq 90^o$ and $0^o \leq \theta + g$. Similarly, for t, there may be a maximum variation band of $+p$ or $-q$, with $p,\ q \geq 0$, and $t + q > 0$. The optimization procedure involves the stages of determining the buckling load at (θ, t), and at the eight other points which occur when the tolerances of the fibre orientation and thickness are accounted for, viz. $(\theta + f, t + p), (\theta + f, t + q), (\theta + f, t), (\theta + g, t + p), (\theta + g, t + q), (\theta + g, t), (\theta, t + p)$ and $(\theta, t + q)$. The highest of these is then selected, and the orientation and thickness values improved to minimize the weight, whilst ensuring that the minimum buckling load constraint is complied with. So, the computational solution consists of successive stages of analysis and optimization until convergence is obtained and the optimal angle θ_{opt} and thickness $H_{\min}$ is determined within specified accuracy. Thus, the design problem may be stated as: determine the solution to min $\mid N_{crit} - N_{\min} \mid$ which leads to a minimum weight, with the manufacturing tolerances accounted for.

In order to illustrate the problem, consider the following scenario. For a eight layer symmetric plate with $\theta_1 = -\theta_2 = \theta_3 = -\theta_4 = -\theta_5 = \theta_6 = -\theta_7 = \theta_8 = \theta$, and layers of equal thickness t, assume that on the intervals $[0^o \leq \theta \leq 90^o]$ and $[5mm \leq H \leq 50mm]$ a manufacturer incurs the following tolerances in the lay-up angle: $\theta + 13^o$ and $\theta - 7^o$, and for the layer thickness: $t + 0.375mm$ and $t - 0.625mm$. Thus, when trying to achieve the value θ, the actual value that results is $\theta - 7^o \leq \theta \leq \theta + 13^o$, and when trying to achieve the value t, the actual value that results is $t - 0.625mm \leq t \leq t + 0.375mm$.

Figure 2-7 shows the effect of the tolerance in θ on the objective (viz. $\mid N_{crit} - N_{\min} \mid$) for such a plate with dimensions $a = 0.75m$, $b = 1m$, $\lambda = 1$ and $H = 4.4mm$. The buckling load requirement here is 10^7N (viz. $N_{\min} = 10^7$), and the tolerance in t has been neglected (for the sake of clarity here). The material properties are those for a typical T300/5208 graphite/epoxy

material. Table 1.2. There are three trendlines given, and these represent the nominal objective (viz. the value at θ), along with the upper and lower bounds (viz. the values at $\theta + f$ and $\theta + g$). It is evident that the effect of the upper and lower tolerances is to shift the nominal trend right and left.

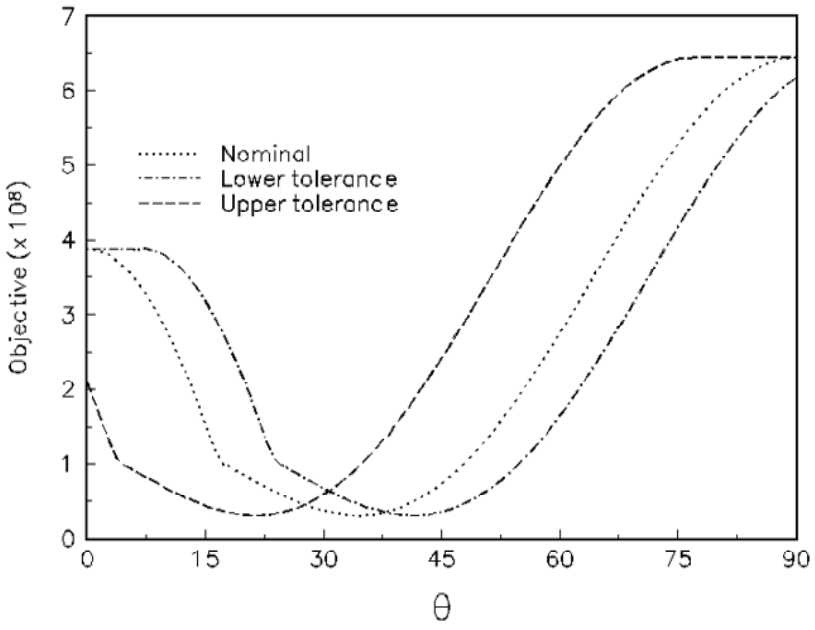

Figure 2-7: Effect of manufacturing tolerances in θ on the Objective with a/b = 0.75, $\lambda = 1$ and H = 4.4mm

The design problem (at this stage with the tolerance in the layer thickness neglected) becomes one of determining the value of θ at which the objective is minimized, with the tolerances in θ accounted for, which effectively becomes one of determining the value of θ for which the trend described by the upper solid line in Figure 2-8 is minimized (viz. designing for the worst case scenario). This occurs at 30.70^o, but for this value of H, the objective has not been minimized sufficiently. The solution would be to determine θ and t so that the value at which the upper solid line is minimal and the objective is effectively zero. When the tolerance in t is also included (and dealt with in the same manner), the design solution is $\theta_{opt} = 30.70^o$ and $H_{\min} = 40.98mm$. These values give a (nominal) buckling load of $1.52245 \times 10^7 N$, which is approximately 34% higher than that required. When the tolerances in the fibre angle and plate

thickness are ignored, the design solution is $\theta_{opt} = 34.00^o$ and $H_{\min} = 34.56mm$ (which give a buckling load of $10^7 N$).

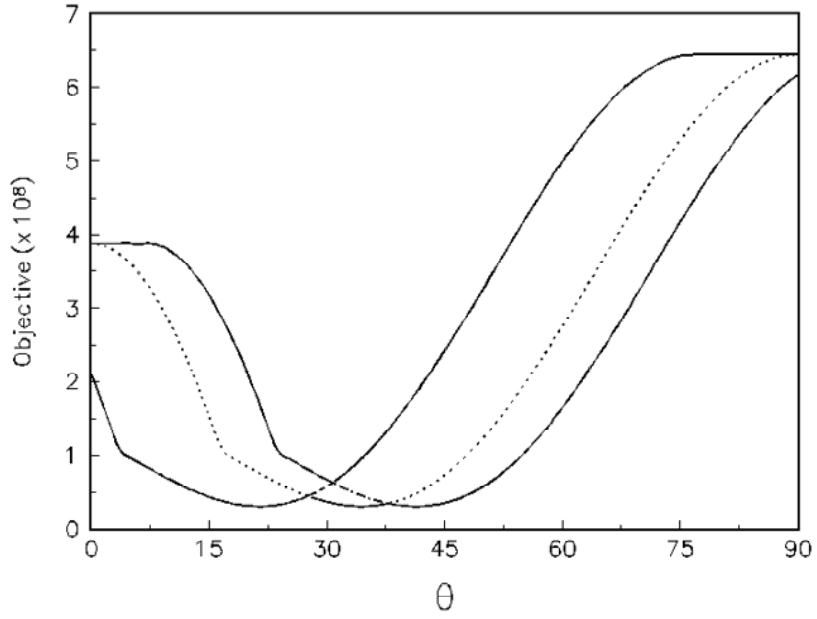

Figure 2-8

It is apparent from this example that the values of the actual optimal results are quite different from those of the nominal, and that if we were to ignore the manufacturing tolerances and choose 34^o as the optimal fibre orientation and $34.56mm$ as the plate thickness, the corresponding buckling load could be as low as $5.37891 \times 10^6 N$ (at $34^o + 13^o$ and $34.56mm - 5mm$), which is 46% less than that required. This fact emphasizes the importance of carrying out optimization in design work with the effects of manufacturing tolerances included. Finally, it should be emphasized that by designing for the worst case scenario, the resulting buckling load will always be at least equal to that required.

The optimization procedure thus involves the stages of determining the objective for a given (θ, t), and $(\theta + f, t + p), (\theta + f, t + q), (\theta + f, t), (\theta + g, t + p), (\theta + g, t + q), (\theta + g, t), (\theta, t + p)$ and $(\theta, t + q)$, selecting the highest of these and improving the fibre orientation and layer thickness to minimize the objective and weight. Thus, the computational solution consists of successive stages of analysis and optimization until convergence is obtained and the optimal angle θ_{opt}

and layer thickness $t_{\min}$ is determined within specified accuracy. In the optimization stage θ_{opt} is determined to within 0.01^o and $t_{\min}$ to within $0.01mm$.

2.6 Problem 5: A technique for optimally designing fibre-reinforced laminated structures for minimum weight with manufacturing uncertainties accounted for

Here a methodology to design symmetrically laminated structures under transverse loads for minimum weight with manufacturing uncertainty in the ply angle, is described. The ply angle and the ply thickness are the design variables, and the Tsai-Wu failure criteria is the design constraint implemented. The finite element method, based on Mindlin plate and shell theory, is implemented, and thus, unlike the previous problems, the effects of bending-twisting coupling are accounted for. The Golden Section method is used as the search algorithm, but the methodology is flexible enough to allow any appropriate finite element formulation, search algorithm and failure criterion to be substituted. In order to demonstrate the procedure, laminated plates with varying aspect ratio and boundary conditions are optimally designed and compared.

2.6.1 Optimal design problem formulation

The objective of the design problem is to minimize the weight of the plate, with manufacturing uncertainty in the lay-up angle θ accounted for. The problem can thus be stated as

$$W_{\min} \stackrel{\Delta}{\equiv} \min_{\theta,H} \left[W(\theta, H)\right], \qquad 0^o \leq \theta \leq 90^o, \ H_{\min} \leq H \leq H_{\max} \tag{2.9}$$

where the weight of a plate is given by

$$W = Hab\rho \tag{2.10}$$

where H is the total thickness of the plate and ρ the density.

In this case the minimum weight can be found by determining

$$\min_{H} \left|F\left(\theta\right) - 1\right| \tag{2.11}$$

at each value of θ until $H_{\min}$ (and thus θ_{opt}) is obtained.

2.6.2 Solution procedure

Assume that for the interval $0^o \leq \theta \leq 90^o$, a manufacturing tolerance in the lay-up angle θ is incurred, and must be accounted for during the design stage, if optimal performance is required. Furthermore, assume that the probability of any tolerance value occurring within the tolerance band, compared with any other, is equal. For example, there may be a maximum variation band of $+g$ or $-h$, with $0^o \leq g, h \leq 90^o$. In addition, when accounted for, it is assumed that $\theta + g \leq 90^o$ and $0^o \leq \theta + h$. In order to illustrate the problem, consider the following scenario: assume a manufacturer incurs the following maximum tolerances, $\theta + 13^o$ and $\theta - 7^o$; viz. when trying to achieve the value θ, the actual value that results is $\theta - 7^o \leq \theta \leq \theta + 13^o$. Figure 2-9 shows the effect of the tolerance on the minimum required plate thicknesses for a laminated CCCC (viz. clamped along each edge) plate with four symmetric layers of equal thickness and with $\theta_1 = -\theta_2 = -\theta_3 = \theta_4 = \theta$.

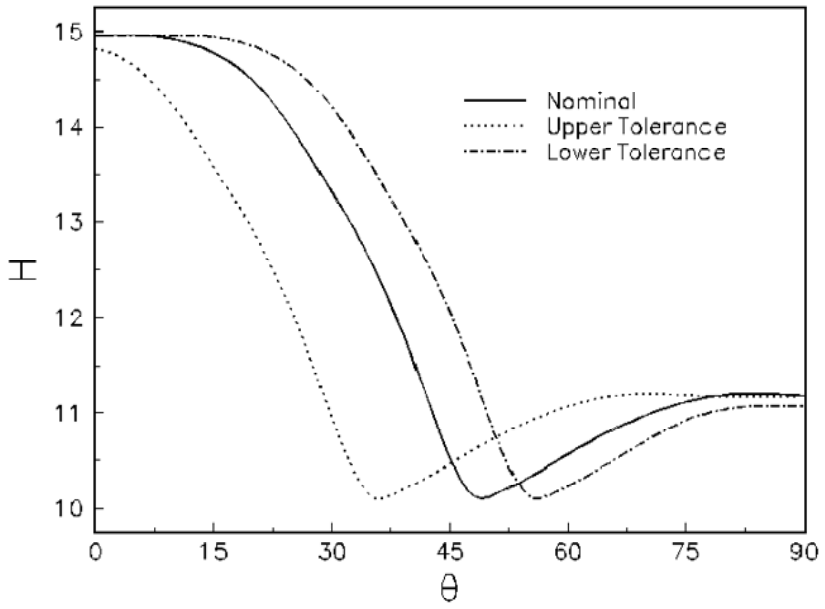

Figure 2-9: Effect of manufacturing tolerance in θ on the minimum plate thickness with $a/b = 1.25$ and (CCCC) boundary condition

The plate has dimensions $a = 1.25m$, $b = 1m$ and is subjected to a uniform transverse

bending pressure of $100000Pa$. The material properties are those for a typical T300/5208 graphite/epoxy material, Table 1.2. There are three trendlines given, and these represent the nominal layer thickness (viz. the value at θ), along with the upper and lower bounds (viz. the values at $\theta + g$ and $\theta + h$; thus the plate thickness required is $H_{lower} \leq H \leq H_{upper}$ due to the presence of tolerance in the lay-up angle). Note that each value in the trendlines has been determined by using Equation 2.11. It is evident that the effect of the upper and lower tolerances is to shift the nominal trends right and left. The design problem becomes one of determining the value of θ at which the layer thickness is minimized thus reducing the weight of the laminate, with the tolerances accounted for, which effectively becomes one of determining the value of θ for which the trend described by the *upper* solid line in Figure 2-10 (which needs no explanation) is minimized (viz. designing for the worst case scenario).

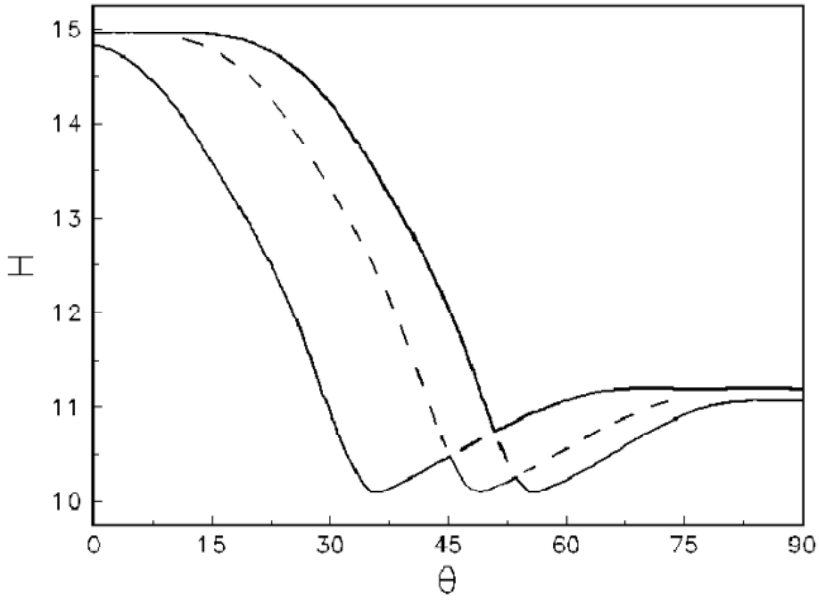

Figure 2-10

In addition, in the event that two or more values of θ correspond to equal minimum thickness values, the one that gives the best value contained within the *lower* solid line should logically be selected. In this case, the optimal value is 51.43^o which corresponds to a plate thickness of $10.89mm$. The optimal values for the nominal case are 48.84^o and $10.10mm$. It is apparent from

this example that the values of the actual optimal results are different from those of the nominal, and that if we were to ignore the manufacturing tolerances and choose 48.84^o as the optimal fibre orientation, the corresponding minimum thickness required could be as high as $11.32mm$ (viz. the value at 48.84^o - 7^o), which is 12% more than the optimal value. Alternatively, if the nominal design values are selected, the plate would fail in practice. This fact emphasizes the importance of carrying out optimization in design work with the effects of manufacturing tolerances included.

The optimization procedure thus involves the stages of determining the minimum layer thickness required for a given θ, $\theta + g$ and $\theta + h$ to satisfy Equation 2.11, selecting the greatest of the three values, and improving the fibre orientation to minimize the greatest value. Thus, the computational solution consists of successive stages of analysis and optimization until convergence is obtained and the optimal angle θ_{opt} and layer thickness $t_{\min}$ is determined within specified accuracy. In the optimization stage here, the Golden Section method is employed to determine both θ_{opt} and $t_{\min}$, and θ_{opt} is determined to within 0.01^o, whilst $t_{\min}$ is determined to within $0.01mm$.

Chapter 3

Results and discussion

3.1 Problem 1: A technique for optimally designing fibre-reinforced plates with manufacturing uncertainties for maximum buckling strength

In order to further illustrate the methodology described above, three different manufacturing tolerance scenarios are used. The first has been described previously, whilst the second may be described as follows. On the interval $[0^o \leq \theta \leq 40^o]_1$ a manufacturer incurs the following maximum tolerances: $\theta + 13^o$ and $\theta - 7^o$. On the interval $[40^o \leq \theta \leq 90^o]_2$, the tolerance is $\theta + 16^o$ and $\theta - 8^o$. The third scenario has tolerances $\theta + 17^o$ and $\theta - 3^o$ on the interval $[0^o \leq \theta \leq 40^o]_1$ and $\theta + 5$ and $\theta - 10^o$ on $[40^o \leq \theta \leq 90^o]_2$. Plates with eight symmetric layers with aspect ratios ranging from $a/b = 0.5$ to 2 are studied.

Figure 3-1 shows the effect on the results when the aspect ratio is changed to $a/b = 1$, for the same scenario studied in Figure 2-1 (viz. scenario 1). Here, it is apparent that the actual optimal value of the fibre orientation and that of the nominal case are the same. In addition, the actual optimal value occurs at the intersection of upper and lower tolerance trendlines, and not near the discontinuity. The value is 45^o, which corresponds to a buckling load of $137766N$, whilst the nominal maximum is $158043N$ (and thus it should again be highlighted that the outcome after manufacture could vary between these two values).

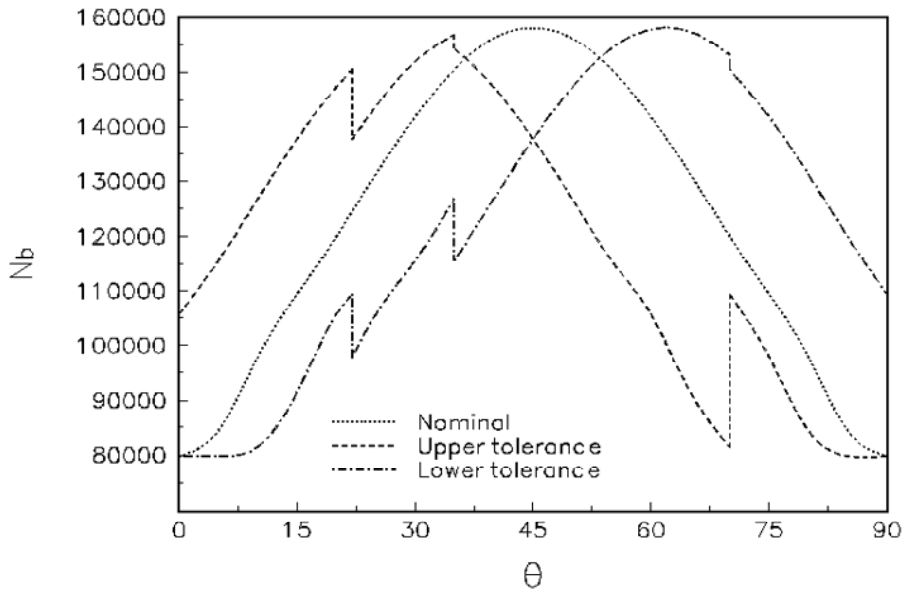

Figure 3-1: Effect of manufacturing tolerances on the buckling load for scenario 1 with a/b = 1 and $\lambda = 1$

When the aspect ratio is increased to 2 as shown in Figure 3-2, the optimal fibre angle occurs at the third intersection of the upper and lower trendlines (the second intersection is at the third discontinuity), viz. at 71^o, whilst the nominal optimal is at 70^o. Finally, Figure 3-3 demonstrates the difference that subjecting the same plate used in the first example (viz. with $a/b = 1.5$) to scenario 2 makes. Once again, the actual optimal value of θ occurs at the intersection of the upper and lower trendlines (viz. at 57^o), whilst the value of the nominal optimal is 63^o. Finally, the discontinuity is barely visible at 40^o

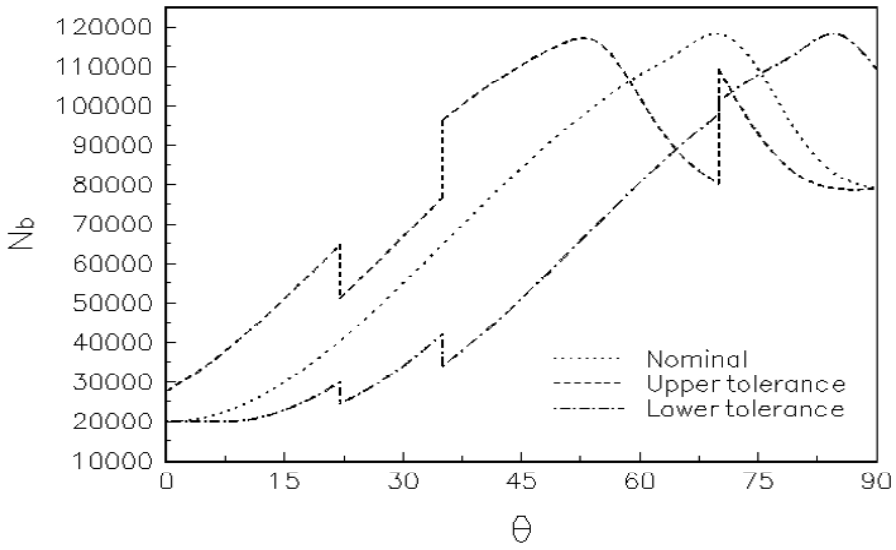

Figure 3-2: Effect of manufacturing tolerances on the buckling load for scenario 1 with a/b = 2 and $\lambda = 1$

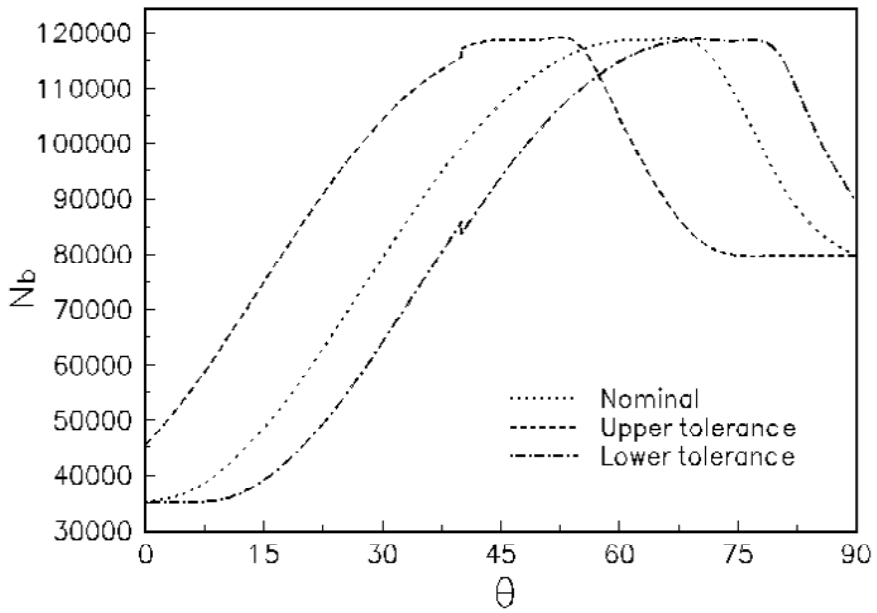

Figure 3-3: Effect of manufacturing tolerances on the buckling load for scenario 2 with a/b = 1.5 and $\lambda = 1$

The values of the actual optimal fibre orientations and the corresponding buckling loads for various plate aspect ratios subjected to scenario 1 and $\lambda = 1$ are given in Table 3.1.

a/b	θ_{opt}	$N_{\max}$	Optimal fibre angle (nominal)	Maximum buckling load (nominal)
0.5	26^o	420756	20^o	472157
0.75	34^o	212599	34^o	222331
1	45^o	137766	45^o	158043
1.5	71^o	104817	63^o	118847
2	71^o	102405	70^o	118039

Table 3.1: Effect of varying the plate aspect ratio with scenario 1 and λ =1

As expected, as the aspect ratio increases, so the value of θ_{opt} increases and the corresponding buckling load reduces. This is also true for the nominal values. Interestingly, only two plates ($a/b = 0.5$ and $a/b = 1.5$) have actual optimal fibre orientations that are significantly different from the nominal values, but the values of the corresponding buckling loads differ by between about 4.5% (at $a/b = 0.75$) and 13% (at $a/b = 2$).

a/b	θ_{opt}	$N_{\max}$	Optimal fibre angle (nominal)	Maximum buckling load (nominal)
0.5	0^o	612758	0^o	628616
0.75	34^o	332185	34^o	347392
1	43^o	266929	45^o	316086
1.5	45^o	243741	43^o	337343
2	44^o	245909	45^o	316086

Table 3.2: Effect of varying the plate aspect ratio with scenario 1 and λ =0

The effect of decreasing the loading ratio to $\lambda = 0$ for the same plates is demonstrated in Table 3-2. Here, for $0.5 \leq a/b \leq 1$, the values of θ_{opt} increase, and thereafter, remain close to 45^o. Also, there is little difference between the θ_{opt} and the nominal values, while the difference between $N_{\max}$ and the nominal ranges from about 2.5% to 28%. By comparing Table 3.1 and

3.2, it is apparent that (as expected) the resulting buckling loads increase when the applied loads are decreased from $\lambda = 1$ to $\lambda = 0$.

a/b	θ_{opt}	$N_{\max}$	Optimal fibre angle (nominal)	Maximum buckling load (nominal)
0.5	21^o	409621	20^o	472157
0.75	31^o	214265	34^o	222331
1	41^o	147315	45^o	158043
1.5	57^o	112027	63^o	118847
2	62^o	98789	70^o	118039

Table 3.3: Effect of varying the plate aspect ratio with scenario 2 and λ =0

The effect of designing to account for scenario 2 is shown in Table 3.3, for the same plates and with $\lambda = 1$. The same trends observed with Table 3.1 are evident here (viz. as the aspect ratio increases, so θ_{opt} increases while the corresponding buckling load decreases). The affect of changing from scenario 1 to scenario 2 is to reduce the value of θ_{opt}, by as little as about 9% (for $a/b = 0.75$) to as much as about 20% (for $a/b = 1.5$), while the corresponding buckling loads are decreased slightly in some cases (for $a/b = 0.5$ and 2) and increased in the others.

a/b	θ_{opt}	$N_{\max}$	Optimal fibre angle (nominal)	Maximum buckling load (nominal)
0.5	17^o	409621	20^o	472157
0.75	27^o	214265	34^o	222331
1	48^o	153116	45^o	158043
1.5	67^o	117323	63^o	118847
2	70^o	107792	70^o	118039

Table 3.4: Effect of varying the plate aspect ratio with scenario 3 and λ =1

Designing for scenario 3 (which has the same discontinuity point as that for scenario 2 but with slight changes in the tolerances - see Table 3.4) has the affect of decreasing the value of θ_{opt} for $a/b = 0.5$ and 0.75, and increasing it for the rest (when compared to the results for scenario 2). As before, the values of $N_{\max}$ are less than those of the nominal buckling loads even when

θ_{opt} and the nominal optimal fibre angle are the same (e.g. at 70^o), because the technique is aimed at designing for the worst case which results due to the manufacturing tolerances, even though the outcome may be considerably better (as the resulting buckling load varies with the value of θ within the tolerance range).

3.2 Problem 2: A technique for optimally designing fibre-reinforced symmetrically laminated structures for maximum buckling strength with manufacturing uncertainties in the fibre lay-up orientation accounted for

In order to further illustrate the methodology described above, three different manufacturing tolerance scenarios are used. The first has been described previously, whilst the second may be described as follows. On the interval $[0^o \leq \theta \leq 40^o]_1$ a manufacturer incurs the following maximum tolerances: $\theta + 13^o$ and $\theta - 7^o$. On the interval $[40^o \leq \theta \leq 90^o]_2$, the tolerance is $\theta + 16^o$ and $\theta - 8^o$. The third scenario has tolerances $\theta + 17^o$ and $\theta - 3^o$ on the interval $[0^o \leq \theta \leq 40^o]_1$ and $\theta + 5$ and $\theta - 10^o$ on $[40^o \leq \theta \leq 90^o]_2$. Plates with eight symmetric layers with aspect ratios ranging from $a/b = 0.5$ to 2 are studied. In addition, different combinations of free (F), simply supported (S) and clamped (C) boundary conditions are implemented at the four edges of the plate, and here, five different combinations are studied, namely (FSFS), (FSCS), (SSSS), (CSCS) and (CCCC), where the first letter refers to the first plate edge, and the others follow in an anti-clockwise direction as shown in Figure 1-17.

Figure 3-4 shows the effect on the results when the aspect ratio is changed to $a/b = 0.5$, for the same scenario and boundary condition studied in Figure 2-3 (viz. scenario 1 and (CCCC)). Here, it is apparent that the actual optimal value of the fibre orientation and that of the nominal case are the same. In addition, the actual optimal value occurs at the intersection of upper and lower tolerance trendlines. The value is 34^o, which corresponds to a buckling load of 876.5, whilst the nominal maximum is 941.8 (and thus it should again be highlighted that the outcome after manufacture could vary between these two values).

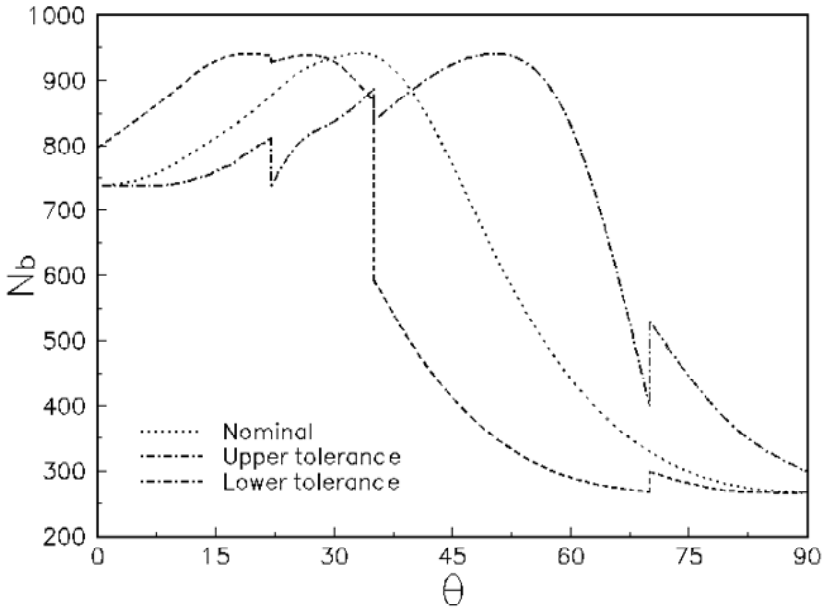

Figure 3-4: Effect of manufacturing tolerances on the buckling load of a plate with a/b = 0.5 and $\lambda = 1$

Finally, Figure 3-5 demonstrates the difference that subjecting the square (CCCC) plate of the first example to scenario 2, makes. Once again, the actual optimal value of θ occurs at the intersection of the upper and nominal trendlines (viz. at 39^o), whilst the value of the nominal optimal is 27^o or 63^o. Finally, the discontinuity is barely visible at 40^o.

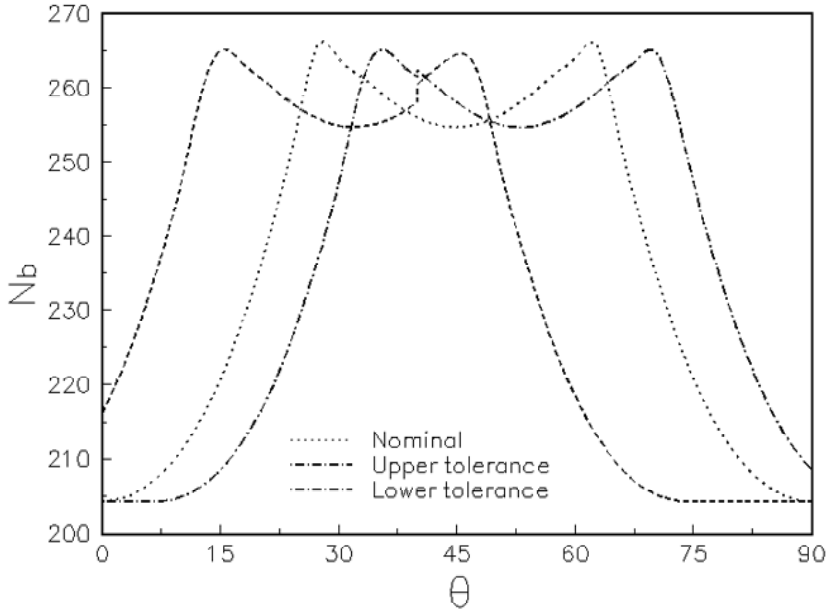

Figure 3-5: Effect of manufacturing tolerances on the buckling load of a plate with a/b = 1 and $\lambda = 1$

The effect of changing the scenario on the results for (CCCC) and (SSSS) plates with $\lambda = 1$ is given in Table 3.5.

a/b	Boundary Condition	θ_{opt}	$N_{b_{\max}}$	θ_{opt} (nominal)	$N_{b_{\max}}$ (nominal)
scenario 1					
0.5	CCCC	34^o	876.5	34^o	941.8
1.0	CCCC	42^o or 48^o	255.2	27^o or 63^o	265.2
2.0	CCCC	71^o	211.2	57^o	230.4
0.5	SSSS	26^o	357.5	25^o	406.0
1.0	SSSS	45^o	114.5	45^o	126.1
2.0	SSSS	72^o	88.2	65^o	101.0
scenario 2					
0.5	CCCC	28^o	866.2	34^o	941.8
1.0	CCCC	39^o	271.7	27^o or 63^o	265.2
2.0	CCCC	57^o	204.2	57^o	230.4
0.5	SSSS	20^o	351.3	25^o	406.0
1.0	SSSS	41^o	119.8	45^o	126.1
2.0	SSSS	63^o	84.9	65^o	101.0
scenario 3					
0.5	CCCC	24^o	866.2	34^o	941.8
1.0	CCCC	48^o	270.3	27^o or 63^o	265.2
2.0	CCCC	62^o	218.6	57^o	230.4
0.5	SSSS	16^o	351.3	25^o	406.0
1.0	SSSS	48^o	123.2	45^o	126.1
2.0	SSSS	70^o	91.6	65^o	101.0

Table 3.5: Effect of implementing different scenarios for (CCCC) and (SSSS) plates with λ =1

It is interesting to note that the value of $N_{b_{\max}}$ remains fairly constant for each particular

choice of aspect value and boundary condition for each scenario studied, but the value of θ_{opt} does not. For example, with $a/b = 0.5$ and the (CCCC) boundary condition, $N_{b_{\max}}$ varies from 876.5 to 866.2 as we swap between scenarios 1, 2 and 3, whilst θ_{opt} changes from 34^o to 28^o to 24^o, respectively. In addition, the difference between the actual and nominal values is greatest for scenario 3. Also, as expected, as the aspect ratio increases, so the buckling load decreases whilst the value of the optimal fibre angle increases.

The effect of varying the plate aspect ratio on the results for (CCCC) and (SSSS) plates subject to scenario 3 and $\lambda = 1$ are given in table 3.6.

a/b	Boundary Condition	θ_{opt}	$N_{b_{\max}}$	θ_{opt} (nominal)	$N_{b_{\max}}$ (nominal)
0.5	CCCC	24^o	866.2	34^o	941.8
0.75	CCCC	23^o	400.3	34^o	446.0
1	CCCC	37^o	258.0	27^o or 63^o	265.2
1.25	CCCC	62^o	233.4	58^o	253.1
1.5	CCCC	62^o	226.0	54^o	238.8
1.75	CCCC	61^o	222.5	59^o	235.1
2	CCCC	62^o	218.6	57^o	230.4
0.5	SSSS	16^o	351.3	25^o	406.0
0.75	SSSS	20^o	182.3	19^o	190.2
1	SSSS	48^o	123.2	45^o	126.1
1.25	SSSS	64^o	105.2	60^o	105.7
1.5	SSSS	68^o	98.2	69^o	105.6
1.75	SSSS	70^o	96.2	67^o	104.4
2	SSSS	70^o	91.6	65^o	101.0

Table 3.6: Effect of varying plate aspect ratio for (CCCC) and (SSSS) plates for scenario 3 and λ =1

Scenario 3 was chosen for demonstration purposes here because it had the most effect on the results and is thus the most interesting (see Table 3.5). This is obvious, as in some cases

there is up to 40% difference in the values of θ_{opt} and θ_{opt} (nominal). As before, as the aspect ratio increases, so the value of θ_{opt} increases and the corresponding buckling load reduces. In both boundary condition cases, the values of θ_{opt} remain fairly constant at around 20^o until $a/b = 1$. Between $a/b = 1.0$ and $a/b = 1.25$ the values of θ_{opt} increase substantially to around 60^o, whereafter, it again remains fairly constant.

The effect of decreasing the loading ratio for some of the same plates is demonstrated in Table 3.7.

a/b	Boundary Condition	θ_{opt}	$N_{b_{\max}}$	θ_{opt} (nominal)	$N_{b_{\max}}$ (nominal)
$\lambda = 1$					
0.5	CCCC	24^o	866.2	34^o	941.8
1.0	CCCC	37^o	258.0	27^o or 63^o	265.2
2.0	CCCC	62^o	218.6	57^o	230.4
0.5	SSSS	16^o	351.3	25^o	406.0
1.0	SSSS	48^o	123.2	45^o	126.1
2.0	SSSS	70^o	91.6	65^o	101.0
$\lambda = 0$					
0.5	CCCC	0^o	2587.3	0^o	2588.6
1.0	CCCC	0^o	599.4	0^o	671.5
2.0	CCCC	43^o	374.9	41^o	392.3
0.5	SSSS	0^o	569.0	0^o	635
1.0	SSSS	47^o	237.8	45^o	242.7
2.0	SSSS	46^o	224.9	44^o	229.5

Table 3.7: Effect of varying loading ratio for (CCCC) and (SSSS) plates subject to scenario 3

By reducing the loading conditions from $\lambda = 1$ to $\lambda = 0$,the θ_{opt} values decrease in both boundary condition cases. Similarly the $N_{b_{\max}}$ values increase. Also, the difference between the

actual and nominal values of θ_{opt} is much less in the case of $\lambda = 0$.

The effect of different boundary conditions on the results for plates subject to scenario 3 and $\lambda = 1$ is shown in Table 3.8.

a/b	Boundary Condition	θ_{opt}	$N_{b_{\max}}$	θ_{opt} (nominal)	$N_{b_{\max}}$ (nominal)
0.5	FSCS	17^o	230.9	25^o	252.6
1.0	FSCS	17^o	58.9	24^o	64.0
2.0	FSCS	75^o	27.3	74^o	28.2
0.5	FSFS	17^o	232.2	25^o	253.2
1.0	FSFS	19^o	51.7	21^o	62.6
2.0	FSFS	17^o	12.2	29^o	15.2
0.5	SSSS	16^o	351.2	25^o	406.0
1.0	SSSS	48^o	123.2	45^o	126.1
2.0	SSSS	70^o	91.6	65^o	101.0
0.5	CSCS	15^o	368.5	23^o	415.5
1.0	CSCS	46^o	356.4	41^o	402.9
2.0	CSCS	62^o	214.3	60^o	226.1
0.5	CCCC	24^o	866.2	34^o	941.8
1.0	CCCC	37^o	258.0	27^o or 63^o	265.2
2.0	CCCC	62^o	218.6	57^o	230.4

Table 3.8: Effect of different boundary conditions for scenario 3 and $\lambda = 1$

Once again, as expected, as the number of degrees of freedom is reduced, so the values of buckling loads are reduced and θ_{opt} increases. The most difference between the actual and nominal values is apparent when the boundary condition is specified as (CCCC).

In closure, it is important to note that the various tables demonstrate that there is generally

a difference between the values of actual and nominal optimal fibre angles, that in some cases, the difference is large, and is affected by the aspect ratio and loading ratio, boundary condition and scenario. It is thus important to design with the manufacturing uncertainty in the ply angle accounted for, so that the effect is minimized, and the best design is determined.

3.3 Problem 3: A technique for optimally designing fibre-reinforced laminated plates under in-plane loads for minimum weight with manufacturing uncertainties accounted for

In order to further illustrate the methodology described above, three different manufacturing tolerance scenarios are used. The first has been described previously, whilst the second may be described as follows. On the interval $[0^o \leq \theta \leq 40^o]_1$ a manufacturer incurs the following maximum tolerances: $\theta + 13^o$ and $\theta - 7^o$. On the interval $[40^o \leq \theta \leq 90^o]_2$, the tolerance is $\theta + 16^o$ and $\theta - 8^o$. The third scenario has tolerances $\theta + 17^o$ and $\theta - 3^o$ on the interval $[0^o \leq \theta \leq 40^o]_1$ and $\theta + 5$ and $\theta - 10^o$ on $[40^o \leq \theta \leq 90^o]_2$. Plates with eight symmetric layers with aspect ratios ranging from $a/b = 0.5$ to 2 are studied.

Figure 3-6 shows the effect on the results when the aspect ratio is changed to $a/b = 1$, for the same scenario studied in Figure 2-5 (viz. scenario 1). Here, it is apparent that the actual optimal value of the fibre orientation and that of the nominal case are the same. In addition, the actual optimal value occurs at the intersection of upper and lower tolerance trendlines, and not near a discontinuity. The value is 45^o, which corresponds to a layer thickness of $1.09mm$, whilst the nominal minimum is $1.04mm$ (and thus it should again be highlighted that the outcome after manufacture could vary between these two values).

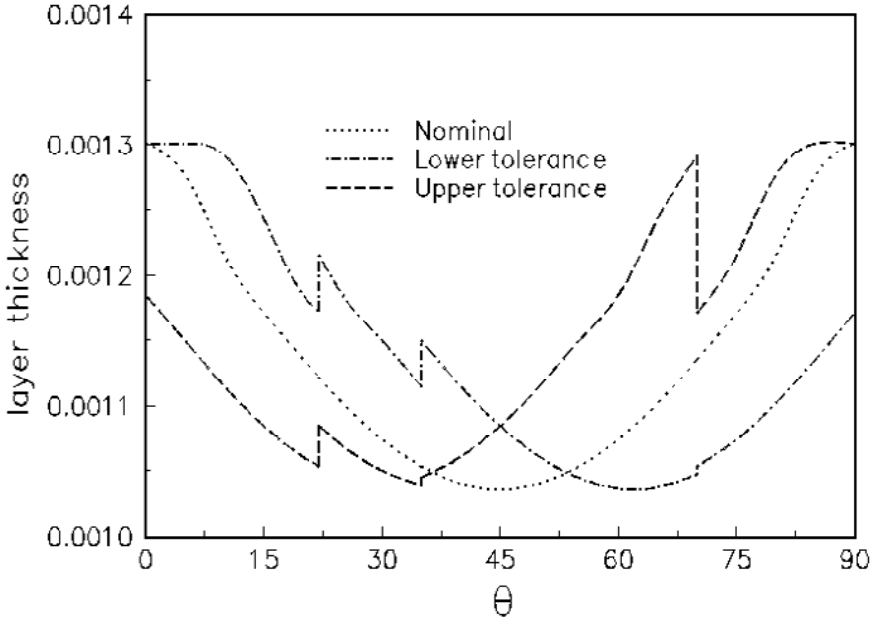

Figure 3-6: Effect of manufacturing tolences on the layer thickness for scenario 1 with a/b = 1 and $\lambda = 1$

When the aspect ratio is increased to 2 shown in Figure 3-7, the optimal fibre angle occurs at the third intersection of the upper and lower trendlines (the second intersection is at the third discontinuity), viz. at 71^o, whilst the nominal optimal is at 70^o.

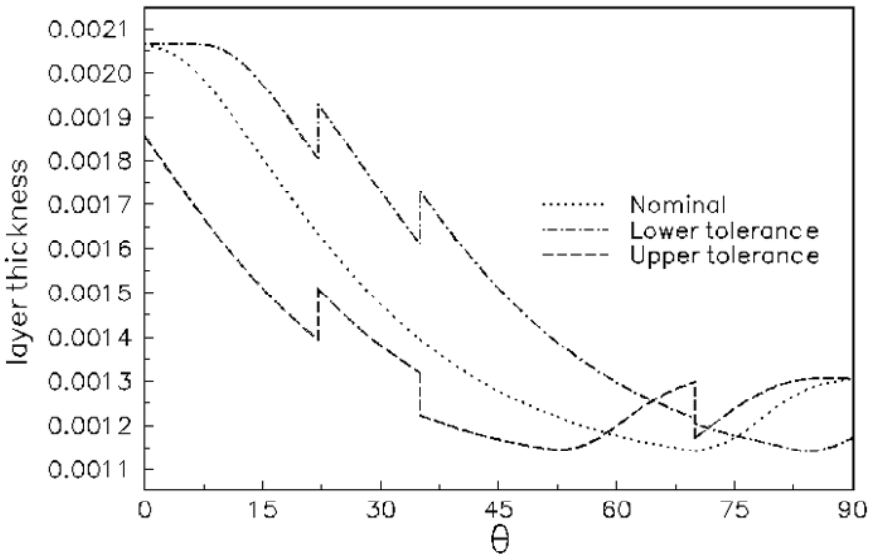

Figure 3-7: Effect of manufacturing tolences on the layer thickness for scenario 1 with a/b = 2 and $\lambda = 1$

Finally, Figure 3-8 demonstrates the difference that subjecting the same plate used in the first example (viz. with $a/b = 1.5$) to scenario 2 makes. Once again, the actual optimal value of θ occurs at the intersection of the upper and lower trendlines (viz. at 57^o), whilst the value of the nominal optimal is 63^o. Finally, the discontinuity is barely visible at 40^o.

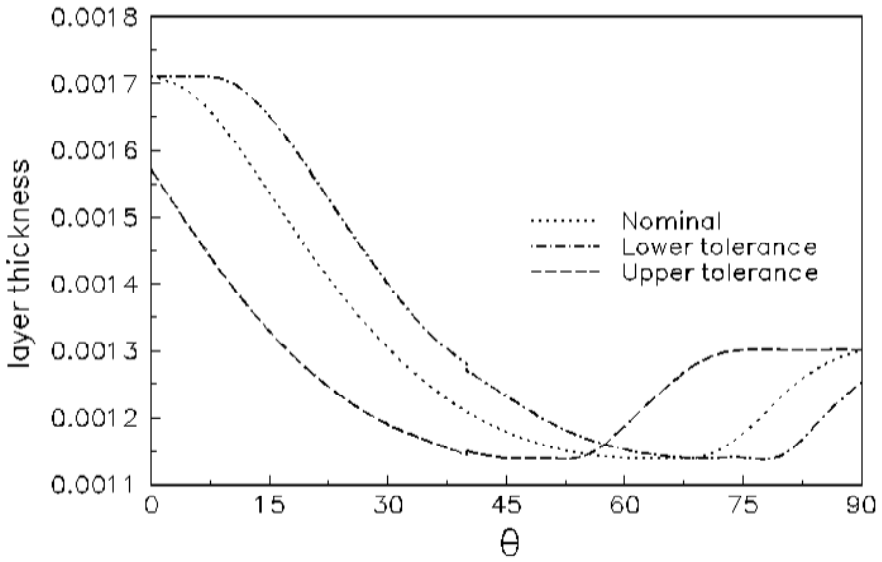

Figure 3-8: Effect of manufacturing tolerances on the layer thickness for scenario 2 with a/b = 1.5 and $\lambda = 1$

The values of the actual minimized plate thickness values (rounded to the nearest 0.1mm) and the corresponding optimal fibre orientations for various plate aspect ratios subjected to scenario 1 and $\lambda = 1$ are given in Table 3.9, with $N_{\min} = 90000\ N$. In addition, the value N_{act} is the value of the actual buckling load that results from the rounding off the thickness values. Also, the nominal optimal fibre angle and nominal $H_{\min}$ are reported, for comparison purposes.

a/b	θ_{opt}	$H_{\min}$	N_{act}	Optimal fibre angle (nominal)	$H_{\min}$ (nominal)
0.5	26^o	6.0	97152	20^o	5.8
0.75	34^o	7.5	93796	34^o	7.4
1	45^o	8.7	104072	45^o	8.3
1.5	71^o	9.5	100833	63^o	9.1
2	71^o	9.6	104202	70^o	9.1

Table 3.9: Effect of varying the plate aspect ratio with scenario 1 and $\lambda = 1$

As expected, as the aspect ratio increases, so the value of θ_{opt} increases (except once $a/b =$

1.5) and the corresponding plate thickness increases. This is also true for the nominal values. Interestingly, only two plates ($a/b = 0.5$ and $a/b = 1.5$) have actual optimal fibre orientations that are significantly different from the nominal values. Also, due to the rounding, some of the buckling loads that result in the case of the 'nominal' values of t are less than the minimum required. This occurs when $a/b = 1.5$ and $a/b = 2$ with the values $89559N$ and $88951N$ respectively.

a/b	θ_{opt}	$H_{\min}$	N_{act}	Optimal fibre angle (nominal)	$H_{\min}$ (nominal)
0.5	0^o	5.3	93586	0^o	5.2
0.75	34^o	6.5	95403	34^o	6.4
1	43^o	7.0	108201	45^o	6.6
1.5	45^o	7.2	123897	43^o	6.4
2	44^o	7.2	117920	45^o	6.6

Table 3.10: Effect of varying the plate aspect ratio with scenario 1 and $\lambda = 0$, for N min = 90 000 N

The effect of decreasing the loading ratio to $\lambda = 0$ for the same plates is demonstrated in Table 3.10. Here, for $0.5 \leq a/b \leq 1$, the values of θ_{opt} increase, and thereafter remain close to 45^o. Also, there is little difference between the θ_{opt} and the nominal values, while the difference between $H_{\min}$ and the nominal ranges from about 1.5% to 11%. By comparing Table 3.9 and Table 3.10, it is apparent that (as expected) the resulting plate thicknesses decrease when the applied loads are decreased from $\lambda = 1$ to $\lambda = 0$.

a/b	θ_{opt}	$H_{\min}$	N_{act}	Optimal fibre angle (nominal)	$H_{\min}$ (nominal)
0.5	21^o	6.0	101278	20^o	5.8
0.75	31^o	7.5	93426	34^o	7.4
1	41^o	8.5	96287	45^o	8.3
1.5	57^o	9.3	94667	63^o	9.1
2	62^o	9.7	100586	70^o	9.1

Table 3.11: Effect of varying the plate aspect ratio with scenario 2 and $\lambda = 1$

The effect of designing to account for scenario 2 is shown in Table 3.11, for the same plates and with $\lambda = 1$. The same trends observed with Table 3.9 are evident here (viz. as the aspect ratio increases, so θ_{opt} increases while the corresponding plate thicknesses decrease). The affect of changing from scenario 1 to scenario 2 is to reduce the value of θ_{opt}, by as little as about 9% (for $a/b = 0.75$) to as much as about 20% (for $a/b = 1.5$).

a/b	θ_{opt}	$H_{\min}$	N_{act}	Optimal fibre angle (nominal)	$H_{\min}$ (nominal)
0.5	17^o	6.0	98042	20^o	5.8
0.75	27^o	7.5	92155	34^o	7.4
1	48^o	8.4	93253	45^o	8.3
1.5	67^o	9.2	92285	63^o	9.1
2	70^o	9.4	98041	70^o	9.1

Table 3.12: Effect of varying the plate aspect ratio with scenario 3 and $\lambda = 1$

Designing for scenario 3 (which has the same discontinuity point as that for scenario 2 but with slight changes in the tolerances - see Table 3.12) has the affect of decreasing the value of θ_{opt} for $a/b = 0.5$ and 0.75, and increasing it for the rest (when compared to the results for scenario 2). As before, the values of $H_{\min}$ are greater than those of the nominal plate thickness even when θ_{opt} and the nominal optimal fibre angle are the same (e.g.. at 70^o), because the technique is aimed at designing for the worst case which results due to the manufacturing tolerances, even though the outcome may be considerably better (as the resulting plate thickness varies with the value of θ within the tolerance range).

3.4 Problem 4: A methodology for optimally designing fibre-reinforced symmetrically laminated structures for minimum weight with manufacturing uncertainties in the fibre lay-up orientation and thickness accounted for

In order to further illustrate the methodology described above, some more example results are given and compared below. The values of the actual minimized plate thickness values and the optimal fibre orientations for various plate aspect ratios and $\lambda = 1$ are listed in Table 3.13, with $N_{\min} = 10^7\ N$. In addition, the value N_{act} is the value of the actual buckling load that results. Also, the nominal optimal fibre angle and nominal $H_{\min}$ are reported, for comparison purposes (viz. these give $N_{nom} = 10^7$). As expected, as the aspect ratio increases, so the value of θ_{opt} increases and the plate thicknesses increase. This is also true for the nominal values. When compared to the nominal values, the actual thickness of the $a/b = 0.5$ plate is 18% greater, and 12% greater for the $a/b = 1.5$ plate. The average difference is 14%.

a/b	θ_{opt}	$H_{\min}$	N_{act} (x10^7)	Optimal fibre angle (nominal)	$H_{\min}$ (nominal)
0.5	20.36^o	33.92	1.83887	18.13^o	27.84
0.75	30.70^o	40.98	1.52245	34.00^o	35.56
1	42.00^o	45.51	1.48301	45^o	39.85
1.5	59.83^o	49.25	1.41619	63.15^o	43.82
2	63.64^o	50.91	1.47895	70.06^o	43.91

Table 3.13: Effect of varying the plate aspect ratio with $\lambda = 1$, for $N_{\min} = 10^7\ N$

The effect of decreasing the loading ratio to $\lambda = 0$ for the same plates is demonstrated in Table 3.14. Here, for $0.5 \leq a/b \leq 1$, the values of θ_{opt} increase, and thereafter remain close to 45^o. Also, there is little difference between the θ_{opt} and the nominal values, while the difference between $h_{\min}$ and the nominal ranges from about 15% to 17.5%, with the average being 16%. By comparing Table 3.13 and Table 3.14, it is apparent that (as expected) the resulting plate thicknesses decrease when the applied loads are decreased from $\lambda = 1$ to $\lambda = 0$.

a/b	θ_{opt}	$H_{\min}$	N_{act} (x10^7)	Optimal fibre angle (nominal)	$H_{\min}$ (nominal)
0.5	0^o	30.37	1.76119	0^o	25.15
0.75	30.70^o	36.00	1.61361	33.83^o	30.65
1	42.00^o	37.15	1.61340	45^o	31.63
1.5	41.70^o	37.53	1.75709	42.87^o	30.94
2	41.10^o	37.25	1.62104	45^o	31.63

Table 3.14: Effect of varying the plate aspect ratio with $\lambda = 0$, for $N_{\min} = 10^7$ N.

In order to demonstrate the effect a different tolerance scenario makes to the results, the thickness tolerance to -3mm and +3mm, whilst the orientation tolerance was reduced to -7^o and +7^o. The results for plates with $\lambda = 1$ (viz. similar to those of Table 3.13) are given in Table 3.15. It can be seen that narrowing down the tolerance band has pushed the value of θ_{opt} and $H_{\min}$ closer to that of the nominal values. Similar trends observed in Table 3.13 are evident here, and once again, the difference between $H_{\min}$ and the nominal ranges from about 6.5% to 11.5%, with the average being 8.5%.

a/b	θ_{opt}	$H_{\min}$	N_{act} (x10^7)	Optimal fibre angle (nominal)	$H_{\min}$ (nominal)
0.5	21.95^o	31.41	1.44220	18.13^o	27.84
0.75	34.08^o	38.77	1.29554	34.00^o	35.56
1	45^o	43.17	1.27172	45^o	39.85
1.5	63.87^o	46.97	1.23137	63.15^o	43.82
2	68.05^o	48.09	1.29455	70.06^o	43.91

Table 3.15: Effect of different tolerance scenario of the results for plates with $\lambda = 1$, for $N_{\min} = 10^7$ N

3.5 Problem 5: A technique for optimally designing fibre-reinforced laminated structures for minimum weight with manufacturing uncertainties accounted for

In order to further illustrate the methodology described above, plates with four equal thickness symmetric layers and with aspect ratios ranging from $a/b = 0.5$ to 2 are studied. In addition, the effect of the boundary condition is also considered. The plates have the same material properties and loading as that of Figure 2.9. Also, different combinations of free (F), simply supported (S) and clamped (C) boundary conditions are implemented at the four edges of the plate, and here, five different combinations are studied, namely (FSFS), (FSCS), (SSSS), (CSCS) and (CCCC), where the first letter refers to the first plate edge, and the others follow in an anti-clockwise direction as shown in Figure 1-17.

The effect of the aspect ratio is illustrated in Tables 3.16 and 3.17, for (CCCC) and (SSSS) plates (respectively). Also, the nominal optimal fibre angle and corresponding $H_{\min}$ are reported, for comparison purposes.

a/b	θ_{opt}	$H_{\min}$	Optimal fibre angle (nominal)	$H_{\min}$ (nominal)
0.5	7.59^o	4.46	35.46^o	4.37
0.75	29.54^o	7.65	39.64^o	7.26
1	41.97^o	10.20	45^o	9.30
1.25	51.43^o	10.89	48.84^o	10.10
2	56.71^o	11.09	52.15^o	10.36

Table 3.16: Effect of varying the plate aspect ratio for (CCCC) plates

For Table 3.16, the trend in both the nominal thickness and actual thickness values is generally as expected, viz. as the plate gets longer, so the thickness increases. In addition, the actual values are greater than the nominal values (as expected), with the difference for the square plate being the largest (9.7%). The optimal fibre orientation values show the same (increasing) trend although the actual values are less than the nominal values for $0.5 \leq a/b \leq 1$. When $a/b \succ 1$, the values are greater. The greatest difference occurs for the plate with

$a/b = 0.5$.

a/b	θ_{opt}	$H_{\min}$	Optimal fibre angle (nominal)	$H_{\min}$ (nominal)
0.5	0^o	6.06	0^o	5.73
0.75	0^o	9.79	0^o	8.69
1	90^o	12.50	0 or 90^o	11.78
1.25	90^o	12.46	90^o	11.57
2	90^o	12.43	86.81^o	11.62

Table 3.17: Effect of varying the plate aspect ratio for (SSSS) plates

For Table 3.17, the trend in the thickness values is the same as that observed in Table 3.16, except when $a/b \succ 1$, at which point the values start reducing. Nonetheless, the actual values are always greater than the nominal values due to the uncertainty in θ,and the greatest difference is 12.7% (in the case of the plate with $a/b = 0.75$). The values of the optimal fibre orientations are not particularly interesting, except in the case of the longest plate, which has a nominal θ_{opt} which is neither 0^o or 90^o (although close to 90^o).

Boundary condition	θ_{opt}	$H_{\min}$	Optimal fibre angle (nominal)	$H_{\min}$ (nominal)
(SSSS)	90^o	12.46	90^o	11.57
(CSFS)	38.73^o	21.23	39.98^o	19.84
(CSCS)	84.14^o	7.88	79.69^o	7.82
(CCCC)	51.43^o	10.89	48.84^o	10.10

Table 3.18: Effect of boundary conditions for plates with a/b = 1.25

The effect of the boundary condition on the results for plates with $a/b = 1.25$ is illustrated in Table 3.18. There are no apparent trends in either the thickness or fibre orientation values (although, as usual, the actual thickness values are greater than the nominal values). The greatest difference in the thickness values is 7.6% in the case of the (SSSS) plate. Interestingly, the plate with the free edge, viz. the (FSCS) plate, is almost double the thickness of the thinnest (in both actual and nominal values).

Chapter 4

Conclusions

The work presented in this thesis employed various different search routines and optimization strategies and combined them with analysis methods, like the FEM, to develop four new methodologies to minimize the weight, or maximize the load bearing capacity of laminated structures. Each problem that was investigated is summarised below:

Problem 1: A technique for optimally designing fibre-reinforced symmetrically laminated structures for maximum buckling strength with manufacturing uncertainties in the fibre lay-up orientation accounted for. Here, a procedure to design symmetrically laminated plates for maximum buckling load with manufacturing uncertainty in the ply angle, which is the design variable, is described. In order to illustrate the technique, the designs of simply supported symmetrically laminated plates are optimized. The plates are subjected to three manufacturing tolerance scenarios, and the effect of these, as well as that of changing the aspect ratio and loading ratio is studied. In addition, the value of θ_{opt} is determined to within 1^o, and the optimized designs are compared to those for plates not subjected to manufacturing variations. The results demonstrate that if the manufacturing tolerances are neglected in the optimal design stage, the resulting in-plane load carrying capacity of the plate can be significantly lower than expected. Finally, it should be noted that different problem formulations and methods of solution can also be substituted into the technique when more appropriate.

Problem 2: A technique for optimally designing fibre-reinforced symmetrically laminated structures for maximum buckling strength with manufacturing uncertainties in the fibre lay-up orientation accounted for. In this problem, which is similar to the first, the finite element

method is implemented and used to determine the fitness of each design candidate, and so the effects of bending-twisting coupling are accounted for. In order to illustrate the technique, the designs of symmetrically laminated plates are optimized. Different combinations of free, simply supported and clamped boundary conditions are implemented at the four edges of the plates, which are subjected to three manufacturing tolerance scenarios, and the effect of these, as well as that of changing the aspect ratio and loading ratio is studied. In addition, the value of θ_{opt} is determined to within 1^o, and the optimized designs are compared to those for plates not subjected to manufacturing variations. The results demonstrate that if the manufacturing tolerances are neglected in the optimal design stage, the resulting in-plane load carrying capacity of the plate can be significantly lower than expected. Finally, it should be noted that different finite element formulations can also be substituted into the technique when more appropriate.

Problem 3: A technique for optimally designing fibre-reinforced laminated plates under in-plane loads for minimum weight with manufacturing uncertainties accounted for. Here, a procedure to design symmetrically laminated plates under buckling loads for minimum weight with manufacturing uncertainty in the ply angle, which is the design variable, is described. The constraint implemented is a minimum buckling load carrying capacity constraint, and the objective is to determine the value of the fibre orientation that corresponds to a minimum plate thickness, with the uncertainty included. In order to illustrate the technique, the design optimization of rectangular plates with eight layers is undertaken. The plates are subjected to three manufacturing tolerance scenarios, and the effect of these, as well as that of changing the aspect ratio and loading ratio is studied. In addition, the value of θ_{opt} is determined to within 1^o, and the optimized designs are compared to those for plates not subjected to manufacturing variations. The results demonstrate that if the manufacturing tolerances are neglected in the optimal design stage, the resulting plate may not be capable of carrying the required buckling load. Finally, it should be noted that different problem formulations and methods of solution can also be substituted into the technique when more appropriate.

Problem 4: A methodology for optimally designing fibre-reinforced symmetrically laminated structures for minimum weight with manufacturing uncertainties in the fibre lay-up orientation and thickness accounted for. Here, a procedure to design symmetrically laminated plates under buckling loads for minimum weight with manufacturing uncertainty in the ply angle and plate

thickness, which are the design variables, is described. The search routine implemented is the Downhill Simplex method, but the methodology is independent of the routine, and any suitable substitute could be used. Similarly, the technique is also independent of the solution for the buckling load that is implemented, and a more accurate one than that used here can easily be utilized. In order to illustrate the technique, the designs of simply supported symmetrically laminated plates are optimized, and the effect of increasing aspect ratio and loading on the weight and optimal fibre orientations are studied. The optimized designs are compared to those for plates not subjected to manufacturing variations. The results demonstrate that if the manufacturing tolerances are neglected in the optimal design stage, the resulting weight of the plates can be significantly higher than expected.

Problem 5: A technique for optimally designing fibre-reinforced laminated structures for minimum weight with manufacturing uncertainties accounted for. Here, a methodology to design symmetrically laminated structures under transverse loads for minimum weight with manufacturing uncertainty in the ply angle, is described. The ply angle and the ply thickness are the design variables, and the Tsai-Wu failure criteria is the design constraint used. The finite element method is used, and thus effects like bending-twisting coupling are accounted for. In order to illustrate the technique, the designs of symmetrically laminated plates are optimized.. The plates are subjected to similar UDLs, and the effect of changing the aspect ratio and boundary condition is studied. In addition, the value of θ_{opt} is determined to within 0.01^o whilst H is determined to within $0.01mm$, and the optimized designs are compared to those for plates not subjected to manufacturing variations. The results demonstrate that if the manufacturing tolerances are neglected in the optimal design stage, the plate can be as much as 12% heavier if it were to carry the load without failure, or would be too thin, and fail in practice. Finally, it should be noted that different finite element formulations can also be substituted into the technique when more appropriate.

Bibliography

[1] Reddy, J. N. (1993) An Introduction to the Finite Element Method. Second Edition. McGraw-Hill. Texas. 5-6

[2] Zahavi, E. (1992). The Finite Element Method in Machine Design. Prentice Hall. New Jersey.

[3] Rao, S. R. (1999). The Finite Element Method in Engineering. Butterworth-Heinemann. USA.

[4] Huebner, K. H, Thornton, E. A. & Byrom, T. G. (1995). The Finite Element Method for Engineers, Third edition, Wiley-Interscience, Ney York. 84-86

[5] Matthews, F. L., Davies, G. A. O., Hitchings, D. & Soutis, C. (2000). Finite Element Modelling of Composite Materials and Structures. Woodhead Publishing Limited. Cambridge. England.

[6] Cook, R. D. (1995). Finite Element Modelling for Stress Analysis. John Wiley & Sons, Inc. USA.

[7] Askeland, D. R. (1994) The Science and Engineering of Materials. Third Edition. PWS Publishing Company. Boston. 527-545

[8] Smith, W. F. (2004) Foundations of Material Science and Engineering. McGraw-Hill. New York. 612-614

[9] Gürdal, Z., Haftka, R. T. & Hajela, P. (1999). Design and Optimization of Laminated Composite Materials. Wiley-Interscience. New York.

[10] Herakovich, C. T. (1998). Mechanics of Fibrous Composites. John Wiley & Sons, Inc. USA.

[11] Tsai, S. W. & Pagano, N. J. (1968). Invariant Properties of Composite Materials. In Composite Materials Workshop. 233-253.

[12] Matthews, F. L. & Rawlings, R. D. (1994). Composite Materials: Engineering and Science. Woodhead Publishing Limited, Cambridge, England

[13] Jones, R. M. (1975). Mechanics of Composite Materials. McGraw-Hill. New York. Chapter 4. 166.

[14] Reddy, J. N. (1984). Energy and Variational Methods in Applied Mechanics. Wiley, New York.

[15] Gibson R. F. (1994). Principles of Composite Material Mechanics. McGraw Hill. New York.

[16] Tsai, T. W. & Hahn, H. T. (1980). Introduction to Composite Materials. Technomic Publishing Company. Westport. Connecticut.

[17] Tsai, S. W. & Wu, E. M. (1971). A General Theory of Strength for Anisotropic Materials, Journal of Composite Materials, **5**, 58-80.

[18] Messac, A. & Sundararaj, G. J. (2002). A Robust Design Approach using Physical Programming. AIAA-2000-0562.

[19] Bates, S. J., Sienz, J., Pittman, J. F. T. & Langley, D.S. (2002). Application of Robust Design Optimization to Extrusion slit die Design. Proceedings of the 3rd international conference on engineering computational technology, B.H.V. Topping and Z. Bittnar, Civil-Comp Press, Stirling, Scotland. Paper 62.

[20] Sandgren E & Cameron T. M. (2002). Robust Design Optimization of Structures through consideration of variation. Computers and Structures, **80**,(20),1605-1613.

[21] Liou J. H. & Jang D. Y. (1997). Forging Parameter Optimization considering stress distributions in products through FEM Analysis and Robust Design Methodology. International Journal of Machine Tools and Manufacture, **37**,(6),775-782.

[22] Lee, K. H. & Park, G. J. (2002). Robust Optimization in Discrete Design Space for Constrained Problems. AIAA Journal, **40**,(4),774-780.

[23] Lee, K. H. & Park, G. J. (2001). Robust Optimization considering Tolerances of Design Variables. Computers and Structures, **79**,(1),77-86.

[24] Press, W. H., Teukolsky, S. A, Vetterling, W. T. & Flannery, B. P. (1988). Numerical Recipes in C. Press Syndicate of the University of Cambridge.

[25] Nelder, J. A. & Mead, R. (1965). Computer Journal, Vol. 7, 308-313.

[26] Walker, M., Adali, S. & Verijenko, V. (1996). Optimization of Symmetric Laminates for Maximum Buckling load Including the effects of Bending-Twisting Coupling. Computers & Structures, 58(2):313-319.

[27] Adali, S., Walker, M. & Verijenko, V. E. (1996). Multiobjective Optimization of Laminated plates for Maximum Prebuckling, Buckling and Postbuckling Strength using continuous and discrete ply angles. Composite Structures, **35**,117-130.

[28] Joshi, S. P. & Iyengar, N. G. R. (1985). Optimal Design of Laminated Composite plates under axial compression. Transactions of the Canadian Society of Mechanical Engineers, **9**,45-50.

[29] Miki, M. (1986). Optimal Design of Fibrous Laminated Composite plates subject to axial compression. In Composites 86: Recent Advances in Japan and the United States, edited by K. Kawata, S. Umekawa and A. Kobayashi, Tokyo. 673-680.

[30] Muc, A. (1988). Optimal Fibre Orientation for Simply-Supported, angle-ply plates under biaxial compression. Composite Structures **9**,161-172.

[31] Kam, T. Y. & Chang, R. R. (1993). Design of Laminated Composite plates for Maximum Buckling load and Vibration Frequency. Computer Methods in Applied Mechanics and Engineering, **106**,65-81.

[32] Adali, S. (1994). Lay-up Optimization of Laminated plates under Buckling loads. In Buckling and Postbuckling of Laminated Plates, Edited by G. J. Turvey and I. H. Marshall, Chapman and Hall, London.

[33] Walker, M., Reiss, T. & Adali, S. (1997). Optimal Design of Symmetrically Laminated plates for Minimum Deflection and Weight. Composite Structures, **39**(3 - 4),337-346.

[34] Nemeth M. P. (1986). Importance of Anisotropy on Buckling of Compression-loaded Symmetric Composite Plates, *AIAA*, **24**, 1831-1835.

[35] Whitney, J. M. (1987). The Effect of Shear Deformation on the Bending and Buckling of Anisotropic Laminated plates, Composite structures 4, Elsivier applied science, London. 1109-1121.

[36] Rohwer, K. (1988). Bending-Twisting Coupling Effects on the Buckling Loads of Symmetrically Stacked plates, Composite Materials and Structures, Proceedings of the international conference on composite materials and structures, McGraw Hill, New Delhi: 313-323.

[37] Sherbourne, A. N. & Pandey, M. D. (1991). Diffential Quadrature Method in the Buckling Analysis of beams and Composite plates, Computers and Structures, **40,**903-913.

[38] Walker, M. & Smith, R. E. (2002). A Computational Methodology to select the best Material Combinations and Optimally Design Composite Sandwich panels for Minimum Cost. Computers and Structures, **80**,1457-1460.

[39] Joshi, M. G. & Biggers, S. B. Jr. (1996). Thickness optimization for maximum buckling loads in composite laminated plates. Composites Part B: Engineering, **27,**(2),105-114

[40] Adali, S., Richter, A. & Verijemko, V. E. (1995). Minimum Weight Design of Symmetric angle-ply Laminates under Multiple Uncertain loads. Structural Optimization, **9**,89-95

[41] Tauchert, T. R. & Adibhatla, A. (1984). Design of Laminated plates for Maximum Stiffness. Journal of composite materials, **18**,58-69

[42] Quian, B., Reiss, R. & Aung, W. (1990). The Maximum Stiffness Design of Rectangular Symmetric angle-ply Laminates. Proceedings of the 2nd Int. Conf. on Computer Aided Design in Composite Material Technology. Free University of Brussels/Wessex Institute of Technology, Computational Mechanics Publications, Southampton, 451-464

[43] Kengtung, C. (1986). Sensitivity Analysis and a mixed approach to the Optimization of Symmetric Layered Composite plates. Engineering Optimization, **9**,233-248

[44] Kam, T. Y. & Chang, R. R.(1992). Optimum lay-up of thick Laminated Composite plates for Maximum Stiffness. Engineering Optimization, **19**,237-249

[45] Adali, S., Summers, E. B. & Verijenko,V. E. (1994). Minimum Weight and Deflection Design of thick Sandwich Laminates via Symbolic Computation. Composite Structures, **29**,145-160.

[46] Phillips, J. L. & Gürdal, Z. (1990). Analysis and Optimal Design of Geodesically stiffened Composite panels. Proceedings of the 2nd Int. Conf. on Computer Aided Design in Composite Material Technology. Free University of Brussels/Wessex Institute of Technology, Computational Mechanics Publications, Southampton, 509-520.

[47] Triantafillou, T. C., Kim, P. & Meier, U.(1991). Optimization of Hybrid Aluminium/c.f.r.p box beams. International Journal of Mechanical Sciences, **33**(9),729-739.

[48] Min, K. T. & de Charenteney, F. X. (1986). Optimum Weight Design of Sandwich Cylinders with Orthotropic facings and core under combined loads. Computers and Structures, **24,**(2),313-322.

[49] Ostwald, M. (1990). Optimum Weight Design of Sandwich Cylindrical shells under combined loads. Computers and Structures, 11,247.

[50] Lucoshevichyus, R. S. (1976). Minimizing the Mass of Reinforced Rectangular plates Compressed in two directions in a manner conductive toward stability. Polymer Mechanics, **12**,929-933.

[51] Shin, D. K., Gürdal, Z. & Griffin, O. H. (1991). Minimum Weight Design of Laminated plates for postbuckling Performance. Proc. 32nd AIAA/ASME/ASCE/AHS/ASC Structures, Structural dynamics and materials Conf., Baltimore, Maryland, 267-274.

[52] Walker, M., Reiss, T. & Adali, S. (1997). Minimum Weight Design of Composite Hybrid Shells via symbolic computation, J. Franklin Inst, Vol. 334B(1),47-56

[53] Chiang, Y. J. (1996). Robust Design of the Isopescu shear test specimen for Composites. Journal of testing and evaluation, JTEVA. **24**(1),1-11.

[54] Kristinsdottir, B. P. Incorporating Manufacturing Tolerances in Optimal Design of Composite Structures. Masters Thesis. University of Washington.

[55] Kristinsdottir, B. P. (1996). Incorporating Manufacturing Tolerances in near-optimal Design of Composite Structures, Engineering Optimization. 26:57-62.

[56] Walker, M., Reiss, T. & Adali, S. (1997). A Procedure to select the best Material Combinations and Optimally Design Hybrid Composite plates for Minimum Weight and Cost. Engineering Optimization, **29**,65-83.

[57] Walker, M. & Smith, R. E. A Procedure to select the best Material Combination and Optimally Design Composite Sandwich Cylindrical shells for Minimum Mass. Submitted to Computers & Structures.

[58] Walker, M. & Smith, R. E. (2003). A Methodology to Design Laminated Composite Structures for Maximum Strength. Composites PartB ,**34**,209-214.

[59] Walker, M. & Smith, R. E. (2003). A Simple Self-Design Methodology for Laminated Composite Structures to Minimize Mass, Advances in Engineering Software,(34):601-605.

[60] Walker, M. & Smith, R. E. (2002). A Technique for using Genetic Algorithms and Finite Element Analysis to Minimize the Mass of Laminated Structures. Submitted to Finite Elements in Analysis and Design.

[61] Walker, M. & Smith, R. E. (2003). A Technique for the Multiobjective Optimization of Laminated Composite Structures using Genetic Algorithms and Finite Element Analysis, Composite Structures, **62**,123-128.

[62] Walker, M. & Hamilton, R. (2004). A Technique for Optimally Designing Fibre-Reinforced Laminated plates with Manufacturing Uncertainties for Maximum Buckling Strength, Engineering Optimization **37**,(2),135-144.

[63] Walker, M. & Hamilton, R. (2005). A Methodology for Optimally Designing Fibre-Reinforced Laminated Structures with Design Variable Tolerances for Maximum Buckling Strength, Thin-Walled Structures. **43**,161-174.

[64] Walker, M. & Hamilton, R. A Technique for Optimally Designing Fibre-Reinforced Laminated plates under in-plane loads for Minimum Weight with Manufacturing Uncertainties accounted for. Submitted to Engineering with Computers.

[65] Walker, M. & Hamilton, R. A Methodology for Optimally Designing Fibre-Reinforced Laminated plates under in-plane loads for Minimum Weight with Manufacturing Uncertainty accounted for. Submitted to Journal of Engineering Design.